1978

The synthesis and characterization of reduced scandium halides containing one- and two-dimensional metal bonded arrays

Kenneth Reinhard Poeppelmeier
Iowa State University

INFORMATION TO USERS

This material was produced from a microfilm copy of the original document. While the most advanced technological means to photograph and reproduce this document have been used, the quality is heavily dependent upon the quality of the original submitted.

The following explanation of techniques is provided to help you understand markings or patterns which may appear on this reproduction.

1. The sign or "target" for pages apparently lacking from the document photographed is "Missing Page(s)". If it was possible to obtain the missing page(s) or section, they are spliced into the film along with adjacent pages. This may have necessitated cutting thru an image and duplicating adjacent pages to insure you complete continuity.

2. When an image on the film is obliterated with a large round black mark, it is an indication that the photographer suspected that the copy may have moved during exposure and thus cause a blurred image. You will find a good image of the page in the adjacent frame.

3. When a map, drawing or chart, etc., was part of the material being photographed the photographer followed a definite method in "sectioning" the material. It is customary to begin photoing at the upper left hand corner of a large sheet and to continue photoing from left to right in equal sections with a small overlap. If necessary, sectioning is continued again — beginning below the first row and continuing on until complete.

4. The majority of users indicate that the textual content is of greatest value, however, a somewhat higher quality reproduction could be made from "photographs" if essential to the understanding of the dissertation. Silver prints of "photographs" may be ordered at additional charge by writing the Order Department, giving the catalog number, title, author and specific pages you wish reproduced.

5. PLEASE NOTE: Some pages may have indistinct print. Filmed as received.

University Microfilms International
300 North Zeeb Road
Ann Arbor, Michigan 48106 USA
St. John's Road, Tyler's Green
High Wycombe, Bucks, England HP10 8HR

The synthesis and characterization of reduced scandium halides containing one- and two-dimensional metal bonded arrays

by

Kenneth Reinhard Poeppelmeier

A Dissertation Submitted to the
Graduate Faculty in Partial Fulfillment of
The Requirements for the Degree of
DOCTOR OF PHILOSOPHY

Department: Chemistry
Major: Inorganic Chemistry

Approved:

Signature was redacted for privacy.

In Charge of Major Work

Signature was redacted for privacy.

For the Major Department

Signature was redacted for privacy.

For the Graduate College

Iowa State University
Ames, Iowa

1978

TABLE OF CONTENTS

LIST OF TABLES

LIST OF FIGURES

INTRODUCTION

The element scandium with atomic number twenty-one has the unique position in the periodic table as the first member of the d-block transition metals. Accordingly, the chemical and physical properties of scandium compounds could be expected to reflect this circumstance. However, scandium seldom, if ever, has been considered a transition element since inorganic compounds containing scandium have traditionally been scandium(III) compounds. Scandium's inability to retain valence electrons and exist in any oxidation state less than three is supported by the non-existence of a simple dihalide or monoxide unlike other first row transition metals. In fact the hypothetical compound $ScCl_2$ (solid) has been used to illustrate (1) the importance of considering the stability of a compound in relation to any reaction to which it is unstable. Based on a Born-Haber cycle calculation, which requires as one term an estimation of a lattice energy for the hypothetical solid, the standard free energy of formation at 25°C for $ScCl_2$ (solid) is certainly a negative number. The instability has been related to the decomposition reaction, or disproportionation, which also has a negative free energy

$$3\ ScCl_2(s) \rightarrow Sc(s) + 2\ ScCl_3(s)$$

change at this temperature. The ability to properly model the lattice energy of the hypothetical solid phase is the important limitation with this calculation. In particular the ionic model cannot account for or include metal-metal interactions which result in nonperiodic coulomb forces and metal-metal bonding. As a result, a solid dichloride phase of the layered CdI_2 or $CdCl_2$-type, common to the majority of transition metal dihalides may indeed not be energetically favored but this result does not rule out the possibility of alternative favorable structure types.

Transition metal compounds present a major problem in discussing the role of the metal d electrons in the solid state. The possibilities range from completely localized d states, through incipient cooperative behavior, to complete delocalization. The situation can be further complicated as to whether band formation occurs continuously as conditions are modified, for instance, d-d overlap as a function of pressure, or whether band formation occurs discontinuously. Whereas d band formation has been extensively studied (2) in layered-type transition metal dichalcides and is clearly well-advanced, the opposite situation with transition metal dihalides exists. Compounds of transition metals in what are formally low oxidation states, especially halides, would be expected to have unusual and interesting optical, electrical and structural

properties. Born-Haber calculations notwithstanding the binary transition metal-halide systems Sc-ScX_3; X = Cl,Br,I, offer some unique advantages for study in the areas of synthesis, structure and bonding, and physical properties of low oxidation state materials.

As recently as four years ago, the only rare-earth metal halide compounds with a nonmetal to metal ratio (X:M) less than two were the unusual gadolinium sesquihalide phase $GdCl_{1.5}$ (3), the structure of which had been determined (4), and the stoichiometrically similar phases (5) Sc_2Br_3 and Sc_2Cl_3. The latter two compositions were known not to be isostructural with the gadolinium compound based on x-ray powder data. The early goal of this research project was to grow single crystals of Sc_2Cl_3 in order to structurally characterize this interesting solid. Over the course of a year and a half, and after many attempts to grow single crystals of Sc_2Cl_3, a more complex chemistry between these two elements than anyone else had observed (5,6,7) or expected (8) slowly became apparent.

The newly prepared "$ScCl_x$" phases were initially characterized by x-ray powder diffraction and wet analytical or microprobe analyses. They were shown to have nonintegral empirical compositions such as $ScCl_{1.58(4)}$ and $ScCl_{1.43(3)}$ and in another case the more plausible 1:1 stoichiometry $ScCl_{1.04(3)}$. No one physical method is ideal for the

complete investigation into the nature of these materials. However as the primary investigative tool single crystal x-ray diffraction provides, in most cases, not only a definitive analytical result but also structural data. In addition to single crystal and powder x-ray diffraction, other methods used to characterize these materials have been differential thermal analysis (DTA), magnetic susceptibility, electron paramagnetic resonance (EPR), and x-ray and ultra-violet photoelectron spectroscopy (XPS and UPS).

Compounds of the type $ScCl_x$ ($1.0 \leq x \leq 2.0$) fall into the little understood class of solid materials loosely termed metal-rich compounds. Metal-rich compounds have been defined (9,10) as nonmolecular solids in which part of the metal valence is involved in metal-metal bonding. A few examples covering a wide range of metals and nonmetals are Cs_7O, Ag_2F, Ta_6S, Nb_7P_4, and ZrCl. The metal array found in these and other metal-rich compounds can often be recognized as a fragment of the parent metal and may have quasi one- or two-dimensional character. Such complex yet simple binary compounds offer intriguing possibilities in the areas of conduction, superconductivity, and catalysis.

A natural extension from the binary Sc-Cl system would be to a ternary system capable of stabilizing scandium in

a lower oxidation state. In what has become a classic review (11) on metal-metal interactions in solids, Schäfer and von Schnering emphasized the synergetic relationship between interacting metal sites and the structure of the solid itself. Such a relationship exists between compounds of the general formulae $A_3B_2X_9$ and ABX_3. In these solids the A cation is generally an alkali metal cation or an alkaline earth metal cation, depending on the charge of the anion X. The A cations along with the X anions form nearly close-packed layers with the composition A+3X. The stacking of these layers leads to many possible polytypes (12). Between the A+3X layers the octahedral interstices with only X anions at the vertices are occupied by B cations. For example, in the cubic stacking (ABC•••) sequence the octahedra share corners whereas if the sequence is hexagonal (AB•••) face sharing results. The latter sequence generates quasi one-dimensional chains of metal atoms which can result in cation-cation bonding (13) when d valence electrons are present. Alternatively anti- or ferromagnetic materials are commonplace when strong metal-metal bonds are not formed (14). From a consideration of ionic radii, A was chosen to be Cs and the composition range was limited to $Cs_3Sc_{2+x}Cl_3$; $0 \leq x \leq 1.0$. The two end members of this range, $x = 0$ and $x = 1.0$, are formally scandium(III) and scandium(II) compounds, respectively. The latter compound

is formally isoelectronic and, as it turns out, isostructural with the one-dimensional conductor $BaVS_3$ (15).

The Result section has been divided into two parts covering the binary and ternary systems, Part I and Part II, respectively. Part I follows the chronological publication of three articles. These have been included essentially as reprints although they have been changed to the degree necessary to conform to the required thesis style. The first article deals with scandium monochloride, ScCl; a phase very much like the zirconium monohalides, ZrX; X=Cl,Br. The structure type common to this unusual group of MX compounds consists of essentially close-packed layers sequenced $(-XMMX-)_n$. The second paper describes the phase first identified as $ScCl_{1.43}$ and reveals the composition to be Sc_7Cl_{10}. The third article describes Sc_5Cl_8, a composition originally identified as $ScCl_{1.58(4)}$. Both contain six atom metal clusters condensed to form infinite metal chain structures. Unpublished results on Sc_7Cl_{12} and other $ScCl_x$ phases complete Part I of the Result section. Unfortunately, some overlap exists between the thesis and the articles and among the articles themselves but hopefully this is outweighed by a steadily increasing understanding of the synthetic problems, structural relationships, and physical properties of the $ScCl_x$ phases as it actually developed. In Part II the ternary system, $Cs_3Sc_{2+x}Cl_9$; $0.0 \leq x \leq 1.0$,

is presented as a continuous process of reduction from the insulating scandium(III) state to the metallic scandium(II) state.

The reader should find the results not so much out of the ordinary or contradictory of long held ideas, but instead a direct and simple extension of the trends along which the periodic table is organized. From this perspective the chemistry of scandium rejoins that of the rest of the d-block metals. The result will be a logical and satisfying view into how orbital-rich but electron-poor elements early in the d-series blend the traditional concepts of structure and bonding into the unique circumstances particular to their position in the periodic table.

EXPERIMENTATION

Starting Materials

Scandium metal

Fischer and co-workers (16) in the mid-1930's prepared the first pure (~95%) scandium by electrolytic reduction of $ScCl_3$ dissolved in a LiCl-KCl eutectic. Today, the metal available from the Ames Laboratory is prepared by metallothermic reduction of ScF_3 by triply distilled calcium metal. The purity is of the order >99.9 at. % with respect to all impurities. Depending upon the batch, some variability is unavoidable. The metal used in the synthesis of the trichloride and as the reductant in the early synthetic work had major impurity levels (atomic ppm) of: 70 Fe, 250 Ta, <30 each individual rare earths, <800 each C, O, F (99.996 at. %). When physical characterization methods such as magnetic susceptibility or electron paramagnetic resonance results could possibly be affected by contamination with iron or rare-earth elements, the highest purity metal available was used. Typically, again in atomic ppm, the analysis was: H, 585; C, 146; O, 266; N, 13; F, 164; W, 20; Ta, 17; Cu, 9; Fe, 50; individual rare-earth elements and all others, <1.

Scandium trichloride

Anhydrous scandium trichloride was prepared by the reaction of scandium turnings with electronic grade HCl gas in a flow system of the design used by Löchner (17). The crude scandium trichloride was separated from any small pieces of unreacted metal and carbon and oxygen impurities by sublimation at 650°C under diffusion pumped vacuum ($\sim 10^{-5}$ to 10^{-6} Torr). A two compartment tantalum apparatus (17) was used to sublime the scandium trihalide. The sublimation step is very important in the control of oxy-halide contamination in subsequent reactions. Both oxygen, by the simple metathesis reaction between Sc_2O_3 and $ScCl_3$, and water, through the decomposition of hydrated scandium trichloride, give rise to ScOCl at elevated temperatures.

Oxy-halide contamination can be greatly reduced or completely eliminated by obtaining the sublimed trichloride in crystalline form. In general, powders are extremely hard to handle under working situations and can be highly hygroscopic under ordinary dry box conditions (10 ppm H_2O). The low surface area and the more nearly perfect nature of the surface of crystalline material effectively controls both problems. To obtain crystalline scandium trichloride a steep thermal gradient between the sample compartment and the region where the sublimed material condenses must be maintained. This can be accomplished quite simply by

taking advantage of the natural plateau in the temperature profile near the middle region of a tube furnace and the sharp decrease near the ends of the furnace. Then simply by positioning the tantalum sublimation apparatus in the gradient the crude material can be maintained at 650°C and the first few centimeters of the condenser near 400°C. Once the first solid material coats the interior of the tantalum wall, heat will be transferred poorly through the insulating layer of trichloride and the gradient will become steeper. This can result in a plug of trichloride in the condenser. If a plug is observed a slight repositioning of the tube furnace will remedy the situation. The rate of sublimation is the order of two to three grams per hour.

The sublimation apparatus should be taken apart in a dry box. When the trichloride is removed from the condenser the product should be broken up as little as possible and stored in two to three gram amounts in sealed Pyrex containers. In this way the entire supply is not constantly exposed to working dry box conditions everytime some is used. In addition, accidental loss of the entire supply is avoided. By contrast when "anhydrous" scandium trichloride was stored in a container (jar) in a dry box for long periods of time (months), contamination by ScOCl was a persistent problem for me as it has been for others (5).

Cesium chloride

Baker grade 99.9% cesium chloride was dried by vacuum melting and stored under an inert atmosphere.

Analysis

Reduced $ScCl_x$ phases

When available, 100 mg samples were dissolved in 25-50 ml water in 100 ml volumetric flasks. Rapid mixing was necessary to avoid ignition of the rapidly evolving hydrogen and oxidation of the remaining material to an insoluble form. Determination of scandium (18) was by titration with EDTA using xylenol orange as the indicator in an acetic acid-sodium acetate buffer (pH 4.0). The chloride was determined gravimetrically by precipitation with silver nitrate solution, drying, and weighing as silver chloride.

All microprobe analyses were performed by Fran Laabs in this Laboratory using an Applied Research Laboratories Model EMX electron microprobe. For elements lighter than sodium, a RAP-Johonanson-type four inch spectrometer was used. This method of analysis is ideal for small amounts of sample or individual crystals. Sample transfer was accomplished with a minimum of problems by attaching a plastic glove bag flushed by dry nitrogen to the entry port of the spectrometer.

Ultimately, single crystal x-ray crystallography was used as an analytical method. The empirical compositions determined by the previous two techniques were initially viewed with skepticism or disbelief. The results will show that in all cases the x-ray structures have confirmed the original analytical results.

Synthesis

Since a range of conditions and techniques have been used in the preparation of the reduced scandium chlorides and ternary compounds, each preparation will be dealt with separately in the Results section. This is a reflection of the initial semi-empirical nature of the preparations within only the broadest of thermodynamic guidelines. The variety of techniques will illustrate a growing understanding of how best to prepare these unusual solid state compounds.

All reactions have been carried out in sealed tantalum containers since scandium trichloride readily attacks Pyrex or fused silica under the conditions used. The reaction tubes were cleaned in either tantalum cleaning solution or by induction heating under high vacuum (10^{-9} Torr). The containers were made from 9 mm o.d. tubing and generally were four centimeters long for isothermal equilibrations and as long as necessary for gradient

experiments. One end of the tube was crimped and welded. Next, the sample was loaded and the second end crimped tightly in a dry box. The tube was then transferred quickly (∿ five seconds) through the air and into a heliarc welder and sealed. Since tantalum metal is rapidly oxidized upon heating in air, all containers must be sealed in evacuated fused silica jackets for protection. Temperature was monitored by a sheathed thermocouple attached to the outside of the glass jacket.

Physical Measurements

X-ray methods

A variety of x-ray cameras have been used depending on what information was desired. Routine phase identification was done with a Phillips Debye-Scherrer camera of standard diameter 114.59 mm and nickel-filtered copper K_α radiation. When more precision was needed, excellent quality films (±0.02 mm, ±0.005°) were obtained on the evacuable Model XDC-700 Guinier camera, IRDAB, Stockholm. This camera uses a quartz monochromator to provide a nearly clean copper K_{α_1} incident beam. Weissenberg cameras, Charles Supper Co., were routinely used in evaluation of single crystals and preliminary determination of unit cell constants (19). Single crystal x-ray diffraction data were collected on the Ames Laboratory four-circle diffractometer interfaced with

a PDP-15 computer. Mo K_α radiation monochromatized with a graphite single crystal (λ = 0.70954 Å) was used in all single crystal studies.

Differential thermal analysis

Löchner (17) has described the evacuable apparatus used to maintain isothermal conditions and record differential thermal effects. Temperatures were uniformly regulated with a Thermac-Series 6000 controller (Research, Inc.). The temperature of the sample and the temperature difference between the sample and alumina reference were recorded on an Electronik 194 strip recorder and measured with a Rubicon (Minneapolis-Honeywell) potentiometer. Sodium chloride was used for calibration (m.p. 801°C).

Less than one gram amounts of material were customarily available necessitating small tantalum sample containers. They were made from 9 mm o.d. tubing and were 1.25 cm in length. The entry port and thermocouple well were made from 4 mm o.d. tubing. The entire assemblage was electron-beam welded.

Thermal analysis was used to identify transitions only on prepared and well-characterized samples. If compositions more metal-rich than the eutectic are prepared simply by heating salt and metal together for several hours in the thermal analysis apparatus a serious error is made if equilibrium is assumed to be reached under these conditions.

This has led to no less than three incorrect phase diagrams (5,6,7) reported in the literature on the Sc-$ScCl_3$ binary system. The results presented herein will demonstrate conclusively the important role kinetics play in reaction between scandium metal and scandium trichloride. In light of the relatively large initial solubility of scandium in molten trichloride, 18.5 mole % at eutectic composition (5), this is especially noteworthy.

Magnetic susceptibility

Magnetic susceptibility measurements were made with the Faraday balance constructed by Converse (20) on the phase Sc_7Cl_{10}. These measurements were undertaken on this particular composition in order to substantiate the paramagnetism indicated by electron paramagnetic resonance results. Susceptibility measurements on the reduced scandium halides $ScBr_{1.5}$ (5) and $ScI_{2.15}$ (21) have revealed complex magnetic behavior.

Electron paramagnetic resonance

All EPR spectra were obtained on a Varian Model E-3 spectrometer with a frequency range of 8.8-9.6 GHz and a dial selected magnetic field. Room temperature scans over the range 3400 ± 1000 G have become a routine check for paramagnetic behavior.

Electron spectroscopy for chemical analysis (ESCA)

The x-ray photoelectron spectra of scandium metal and scandium trichloride were obtained using a McPherson ESCA 36 in cooperation with Dr. R. J. Thorn and J. R. McCreary, Argonne National Laboratory. The experimental conditions were: power, 15 kV - 20 ma; source, standard Mg K_α radiation without monochromatization; pressure, 1 x 10^{-7} Torr in the analyzer and 1 x 10^{-9} Torr in the sample chamber. Both were sublimed onto sintered stainless steel targets in the high vacuum chamber in order to obtain spectra free of surface contamination effects. Unfortunately, the reduced compounds cannot be treated in a similar fashion since all vaporize by an incongruent mechanism. Even with the benefit of an attached dry box (6 ppm H_2O) all reduced phases had some surface contamination.

Surface contamination has been largely overcome by improvements in sample handling and dry box conditions. All spectra of reduced compounds have been run on the Ames Laboratory AEI ES 200B ESCA instrument with the assistance of Jim Anderegg. An attached dry box (<1 ppm H_2O, O_2) allowed for easy sample mounting and entry into the spectrometer with a minimum of surface contamination. The samples were mounted on indium, a substrate which conveniently provides an essentially structureless background in the valence band (VB) region. Indium also does not

interfere with any core levels of Sc, Cl or Cs. Unless only core level studies were planned, the sample completely covered the indium substrate so none was visible to x-rays. The pressure in the high vacuum chamber of the Ames Laboratory Spectrometer was maintained at 10^{-9} Torr. The x-ray source, with and without monochromatization, was Al K_{α}. The ultra-violet (UV) source was the He(I) line at 21.2 eV.

The fundamental calibration problem (22) involved with the photoelectron measurement will be described in the result section since, in practice, there is no general technique for all types of samples; conductors, semiconductors and nonconductors. Each phase and composition, especially in the ternary $Cs_3Sc_{2+x}Cl_9$ system, requires an independent evaluation.

RESULTS: PART I. THE BINARY Sc-$ScCl_3$ SYSTEM

Metal-Metal Bonding in Reduced Scandium Halides. The Synthesis and Crystal Structure of Scandium Monochloride (23)[1]

Introduction

Since 1963, a series of publications reporting and disputing the existence of solid, lower chlorides of scandium has appeared. Polyachenok and Novikov (6) first reported a relatively large amount of reaction of the metal with the liquid $ScCl_3$ and the formation of the solid phases $ScCl_{2.67}$ and $ScCl_2$, although the means whereby these compositions were established was not given. Corbett and Ramsey (7) disputed these results based on thermal analysis data, suggesting the earlier results had been perturbed by reaction with the silica container. In a subsequent publication McCollum and co-workers (5) reported on the preparation of solid $ScCl_{1.5}$, scandium sesquichloride, as well as $ScBr_{1.5}$, both of which could be prepared at elevated temperatures when proper attention was paid to avoiding blockage of the metal surface by product. Subsequent efforts

---

[1]Published: K. R. Poeppelmeier and J. D. Corbett, Inorg. Chem., 16, 294 (1977).

to prepare single crystals of $ScCl_{1.5}$ have revealed a complex and unpredicted (8) chemistry in the Sc-$ScCl_3$ system. This paper notes some of the chemistry in the region $2.0 \geq Cl:Sc \geq 1.0$ and reports on the single crystal structure of the stoichiometric monochloride, ScCl.

Experimental section

Materials The metal used had been distilled in tantalum and had typical major impurity levels (atomic ppm) of 70 Fe, 250 Ta, <30 individual rare earths, and <800 each C, O, F. Thin foil strips for reduction of $ScCl_3$ were made from cold rolled scandium sheet which was cut into pieces (4 cm x 1 cm x .12 cm), annealed at 750°C under vacuum (10^{-6} Torr), and again cold rolled to a length of 13-14 cm and a thickness of 0.04 cm. The strips were electropolished to remove any hydrocarbon greases and other surface impurities picked up during the cold rolling process (24) and then washed with copious amounts of acetone, dried, and stored under vacuum. As an alternate reductant scandium powder (<100 mesh) was made by thermal decomposition of the dihydride. This brittle material was ground to less than 100 mesh, spread out so as to barely cover the bottom of a molybdenum boat, and heated at 750°C under dynamic vacuum until the system was below discharge (<10^{-4} Torr). The product metal was found to contain H:Sc = 0.091 by vacuum extraction, a value which corresponds to the expected value

based on the equilibrium data available for the Sc-H system (25).

The trihalide was prepared by reaction of the metal with high purity hydrogen chloride and was vacuum sublimed in a tantalum jacket as before (3). The product after sublimation gave Cl:Sc ratios of 2.99 ± .01 with typical recoveries >99%.

To avoid contamination all reactants and reduced products were stored and manipulated only with standard vacuum-line and dry box techniques. All reactions were carried out in induction cleaned (1800°C) tantalum containers which were in turn welded and jacketed in fused silica tubes under vacuum.

Analyses All wet chemical analyses were done as before (5) while the microprobe analyses were performed in this Laboratory using an Applied Research Laboratories Model EMX Electron Microprobe.

Syntheses The initial preparation of the ScCl phase was through the reduction of $ScCl_{1.5}$ with metal foil. Preparation of $ScCl_{1.5}$ as before (5) seemingly leaves a blocked metal surface and stops the reduction process since evidence for a more reduced phase on the foil surface was never found, even with careful and repeated scrutiny. However, under more reducing conditions a number of new phases can be detected by reequilibrating fresh scandium

strips with $ScCl_{1.5}$ at temperatures greater than the peritectic melting point of $ScCl_{1.5}$ (877°C). Several different phases are obtained depending upon various factors: the amount of $ScCl_{1.5}$ used, surface area of the scandium metal, temperature, and especially the length of time the system is allowed to "equilibrate". However, this procedure only gives amounts sufficient for identification by x-ray powder diffraction patterns (Debye-Scherrer) and for microprobe analysis. The latter consistently detected only Sc and Cl in these compounds, but unfortunately contamination by elements lighter than Na, especially C, N, O and F, cannot be ruled out. The interaction of the electron beam with these compounds to change their composition through loss of $ScCl_3$ has prevented reproducible reliable quantitative results from being obtained by the microprobe method (see note (26) for correction). Of particular interest was the powder pattern of one of these new phases which resembled those of ZrCl (single crystal data (27)) and ZrBr (powder data (28)) and which led to this effort to determine whether a monochloride of scandium existed.

In order to overcome the problem of the severely limited yields of these reduced compounds powdered metal and $ScCl_3$ were reacted directly. Thus, ca. 0.25 g of Sc and 0.4 g of $ScCl_3$ were added to a 4 cm long, 9 mm o.d. tantalum tube, and this was welded, sealed in a fused silica

jacket, and heated at 800°C for several weeks. All reactants were completely consumed in the reaction and the product was a mass of black crystalline material analytically determined to be Cl:Sc = 1.04 ± 0.03 and by x-ray powder diffraction to be the scandium monochloride phase. Single crystals were prepared in a similar manner by heating a mixture of Sc powder and $ScCl_3$ (Cl:Sc = 1.0) at 960°C for two months. The temperature was monitored by a thermocouple attached to the outside of the glass jacket. The reaction tube was cooled at a rate of 1.25°/h to 900°C and was then air-quenched. The crystals were examined in a specially designed inert-atmosphere box constructed with a nearly horizontal window to facilitate the use of a stereozoom microscope (27). The crystals were found embedded in a gray-black mass, identified as $ScCl_3$ by x-ray powder diffraction, which had been molten at temperature. About 80 wt % was the shiny gray-black and easily cleaved ScCl. Two other phases of unknown composition were found in small quantities in separate parts of the tantalum tube implying, of course, that this had not been an isothermal equilibrium experiment at 960°C.

Data collection A single crystal of ScCl of extreme dimensions 0.2 x 0.15 x 0.02 mm was used for x-ray data collection at ambient temperature on an automated four-circle diffractometer designed and built in the Ames

Laboratory (29). The data set was collected on the basis of a hexagonal unit cell using Mo K_α radiation (λ = 0.70954Å) monochromatized with a graphite single crystal. All data within a sphere defined by $2\theta < 50°$ were collected in the HKL and $H\bar{K}L$ octants using an ω-scan mode. Peak heights of three standard reflections which were remeasured every 75 reflections did not show any significant change over the data collection period. A total of 227 reflections were observed from a total of 688 reflections checked. Final trigonal cell parameters and their estimated standard deviations were obtained from the data crystal utilizing a least-squares refinement with $\pm 2\theta$ values from 13 independent reflections randomly distributed in reciprocal space for which $2\theta > 25°$. The lattice constants were $\underline{a} = \underline{b} = 3.473(2)$Å and $\underline{c} = 26.71(4)$Å. These lattice parameters match those calculated from preliminary oscillation and Weissenberg films. In general the films characteristically exhibited axial streaking and broad diffraction maxima. The data crystal, however, uncharacteristically gave relatively minor axial streaking but still slightly broadened, coherent diffraction maxima, necessitating the ω-scan.

Structure determination The observed intensities were corrected for Lorentz-polarization effects and the standard deviations calculated as previously described (30)

to give reflections with $I > 3\sigma(I)$. An absorption correction was not considered necessary ($\mu = 48$ cm^{-1}). Examination of the data set revealed the systematic extinction condition $-h + k + \ell \neq 3n$ which fixes the space group as a trigonal equivalent of a rhombohedral space group. Belov (31) has shown that close-packed structures can have only two R space group symmetries, $R\bar{3}m$ and R3m, and the former, with Z = 6 and atoms in 6c special positions, was selected in view of the obvious similarity in unit cell dimensions to those of ZrCl (27) and the earlier observation from powder patterns that ScCl was similar to ZrBr and ZrCl. Appropriate averaging yielded 79 independent reflections for the final data set.

The obvious trial structure based on the ZrCl fractional coordinates resulted in R = 0.80 but switching the metal layers ($z' = 0.33 - z$) with respect to packing so that the halogen atoms have prismatic coordination as in ZrBr (28) gave $R = \Sigma||F_o| - |F_c||/\Sigma|F_o| = 0.174$. Conversion to anisotropic thermal parameters gave convergence at R = .088 and $R_w = .111$ where $R_w = [(\Sigma\omega(|F_o| - |F_c|)^2/\Sigma\omega|F_o|^2]^{1/2}$ and $\omega = \sigma_F^{-2}$. The stronger reflections were observed to have larger values of $\omega||F_o| - |F_c||$ so the data set was reweighted in ten overlapping groups sorted according to F_o so that $\omega\Delta^2$ was constant, giving final converged values of R = .088 and $R_w = .101$. Variation of occupation

parameters at this point for both scandium and chlorine positions gave converged values of 1.000(3), indicating no significant deviation from the simple stoichiometry. A final difference Fourier synthesis map was flat to $\leq$0.5 electrons/Å^3 in all regions between atoms and $\leq$2 electrons/Å^3 on atom sites.

Sources of atomic scattering factors for neutral atoms (which included corrections for both real and imaginary parts of anomalous dispersion) and of the computing programs used were referenced before (27,32).

Results: description and discussion of the structure

The final parameters together with important distances and angles are given in Table I, while the (110) projection of the structure in shown in Figure 1. Observed and calculated structure factors are available in Appendix A.

The four layer sheet structure found for ScCl is polytypic with ZrCl (allowing for the change in metal atom) and isomorphous with ZrBr. The basic unit is a sheet composed of four close-packed and tightly bound layers Cl--Sc-Sc-Cl with the usual description of the layering geometry ···|abca|cabc|bcab|··· or alternately, in terms of layer sheets, ··ACB·· where the capital letters follow the relative orientation of the outer halide layers of each sheet. The result is antiprismatic coordination of the metal atoms and prismatic coordination of the halogen atoms.

Table I. Final atom parameters, interatomic distances and angles in ScCl

Cell: Trigonal, Space Group $R\bar{3}m$, a = 3.473(2), c = 26.71(4)Å, Z = 6

R = 0.088, R_w = 0.101, 79 reflections

Atom Parameters:	x	y	z	$B^a_{11}=B_{22}$	B_{33}	$B_{12}=\frac{1}{2}B_{11}$	$B_{13}=-B_{23}$
Sc	0.0	0.0	0.2137(1)	0.9(1)	3.8(2)	0.45(5)	0.0
Cl	0.0	0.0	0.3914(1)	1.0(1)	3.8(2)	0.50(5)	0.0

Distances (Å):

Intralayer		Interlayer	
Sc-Sc	3.473(2)	Sc-Sc	3.216(6)
Cl-Cl	3.473(2)	Cl-Cl	3.695(8)
		Sc-Cl	2.591(4)

Interlayer Angles (deg.):

Angles defining the anti-prismatic coordination of Sc		Angles defining the prismatic coordination of Cl	
Sc-Sc-Sc	65.3(1)	Cl-Cl-Cl	56.1(1)
Cl-Sc-Sc	104.7(1)	Cl-Cl-Sc	96.4(1)
Cl-Sc-Cl	84.1(2)	Sc-Cl-Sc	84.1(2)

[a]The general thermal parameter expression used is $\exp-[\frac{1}{4}(B_{11}h^2a^{*2} + B_{22}k^2b^{*2} + B_{33}\ell^2c^{*2} + 2B_{12}hka^*b^* + 2B_{13}h\ell a^*c^* + 2B_{23}k\ell b^*c^*)]$.

Figure 1. The $(11\bar{2}0)$ projections of the structures of ScCl (left) and ZrCl (right). The lower case letters refer to relative positions of close-packed layers along [001]; the capital lettering, to packing of four layer sheets. Arbitrary isotropic temperature factors were used.

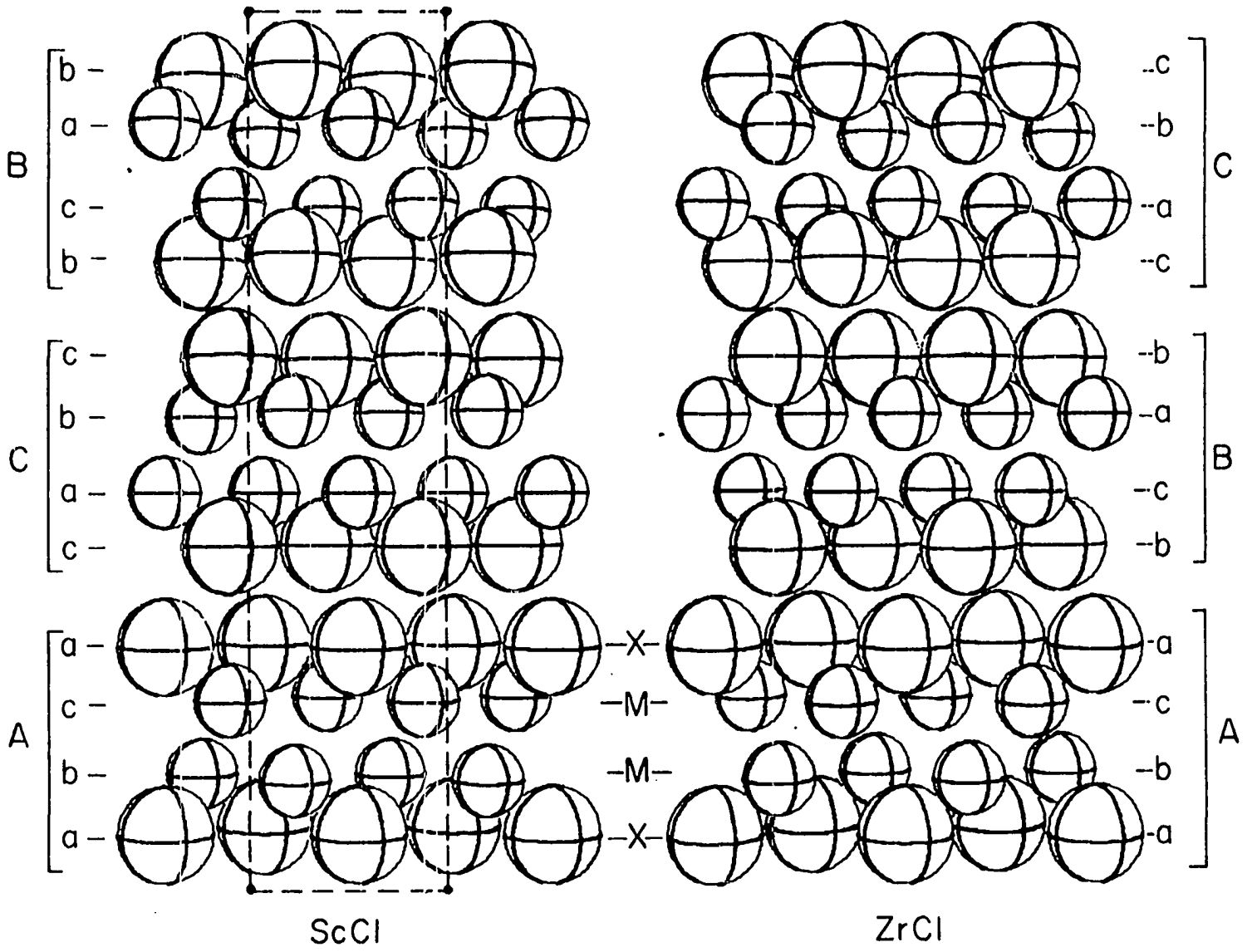
B
b –
a –
c –
b –
C
c –
b –
a –
c –
A
a –
c –
b –
a –
–X–
–M–
–M–
–X–
--c
--b
--a
--c
C
--b
--a
--c
--b
B
-a
--c
--b
-a
A
ScCl
ZrCl

The ScCl arrangement is contrasted in Figure 1 with that of ZrCl (••ABC•• packing) where there is antiprismatic coordination of halogen.

Each scandium atom in ScCl has three metal neighbors in the next layer at 3.22Å, six metal neighbors in the same layer at 3.47Å and three chlorine neighbors in the opposite layer at 2.59Å (Table I). The two different short metal-metal distances, 3.22 and 3.47Å, indicate strong metal-metal bonding between the metal layers and a somewhat lower bond order for the metal-metal bonds between atoms in a layer, the latter separation of course being dictated by the Cl-Cl period in the planar sheets. In hcp scandium metal the metal-metal distances are 3.26 and 3.31Å for inter- and intralayer distances, respectively, the difference arising because of a small distortion from the ideal c/a ratio for close-packed structures (33). The distortion in ScCl is even greater but chemically reasonable since each metal layer is now adjacent to a chlorine layer. The 8% difference in scandium-scandium distances and corresponding angular distortions indicates the degree of approximation necessary in a description of the double metal layer structure in terms of metal octahedra (trigonal antiprisms) each of which shares six edges.

The scandium-chlorine distance observed, 2.59Å, compares closely with 2.58Å in $ScCl_3$ (34) even though the

latter involves octahedral coordination about scandium(III). Intralayer Cl-Cl distances are 3.47Å while interlayer Cl-Cl distances are 3.70Å, very appropriate distances between chlorine atoms bound to common scandium atoms and for weak van der Waals interactions between halogen sheets, respectively. The weak interlayer binding in this and related compounds is of course responsible for their graphitic properties and easy physical damage. The larger thermal parameters exhibited normal to the layers (Table I) parallel very closely the behavior found for ZrCl (27) and are taken to be a manifestation of crystal imperfection in the weakly bound direction. An error resulting from the lack of an absorption correction is considered unlikely here as (a) this correction was carried out for ZrCl with the same results, and (b) the ellipsoid elongation is in the direction of the thin dimension of the crystal platelet, contrary to the usual evidence for an absorption error.

A remarkable feature of the ScCl structure is that it is polytypic with ZrCl (and isostructural with ZrBr) even though there are formally only <u>two</u> rather than <u>three</u> electrons per metal involved in binding the double-metal sheets. The effects of this reduction are discernible particularly in the interlayer metal-metal separation (Table II), even when the difference in core radii is allowed for; on the other hand, intralayer metal bonding

Table II. Some distance comparisons for the polytypic ScCl and ZrCl and the metals (Å)

Type		Distances, Å[a]			
		ScCl	ZrCl[b]	Sc	Zr[c]
M-M	interlayer	3.22	3.09	3.26	3.18
	intralayer	3.47	3.42	3.31	3.23
M-Cl		2.59	2.63		
Cl-Cl	interlayer	3.70	3.61		
	intralayer	3.47	3.42		

[a]Estimated standard deviations for all $\leq$ 0.01Å.

[b]Reference 27.

[c]Reference 33.

changes are largely obscured by the nearly fixed period of the chloride layers. Some charge redistribution in the metal-metal bonding is probable on the transition from ZrCl to ScCl, in part because of the change in second nearest neighbors. Such a change seems implicit in the XP spectra of ZrCl and ZrBr (28) where only the packing is changed. The apparent effects of second nearest neighbors is also evident in the physical properties; ScCl is much less graphitic, and is more brittle and easy to cleave than ZrCl, while its sensitivity to oxygen and moisture is appreciably greater.

The two types of packing observed in these zirconium and scandium monohalides may arise from a competition between electrostatic second nearest neighbor effects in the case of ZrBr and ScCl vs. a predominance of polarizability of the chlorine layer by the adjacent metal layer in ZrCl which provides an alternate second nearest neighbor potential. The antiprismatic chlorine coordination in ZrCl places each chlorine atom 180° in the $[1\bar{1}6]$ direction from a second nearest neighbor metal atom so that polarization effects must predominate. However, in ZrBr and ScCl, both with somewhat greater a lattice parameters, the prismatic halogen coordination positions each halogen atom directly over a second nearest neighbor metal atom in the neighboring sheet along the [001] direction and provides a direct

electrostatic interaction with the positive ion cores of the metal atoms.

Although the Sc-$ScCl_3$ phase study is not complete in the region 2.0 $\geq$ Cl:Sc $\geq$ 1.0 crystal structure determinations are presently underway on two more of the plethora of phases that exist. Evidence of strong metal-metal interactions in isolated groups and extended chains of scandium in these compounds is already in hand. This system seems to provide the ideal opportunity to study the correlation between structure and degree of reduction, in other words, localized (cluster) vs. extended electron delocalization. Two implications of these results are immediately apparent. First, the results for many of the lanthanide-halogen systems merit a closer inspection and reappraisal. Perhaps prior expectations have placed too much emphasis on the divalent state. Born-Haber cycles, which do not (or cannot) allow for stabilization energies resulting from metal-metal interactions, do not provide useful guidelines. A hint of a more reduced chemistry has existed for several years in the $GdCl_3$-Gd system where the very incongruently melting $GdCl_{1.5}$ forms (3); this is a compound containing elongated metal octahedra sharing edges to form chains (4). The present results together with the checkered history of published results of the Sc-$ScCl_3$ system (cf. Introduction) should give experimentalists due caution regarding kinetic

barriers in seemingly tractable systems even at as high as 877°C, the temperature where decomposition of $ScCl_{1.5}$ seemingly first allows access to so much new chemistry. We have found evidence for a similar chemistry (Appendix B) in the Y-YCl_3 and La-$LaCl_3$ systems where previous work did not provide any direct evidence for reduced phases (35,36) and a preliminary note on the formation of GdCl and TbCl, isostructural with ZrCl, has just been published by Simon et al. (37).

The second more speculative implication may involve the 4d and 5d metal-halogen systems for niobium and tantalum. Their cluster chemistry is well-known but perhaps a kinetic, not a thermodynamic, barrier there limits the formation of extended metal-metal bonded structures which would be similar to those in ScCl and ZrCl. It remains to be seen whether these will be manifest as ZrX-type structures with four electrons per atom in the band, $M^{V}X_2$ structures which are isoelectronic in the metal-metal bonding of ZrX, or perhaps most likely, in intermediate states with extended metal-metal bonding in more nearly one dimensional aggregates (ribbons, strings, dimers, etc.), as these can better accommodate the greater number of anions.

The once totally uninteresting chemistry of the Sc-$ScCl_3$ system now seems just the opposite, rich and full of fascinating synthetic, structural, and physical problems for investigation.

Metal-Metal Bonding in Reduced Scandium Halides. The Synthesis and Characterization of Heptascandium Decachloride (Sc_7Cl_{10}). A Novel Metal Chain Structure (23)[1]

Introduction

Heptascandium decachloride, Sc_7Cl_{10}, is the second in a plethora of reduced scandium chloride phases to be isolated and characterized. The checkered history and inherent problems with attaining equilibrium in the Sc-$ScCl_3$ system have been discussed in an earlier publication (38). Briefly, a highly fibrous Sc_2Cl_3 ("mouse fur") can be obtained in small amounts when metal sheet is reacted at 700-800°C with liquid or, better, gaseous $ScCl_3$ in sealed tantalum tubing (5). The combination of sesquichloride on metal exhibits a remarkable metastability up to the former's decomposition (melting) point of 877°C in that their further reaction below this temperature over a period of several weeks is extremely limited and does not yield recognizable amounts of any intermediate phase. Notwithstanding, at least five phases can be recognized in x-ray powder diffraction patterns of products obtained from the same Sc_2Cl_3-Sc reaction above this temperature, although the

---

[1]Published: K. R. Poeppelmeier and J. D. Corbett, Inorg. Chem., 16, 1107 (1977).

formation reactions are still very slow, presumably because of kinetic problems associated with the generation of extended metal-metal bonded networks. The problem of limited yield is reduced somewhat through the use of powdered Sc metal as the reductant in place of foil or turnings. The first phase identified in this study was ScCl, a double metal-double halogen sheet structure which is isostructural with ZrBr and closely related to ZrCl (27,38). The present paper reports the preparation, crystal structure, magnetic and electron paramagnetic resonance properties of a second phase, Sc_7Cl_{10}.

Experimental section

Synthesis All preparations, manipulations, and analyses of materials were as previously described for ScCl (38). The metal utilized had atomic impurity levels in ppm as follows: H, 585; C, 146; O, 266; F, 164; W, 20; Ta, 17; N, 13; Cu, 9; Fe, 50; individual rare-earth elements and all other, <1. Powdered (<100 mesh) metal was again used as the reductant; for example, ca. 0.20 g Sc and 0.59 g $ScCl_3$ (Cl:Sc = 1.4 overall) were placed in a 4 cm long, 9 mm o.d. tantalum tube, this welded and sealed in a fused silica jacket, and the contents heated in a gradient of 880/900°C for six weeks. The crystals of interest here ($ScCl_{1.43}$) deposit as needles in the hottest reaches of the reaction container. Approximately 70% of the product by

weight is found as a fibrous mass of very thin whiskers in the cold end of the reaction tube as another phase previously identified as Cl:Sc = 1.45 ± 0.03 by chemical analysis. The whiskers resemble the reported scandium sesquihalide phase (5) in habit but they exhibit a quite different powder diffraction pattern and have a measurably different composition. The same $ScCl_{1.45}$ may also be obtained directly from $ScCl_{1.50}$ by reduction with metal foil between 877° and 885°C. This material has the unusual property of undergoing an irreversible, erratic and exothermic decomposition over the temperature range 885 - 895°C according to thermal analysis. X-ray powder diffraction showed that $Sc_7Cl_{10}(ScCl_{1.43})$ was the principal decomposition product on heating $ScCl_{1.45}$ at 900°C for 30 min in sealed Ta tubing followed by air-quenching. These observations led to the choice of the temperature gradient employed for single crystal preparation.

Magnetic susceptibility Measurements were made on a Faraday apparatus constructed and calibrated in this Laboratory (39). The null balance employed was a Cahn RG electrobalance with a sensitivity of 10^{-6} g. Approximately 100 mg of transported $ScCl_{1.43}$ was sealed under vacuum in a Pyrex ampoule that had been cleaned in boiling aqua regia. Susceptibilities were determined between 77 and 297 K with the temperature monitored by a copper constantan thermocouple

bonded to the inner surface of the heater assembly and in the presence of 100 μ He exchange gas to reduce temperature gradients between the heater and sample. The balance was zeroed with each temperature increment to allow for any possible convection currents. The Honda-Owen (40) method for determination of field dependence was utilized; force measurements were made at five settings between 6 and 12 kOe at each temperature and $\chi(H = \infty)$ obtained by extrapolation. Then $\chi(\infty H)$ was corrected for the temperature dependent susceptibility of the Pyrex container, the data converted to a molar basis, and finally diamagnetic core corrections applied for Sc^{3+} and Cl^{-} (Selwood). Measurements of the room temperature susceptibility before and after the low temperature study demonstrated the absence of any hysteresis.

Electron paramagnetic resonance The EPR spectrum was obtained at room temperature for a 10 mg polycrystalline sample from the same reaction product utilized for the magnetic susceptibility measurements and the structural determination. The spectrum was recorded on a Varian Model E-3 spectrometer with a frequency range of 8.8 to 9.6 GHz and a dial-selected magnetic field. The magnetic field was calibrated using strong pitch (g = 2.0028).

Crystal selection Relative to $ScCl_{1.50}$ or $ScCl_{1.45}$ the $ScCl_{1.43}$ crystals are still quite fibrous but have a marked increase in cross section. Considerable care must

be taken not to fray them into whiskers by abuse or cutting. Suitable specimens were sealed in 0.3 mm i.d. Lindemann glass capillaries in a specially designed inert atmosphere box constructed with a nearly horizontal window to facilitate the use of a stereozoom microscope. Preliminary zero-level Weissenberg photographs (h0ℓ) revealed the crystals exhibited a range of imperfections in the a*c* network, ranging from those which produced 2 or 3 distinct diffraction maxima parallel to the film translation ([010]) through streaks to single diffraction maxima. Data were collected on two crystals over the period of this study with final parameters coming from one of the smaller crystals (0.55 x 0.06 x 0.06 mm) which exhibited discrete and sharp diffraction maxima. Contrasts between these results and those from a similar sized crystal which gave broad but discrete peaks will be considered later. The fibrous character of the crystals and the striations on the long faces (2-μ period) which were clearly visible under high magnification (150X) are both manifestations of the microscopic chain structure found.

The data crystal was mounted with the needle axis b nearly colinear with ϕ on a four-circle diffractometer designed and built in the Ames Laboratory (29), and four ω-oscillation photographs were taken at various ϕ settings. From these photographs 12 independent reflections were

selected and their coordinates input into an automatic indexing program (41). The reduced cell and reduced cell scalars which resulted indicated monoclinic symmetry and this was then confirmed by inspection of ω-oscillation photographs taken about each of the three reciprocal axes. Only the b axis showed the presence of a mirror plane and all three layer line spacings observed agreed with those predicted by the indexing routine.

Data collection X-ray data were collected at ambient temperature using Mo K_α radiation (λ = 0.70954Å) monochromatized with a graphite single crystal. All reflections within a sphere defined by $2\theta \leq 50°$ in the octants HKL and $HK\bar{L}$ were checked using an ω-scan mode. The peak heights of three standard reflections remeasured every 75 reflections to check on instrument and crystal stability did not show any change over the data collection period. Final cell parameters and their estimated standard deviations were obtained from the same data crystal by a least-squares refinement (42) of ±2θ values of 19 independent reflections randomly distributed in reciprocal space for which $2\theta > 25°$. The lattice parameters were a = 18.620(7), b = 3.5366(7), c = 12.250(5)Å and β = 91.98(4)°. The initial portion of the data set was collected on the basis of a primitive monoclinic cell but after measurement of a few hundred reflections the condition

for C-centering, h + k = 2n, was obvious and this Bravais lattice type was imposed thereafter.

Structure determination and refinement Programs for data reduction, structure solution, illustration, and sources of atomic scattering factors for neutral atoms (including corrections for both real and imaginary parts of anomalous dispersion) were as referenced before (27,32). The observed intensities were corrected for Lorentz-polarization effects and their standard deviations calculated as previously described (30) to yield 730 observed reflections ($I>3\sigma(I)$) from a possible 877. Appropriate averaging of duplicate reflections yielded 705 independent data.

A preliminary structure determination of $ScCl_{1.43}$ phase was first completed in the triclinic space group $P\bar{1}$ utilizing a crystal which gave broad but discrete peaks and provided at best satisfactory diffraction data. Initial atomic positions were obtained by direct methods using MULTAN (43) and once the scandium and chlorine atoms were correctly differentiated three cycles of full-matrix least-squares refinement with isotropic thermal parameters converged at $R = \Sigma||F_o|-|F_c||/\Sigma|F_o| = 0.146$. At this point a C-centered monoclinic cell appeared likely, the triclinic structure limiting the monoclinic space group to C2/m with three scandium atoms and five chlorine atoms each on special position 4i and one scandium atom on special position 2a. Triclinic cell positions and

data indices were then converted to the monoclinic basis for further refinement (see Discussion section). Similar atom parameters were used as initial input for refinement with the better data set obtained from the crystal which gave sharper diffraction maxima. In this case three cycles of full-matrix least-squares refinement, varying the scale factor, positional parameters and isotropic thermal parameters, converged at $R = 0.077$ and $R_w = 0.099$ where $R_w = [\Sigma\omega(|F_o|-|F_c|)^2/\Sigma\omega|F_o|^2]^{1/2}$ and $\omega = \sigma_F^{-2}$. Further refinement with anisotropic parameters for all atoms gave convergence at $R = 0.059$ and $R_w = 0.072$. An absorption correction (44) appropriate to the correct stoichiometry ($\mu = 43$ cm^{-1} (45)) and crystal shape was not considered necessary since transmission factors varied only from 0.813 to 0.834. At this point variation of all occupation parameters for both scandium and chlorine atoms gave converged values of 1.00(1), indicating no significant deviation from the stoichiometry Sc_7Cl_{10}. A final difference Fourier synthesis map was flat to ≤ 1 e/Å^3 on atom sites and ≤ 0.5 e/Å^3 elsewhere.

Results

Structure description Final positional and thermal parameters for Sc_7Cl_{10} are listed in Table III, and important interatomic distances and angles are given in Table IV. Structure factor results are available in Appendix C.

Table III. Crystallographic data for Sc_7Cl_{10}

Composition: Sc_7Cl_{10}

Cell: Monoclinic, C2/m (No. 12)

Lattice Parameters: $\underline{a}$ = 18.620(7)Å β = 91.98(4)°
$\underline{b}$ = 3.5366(6)
$\underline{c}$ = 12.250(5)

Refinement: R = 0.059, R_w = 0.072 (705 reflections, $2\theta \leq 49.9$)

Atom Positions:

	x	y	z	B_{11}[a]	B_{22}	B_{33}	B_{13}
Sc1	0.0	0.0	0.0	1.25(14)	1.67(12)	1.26(12)	0.27(9)
Sc2	0.3314(1)	0.0	0.2466(2)	1.25(14)	0.95(8)	1.37(7)	0.46(9)
Sc3	0.1891(1)	0.5	0.2935(2)	1.39(13)	1.08(8)	1.44(6)	0.36(10)
Sc4	0.3164(1)	0.5	0.4693(1)	0.97(14)	1.15(9)	1.14(6)	0.27(9)
Cl1	0.4155(1)	0.0	0.4042(2)	1.39(13)	1.40(11)	1.62(12)	0.36(10)
Cl2	0.0988(1)	0.0	0.3548(2)	1.25(14)	1.24(11)	1.50(12)	0.18(9)
Cl3	0.0565(1)	0.5	0.1192(2)	2.08(14)	1.27(11)	1.98(12)	0.27(9)
Cl4	0.2150(1)	0.0	0.1407(2)	1.39(13)	1.36(8)	1.50(12)	0.09(9)
Cl5	0.3902(1)	0.5	0.1208(2)	2.35(14)	1.20(10)	2.58(12)	1.55(9)

[a] $T = \exp[-\frac{1}{4}(B_{11}h^2a^{*2} + B_{22}k^2b^{*2} + B_{33}\ell^2c^{*2} + 2B_{12}hka^*b^* + 2B_{13}h\ell a^*c^* + 2B_{23}k\ell b^*c^*)]$. $B_{12} = B_{23} = 0$ by symmetry.

Table IV. Bond distances (Å) and angles (deg.) in Sc_7Cl_{10}

Metal Octahedra:

	Distance
Sc2 - Sc3	3.253(2)Å
Sc2 - Sc4	3.271(2)
Sc3 - Sc4	3.147(3)
Sc3 - $Sc4^a$	3.407(3)
Sc4 - $Sc4^a$	3.153(3)
Sc1 - $Sc1^c$	3.5366(6) (b axis)

	Angle		Angle
Sc4 - Sc2 - Sc3	57.69(6)°	Sc3 - $Sc4^a$ - $Sc3^b$	62.54(5)°
Sc3 - Sc4 - Sc2	60.87(6)	Sc4 - Sc4 - Sc4	55.89(4)
Sc2 - Sc3 - Sc4	61.43(5)	Sc4 - $Sc4^a$ - $Sc4^b$	68.23(8)
Sc3 - Sc4 - $Sc4^a$	65.46(7)	Sc3 - $Sc3^b$ - Sc2	57.07(3)
Sc4 - $Sc4^a$ - Sc3	56.19(6)	Sc3 - Sc2 - $Sc3^b$	65.86(5)
$Sc4^a$ - Sc3 - Sc4	57.36(6)	Sc2 - Sc4 - $Sc4^b$	57.27(3)
$Sc4^a$ - Sc3 - $Sc3^b$	58.73(3)	Sc4 - Sc2 - $Sc4^b$	65.46(6)

Chlorine Atoms on Metal Chain:

Sc4 -- Cl1	2.695(2)Å	Sc4 - Cl1 - Sc4[b]	82.02(9)°
Sc2 -- Cl1	2.443(3)	Sc4 - Cl1 - Sc2	78.91(8)
Sc4[a] -- Cl2	2.627(3)	Sc4[a] - Cl2 - Sc3	81.91(8)
Sc3 -- Cl2	2.570(2)	Sc3 - Cl2 - Sc3	86.96(9)
Sc2 -- Cl4	2.487(3)	Sc3 - Cl4 - Sc3[b]	84.45(9)
Sc3 -- Cl4	2.631(2)	Sc3 - Cl4 - Sc2	78.86(9)

Bridging Chlorine Atoms:

Sc3 -- Cl3	3.208(4)Å	Sc3 - Cl3 - Sc1	133.37(5)°
Sc1 -- Cl3	2.502(2)	Sc1 - Cl3 - Sc1[c]	89.95(9)
Sc2 -- Cl5	2.443(3)	Sc2 - Cl5 - Sc1[d]	134.36(6)
Sc1[d] -- Cl5	2.566(3)	Sc2 - Cl5 - Sc2[c]	85.28(9)

Chlorine Around Isolated Metal Atoms:

Cl5 - Sc1[d] - Cl3[d]	90.54(8)°
Cl3 - Sc1 - Cl3[b]	89.95(9)

---

[a] 1/2 - x, 1/2 - y, 1 - z.

[b] x, y - 1, z.

[c] x, y + 1, z.

[d] 1/2 + x, 1/2 + y, z.

Figure 2 is an ORTEP drawing of the structure viewed along the b axis which illustrates the spatial arrangement of all atoms in the unit cell. (Superscript letters refer to symmetry operations defined in Table IV.) The occurrance of all atoms at y = 0 or 0.5 along the 3.54Å b axis generates regular chains of scandium atoms in that direction, as shown in Figure 3. This remarkable consequence can be best constructed in two stages -- first, infinite chains of distorted octahedra of scandium which share opposite edges Sc3 - Sc4 and $Sc3^a$ - $Sc4^a$, and, then, pairs of these chains displaced by b/2 and joined at a common edge, Sc4 - $Sc4^a$. The octahedra are appreciably distorted; the waist of the octahedra as viewed in Figure 3 is a rectangle 3.15 x 3.54Å, and the apex $Sc4^a$ is off-center with distances of 3.15 and 3.41Å to the waist atoms, a displacement which allows the formation of the short (3.15Å) $Sc3^a$ - $Sc4^a$ bond in the other chain. The other apex Sc2 is relatively well centered above the waist rectangle at distances of 3.25 - 3.27Å.

All chloride atoms have three metal neighbors. Chlorine atoms 1, 2 and 4 cap all outward facing Sc triangles of the chain structure as illustrated in Figure 2 (e.g.. Sc3 - $Sc3^b$ - $Sc4^a$) but do not cover those which are inward facing (e.g., Sc3 - Sc4 - $Sc4^a$) or those between apices of the octahedra (e.g., Sc2 - $Sc2^c$ - Sc3) which would be too close to neighboring chloride atoms (Cl4). Scandium-chloride

Figure 2. View of the Sc_7Cl_{10} structure down the short b axis. Atoms Sc1, Sc2, Cl1, Cl2 and Cl4 are at y = 0, the remainder at y = 0.5. Superscript atoms are related through the operation 1/2 - x, 1/2 - y, 1 - z.

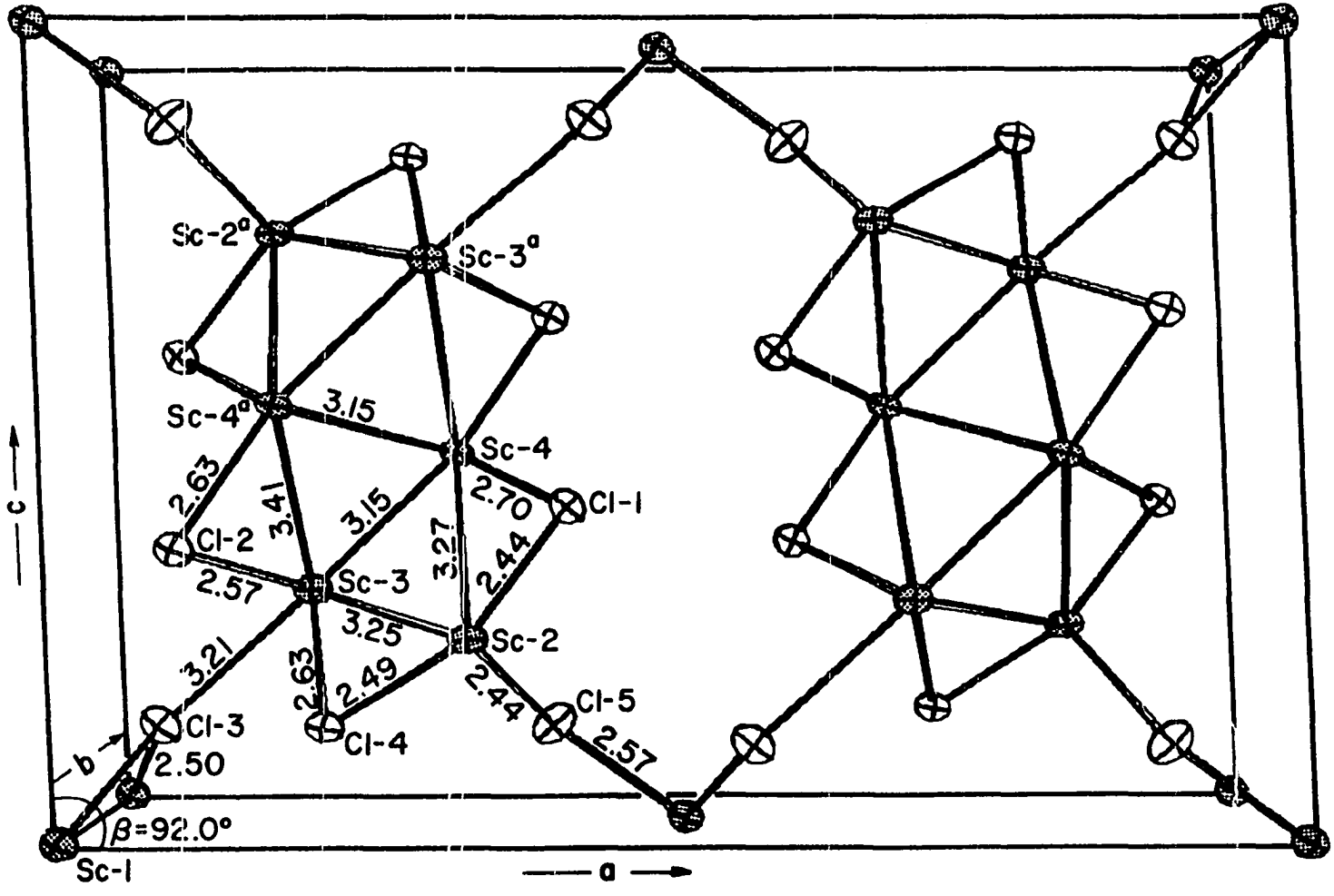
Sc-2a
Sc-3a
Sc-4a
3.15
Sc-4
2.63
3.41
3.15
2.70
Cl-1
Cl-2
3.27
2.44
2.57
Sc-3
3.25
Sc-2
3.21
2.63
2.49
2.44
Cl-5
Cl-3
Cl-4
2.57
2.50
b
β=92.0°
Sc-1
a
c

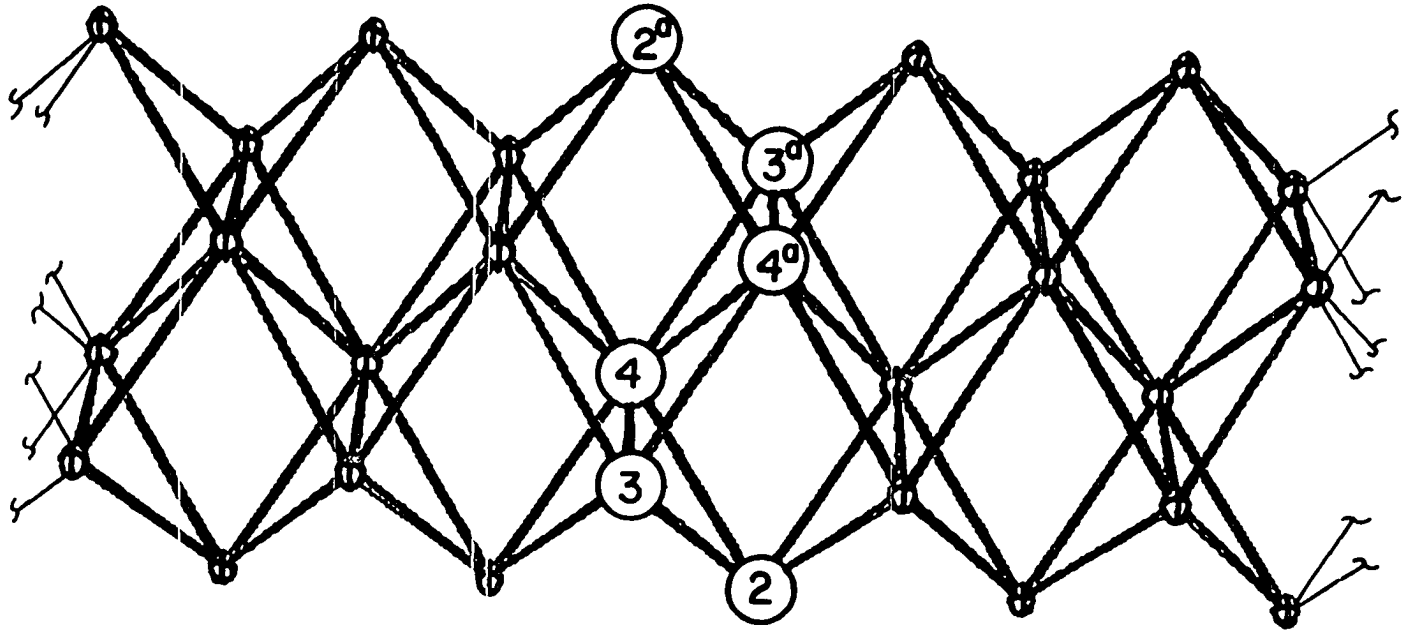

Figure 3. View of the metal chain structure of Sc_7Cl_{10} with the b axis horizontal. The distorted octahedra are discussed in the text in terms of those with apices 2 - 4^a and 4 - 2^a.

distances for this compound range from 2.44 to 2.70Å compared with 2.58Å in $ScCl_3$ (34) and 2.59Å in ScCl (38), a similarity which again emphasizes the apparent disposition of the reduction electrons within the chains. Additional chlorine atoms 3 and 5 bridge between the metal chains and the isolated Sc1 atoms in a complementary fashion; that is, Cl3 edge-bridges two Sc1 atoms at a distance of 2.50Å and interacts with Sc3 through a long Sc-Cl bond, 3.21Å, whereas Cl5 bridges between two Sc2 apices atoms in the chains at 2.44Å and in addition is bonded to Sc1 at 2.57Å (as shown at 1/2, 1/2, 0).

Another structural regularity is found in the two close-packed chlorine layers generated about (001) by chlorine atoms 3, 4 and 5, where the isolated Sc1 (presumably scandium(III)) atoms occupy one-third of the octahedral interstices, as shown in Figure 4. The octahedra containing these isolated metal atoms also form chains parallel to the b axis.

Magnetic and EPR data The gram-susceptibility of $ScCl_{1.43}$ (χ_g) as a function of temperature is provided in Table V, and Figure 5 is a plot of reciprocal ($\chi_M^*-\chi_D$) versus temperature where χ_M^* is the molar paramagnetism assigned to the metallic scandium, that is, chain metal atoms Sc2, 3 and 4 but not the unique Sc1 (46). The compound exhibits Curie-Weiss behavior above about 120 K, and the data yield values

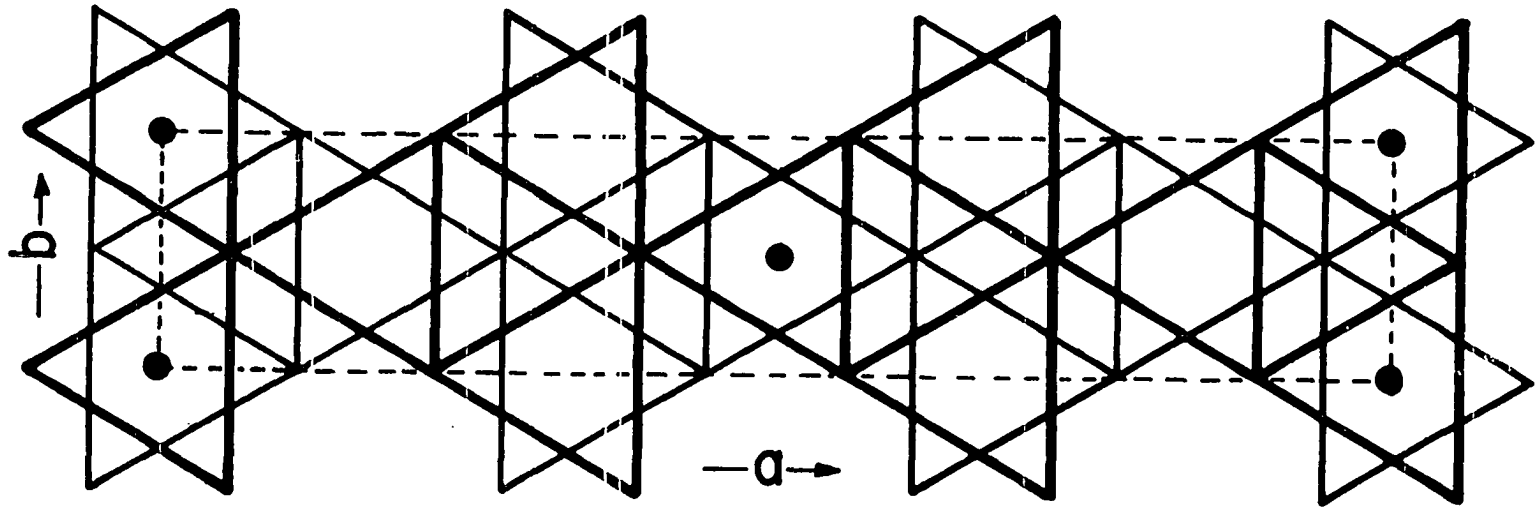

Figure 4. The (001) section of the Sc_7Cl_{10} structure viewed down c. The close packed layers generated by Cl3, 4, 5 and (face centered) octahedral interstices occupied by Sc1 are shown.

Table V. Susceptibility of polycrystalline $ScCl_{1.43}$

Temp. °K	χ Sample[a], (emu/g) x 10^6
79	2.20(4)
83	2.04(1)
86	1.99(2)
90	1.85(1)
95	1.78(4)
100	1.81(1)
105	1.69(1)
110	1.73(3)
115	1.71(4)
120	1.59(1)
130	1.60(4)
140	1.54(2)
160	1.43(5)
180	1.34(4)
200	1.34(3)
225	1.28(3)
250	1.24(4)
275	1.23(7)
297	1.14(4)

[a]The uncertainties in parentheses are standard deviations derived from the Honda-Owen plot.

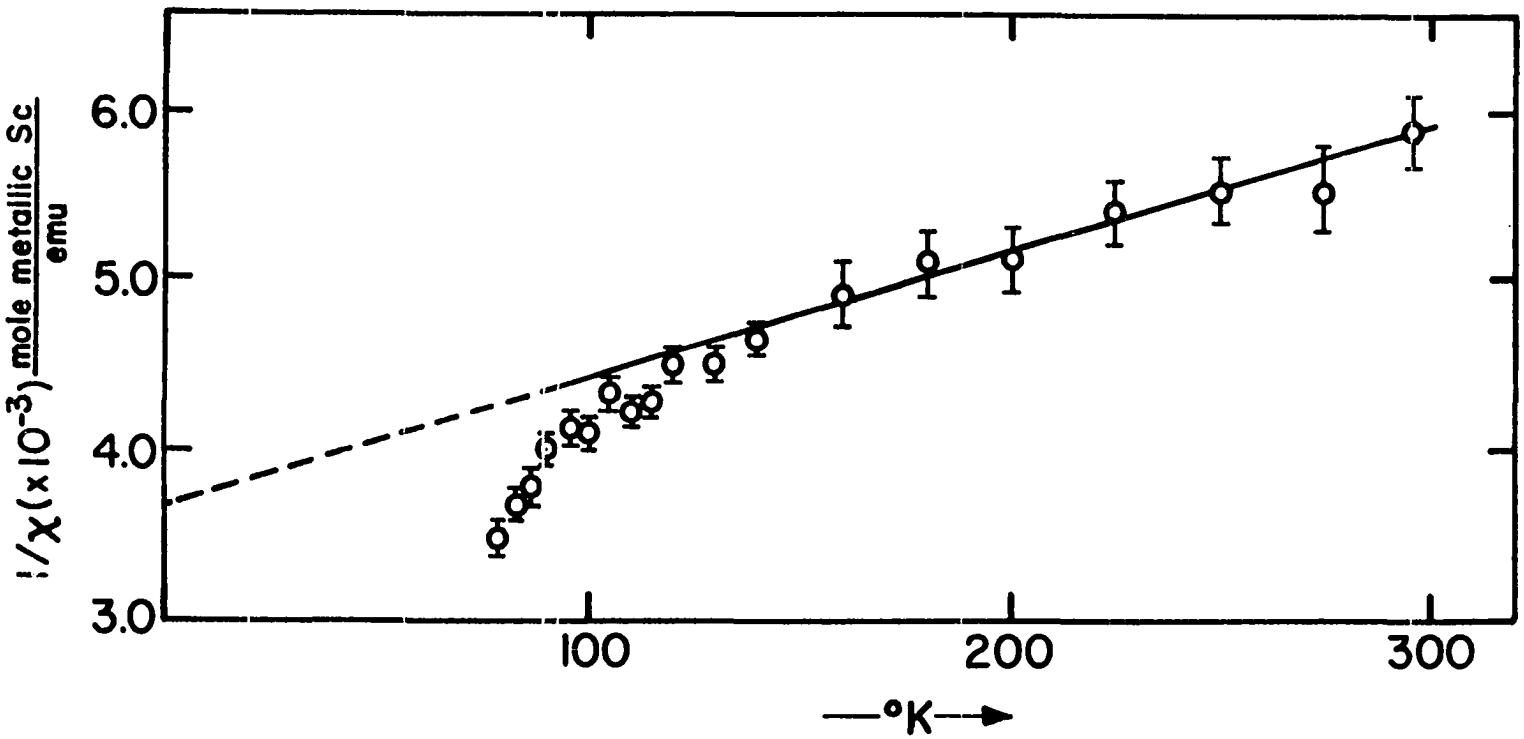

Figure 5. Reciprocal molar (per mole of metallic scandium) magnetic susceptibility vs. temperature for polycrystalline Sc_7Cl_{10}.

of 1.04 μ_B and -498 K for μ_{eff} and θ, respectively. Although the low temperature magnetic behavior is not yet known, the data shown suggest the compound may order antiferromagnetically with T_N somewhat below 79 K. Figure 6 is a reproduction of the EPR spectrum of $ScCl_{1.43}$ at room temperature from which the g factor is calculated to be 1.97.

Discussion

The Sc_7Cl_{10} structure represents an intermediate degree of metal-metal bonding relative to two other very reduced (Cl:M < 2.0) rare-earth metal chlorides, $GdCl_{1.5}$ (4) and ScCl (38). The gadolinium compound contains infinite chains of elongated octahedra which are clearly conceptual precursors of the double chains of metal octahedra found here and which also show the same type of face capping by chloride. Alternatively, the double chain of octahedra can be generated by extracting a section through the ScCl structure, the original Cl-Sc-Sc-Cl layers running vertically and normal to the paper in the section shown in Figure 2. The present structure retains the same capping halogen atoms 1 and 2 and "stitches up" the edges of the chains with Cl4 and Cl5.

A useful description of the present structure can be obtained in terms of atom connectivity, an approach which has found considerable utility with discrete clusters (11).

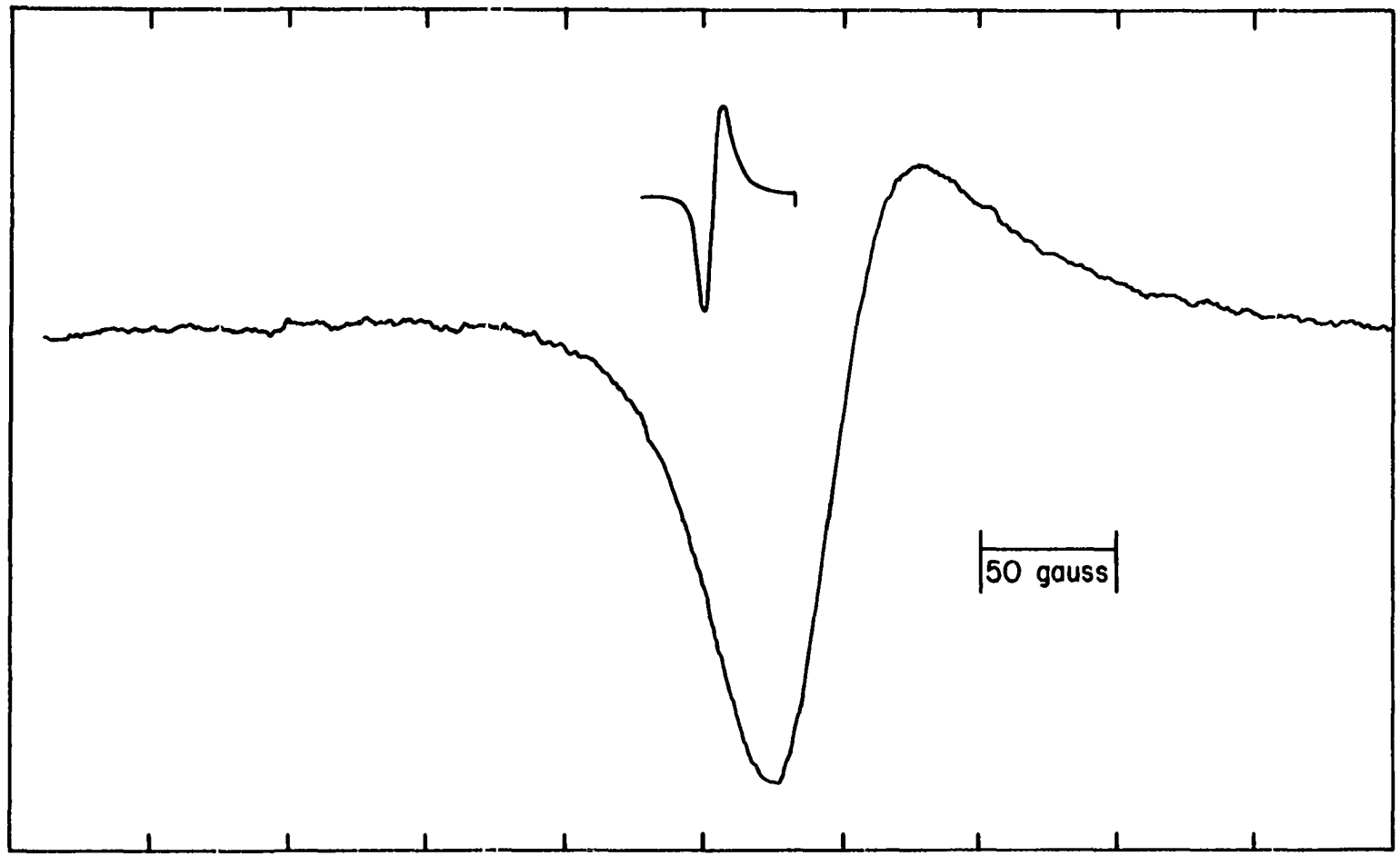

Figure 6. EPR spectrum of polycrystalline Sc_7Cl_{10} at room temperature.

If the long Sc3 - Cl3 interaction (3.21Å) is considered unimportant, the structure sorts out as

$$[Sc(Cl3)_{4/2}(Cl5)_{2/3}]_\infty[Sc_6Cl_6(Cl5)_{4/3}]_\infty$$

where the first portion contains the isolated Scl atom and associated bridging chlorines, the subscripts denoting the degree of sharing, and the second pair of brackets includes the integral repeating parts of the metal-bonded chain with capping and bridging Cl5 atoms. The isolated Scl atom must be taken as scandium(III) judging from distances to neighboring chlorine atoms since an added electron should markedly increase the effective radius. Thus, there is an obvious element of electron transfer from Scl to the metal chain and some chlorine transfer as well is implied by the above formulation.

A striking feature of this remarkable structure is the short metal-metal bonds; the shared edges between the octahedra in each chain (Sc3 - Sc4), and between chains (Sc4 - $Sc4^a$) at 3.147(3) and 3.153(3)Å, respectively, are the shortest scandium metal-metal distances known, considerably less than the shortest metal-metal distance in ScCl (38), 3.216(6)Å, and in the metal itself, 3.26Å (33). The short distances correspond to a Pauling (33, p. 400) bond order of about 0.4 to the extent that this calculation is meaningful for such an asymmetric environment.

Undoubtedly, the one-dimensional strongly bound metal-metal chains in Sc_7Cl_{10} constitute the backbone of the structure, with only van der Waals interactions between parallel chains save for the indirect chlorine bridging between chains provided principally by Cl5 via the isolated Sc1 atoms. The fibrous crystal habit and the parallel striations observed on the crystal surfaces also attest to the highly anisotropic bonding. An interesting measure of these effects are the differences in structural parameters obtained with diffraction data from two crystals of evidently different degrees of perfection utilizing the same instrument and techniques. The widths of "sharp" diffraction peaks out the axes of the final data crystal (e.g., (400), (040), (008)) were 0.06 to 0.10° at half height, while these same diffraction maxima were 2.4 - 4 times broader with the less perfect crystal studied first. Likewise, the refined structure deduced from the first crystal was satisfactory but not great (R = 0.101 for 642 reflections), the standard deviations of the parameters being 1.5 - 3 times those reported here. More remarkable is the consistent shift to shorter as well as more precisely determined interatomic distances and cell lengths in the better refined and "tighter" crystal. Unit cell dimensions in the latter were consistently smaller, 0.19(5), 0.17(2), 0.19(5)% respectively, leading to a remarkable 0.5%

reduction in the cell volume, 810.48(26) to 806.22(51)$\AA^3$ or a difference of 7σ! Presumably, the increased degree of perfection occurs particularly in the packing or order of one scandium chain relative to the other along crystal defects. Although most thermal parameters were simply better defined with the better crystal data and not significantly different, the values of B_{11} for all the chain atoms uniformly decreased by 9 - 10σ. Although the bridging atoms Cl3, Cl5 and Sc1 are crystallographically unique and perhaps less tightly bound, the relatively large values for B_{11} and B_{33} for Cl5 (and Cl3 to a smaller degree) and for B_{22} for the isolated Sc1 (Table III) may or may not reflect remnant crystal defects (47).

The magnetic and EPR data for $ScCl_{1.43}$ are particularly helpful in assessing something of the electron distribution in the metal-metal bonded chains. The magnetic behavior also contrasts with that of either the two-dimensional metallic halides ThI_2 and LaI_2 (48, 49) which exhibit only temperature-independent Pauli paramagnetism or the one-dimensional $GdCl_{1.5}$ where the dominant $4f^7$ cores obscure any possible details regarding the bonding (50). However, the $ScCl_{1.43}$ data show a considerable parallel with the magnetic behavior of scandium metal (51) where a Curie-Weiss behavior with μ_{eff} = 1.65 μ_B and θ = -850 K compares with 1.04 μ_B and -498 K here. If the one-dimensional character

of the scandium metal chains of octahedra in $ScCl_{1.43}$ and the reduction in the number of free valence electrons per metal atom corresponding to partial oxidation are considered, the smaller magnitude of both the magnetic moment and Weiss constant found here seem reasonable and plausible. For this low-dimensional and anisotropic compound an interpretation of the results in terms of partially localized spin states is at least instructive if not necessary (52). Symmetry does not restrict all metal atoms to magnetic equivalence in $ScCl_{1.43}$; in fact, consideration of the differences in bond lengths, coordination, etc., between metal atoms Sc2, 2, 4 and 2^a, 3^a, 4^a leads to the opposite assumption. The effective magnetic moment calculated for the molar composition Sc_7Cl_{10} is 2.57 μ_B, a value close to the spin-only value for two unpaired electrons. Although these could be localized on any pair or, in part, pairs of metal atoms in the Sc_7Cl_{10} repeating unit, the symmetry uniqueness of the Sc2 apical sites and their longer bond distances to waist sites are consistent with unpaired electrons localized on these sites (Sc2 and $Sc2^a$). The room temperature EPR spectrum clearly supports the presence of localized and relative weakly coupled electrons (50-G line width), as should be the case for these Sc2 sites. With an experimental g factor of 1.97 the calculated $\mu_{eff} = 2^{1/2}(1.97)[(1/2)(1/2+1)]^{1/2} = 2.41$ is in good agreement with that determined from the magnetic susceptibility (2.57).

The plethora of reduced phases known to exist in the $Sc-ScCl_3$ system (38) will undoubtedly reveal phenomenologically the more or less continuous process of metal catenation and electron delocalization as a function of metal content and oxidation state. A phase is presently under investigation which clearly contains discrete six atom metal clusters (53) (bond distances 3.21 - 3.23Å), thus representing the end member of the metal-metal bonded series extending from isolated octahedral metal clusters through chains to two-dimensional sheets of shared metal octahedra. In addition, the phase $ScI_{2.15}$ in a CdI_2-type structure evidently exhibits a metallic conduction for only single sheets of metal atoms (21). Seldom has one element provided such a versatile and exciting opportunity to view metal-metal bonding and the properties derived thereby over such a range of structural complexity and, presumably, electron delocalization.

The didactic concept of cluster condensation recently put forth by Simon (9,37) to account for structural similarities in metal-rich compounds works quite well to describe the chains to shared but distorted octahedra in Sc_7Cl_{10}. However, the presence of isolated scandium(III) ions is not predicted or accounted for by this type of modeling. This new variation reveals another important dimension in the structure of metal-rich phases, one that emphasizes the

need for electronic models to complement a geometric scheme of cluster condensation. Obviously, the radial extension of 3d orbitals early in the series is favorable to metal-metal bonding, contrary to some expectations, but the richness and diversity of this feature with scandium requires further definition of more subtle factors than just the commonly accepted (54,55) orbital size.

Sc_7Cl_{12}: The First Example of a Transition Group (III) M_6X_{12}-Type Cluster

Introduction

Among the early transition metals, halogen-bridged clusters of the binary types $M_6X_{12}^{n+}$ (n = 2, 3, 4) and $M_6X_8^{m+}$ (m = 4 mainly), which contain an octahedral cluster of metal atoms, have become well known. The transition metals receiving the most attention have been those in the second and third transition series located in the lower left of the periodic table: Nb, Ta, Mo, and W. The ability of these particular metals to form strongly bonded clusters has been attributed to several factors: the radial extension of their outermost valence orbitals, the effective charge on the metal and the formal oxidation state, the

number of electrons available for filling bonding orbitals, and the steric considerations of a particular nonmetal: metal ratio (composition). Examples of a similar cluster chemistry in the first transition series have been most notable by their absence. This has been attributed to the combination of the small size of the 3d valence orbitals available for overlap and too few electrons even in usual low formal oxidation states to form stable metal clusters. The significance of the synthesis of the phase Sc_7Cl_{12} along with the zirconium examples Zr_6Cl_{15} (56) and more recently Zr_6I_{12} (57) suggests the scarcity of these examples may be attributed to kinetic (11) rather than thermodynamic limitations. At present Sc_7Cl_{12} represents the end member in the range $ScCl_x$; $1.0 \leq x \leq 2.0$, and as the most chlorine-rich composition (Cl:Sc = 1.71) has discrete six-atom metal clusters. A communication has appeared previously (53).

Experimental

Synthesis The cluster synthesis reaction of Sc_7Cl_{12} is one of the least understood reactions in the binary Sc-$ScCl_3$ system yet one of the most studied. As the most chlorine-rich phase disproportionation of a higher halide composition, for example, solid dichloride, is not possible. On the other hand the composition 42.9 mole % Sc in $ScCl_3$ (Cl:Sc = 1.71) is very much more reduced than either the

eutectic at 18 mole % Sc or metal-rich liquidus at ~25 mole % Sc and 950°C as determined by conventional thermal analysis (5). Not only must the solid phase be metal-rich but structurally complex as well. As a consequence, the reduction of the liquidus with metal is difficult to achieve. The problem is, basically, how can the composition and temperature variables be controlled in a way that equilibration of a particular Cl-Sc composition results in the equilibrium phase? The metal-rich compound NbO cannot be prepared at less than 1500°C by the direct combination reaction of Nb_2O_5 and Nb metal although NbO is a stable oxide phase in the Nb-O system (58).

One approach to the problem of reactivity has been to use powdered metal as the reductant. This approach has been successful in the preparation of ScCl where higher temperatures can be used without thermal decomposition of the product. Isothermal reactions of powdered scandium metal and scandium trichloride at the composition Cl:Sc = 1.71 at various temperatures in the range 800-900°C have resulted in nonequilibrium mixtures of unreacted scandium trichloride and solid phases more reduced than Sc_7Cl_{12}. Often the metastable solid phase $ScCl_{1.45}$ was found as the main product. The upper limit of 900°C for thermal stability of Sc_7Cl_{12}, although somewhat arbitrary, is based upon reactions where Sc_7Cl_{12} has been identified.

One such reaction has been the reaction of scandium foil with scandium trichloride in a temperature gradient 850-1000°C (59). Small monocrystals of Sc_7Cl_{12} were found deposited in a zone nearest the cold end where the scandium trichloride had originally been placed. Larger crystals were subsequently prepared by starting with the reduced composition Cl:Sc = 1.45 and using a narrow gradient, 880-900°C. The circumstances of this reaction have been described before (60). The long whiskers of $ScCl_{1.45}$ were found to extend from the cold end (880°C) into the middle region of the reaction container. The gem-like crystals of Sc_7Cl_{12} were found attached at the end of a whisker on a face. This unusual habit has also been observed for Zr_6I_{12} (57).

One explanation for the unusual growth habit of Sc_7Cl_{12} may depend on how the long whisker crystals of $ScCl_{1.45}$ grow in the first place. A possible vapor-liquid-solid (VLS) mechanism postulates (61) the presence of a tiny liquid droplet which acts as a preferred site for whisker growth from the vapor. At saturation values well below any critical pressure molecules from the vapor deposit in a liquid droplet since the sticking factor for impinging molecules is higher for a liquid than that of a solid. With a source of whisker material in the vapor continuously depositing in the droplet, precipitation and growth of the

solid phase (whisker) occurs moving the liquid droplet along at its tip. This liquid droplet after some time and change in growth conditions may then act as the seed for the new solid phase, which in this case is Sc_7Cl_{12}. The growth of this phase is nearly isotropic and provides for beautiful growth on all faces since the whisker mount essentially suspends the growing crystal in the vapor. These crystals were used for the single crystal x-ray diffraction study and in comparison to all the other reduced scandium chlorides studied by diffraction, these crystals were the most nearly perfect specimens.

Data collection, structure determination and refinement

The crystals of Sc_7Cl_{12} were sealed in Lindemann glass capillaries under an inert atmosphere. The data crystal was 0.16 mm on a side when approximated as a cube. Diffraction data was originally collected on the basis of a primitive triclinic cell. The preliminary atomic coordinates for the structure determination were obtained by direct methods (43) in the space group $P\bar{1}$. After solution, the spatial arrangements of the atoms were observed by inspection to have the higher symmetry of space group $R\bar{3}$. The entire hemisphere of observed data collected for the triclinic cell (1395 reflections $I > 3\sigma(I)$) was reindexed and symmetry equivalent reflections (Laue $\bar{3}$) averaged to yield 483 reflections. In the averaging step

only two reflections were eliminated based on $|F_o-F_A|/F_A > 0.20$ where F_A is the average value. This successful averaging shows the validity of the higher symmetry trigonal cell. Triclinic cell positions were subsequently converted to the trigonal basis and the refinement carried out in the space group $R\bar{3}$. After three cycles, the full-matrix least-squares refinement converged at $R = \Sigma||F_o|-|F_c||/|F_o| = 0.16$ for the composition $Sc_{21}Cl_{36}$ (Sc_7Cl_{12}, Z = 3). A difference map at this stage revealed a peak of electron density of $8e/Å^3$ on the special position (0,0,1/2) or the cluster center. A chlorine atom with variable occupancy was added to the atom list and subsequently a residual of 9.8% was obtained with an occupancy factor for the special position (0,0,1/2) of 0.43(1). At this point variable of occupation parameters for all other positions revealed no significant deviation from unit occupancy. Further refinement varying the overall scale factor, positional parameters, anisotropic thermal parameters and the occupancy factor at the (0,0,1/2) site converged readily after three cycles to yield R = 0.053 and $R_w = 0.064$ where $R_w = [\Sigma\omega(|F_o|-|F_c|)^2/\Sigma\omega|F_o|^2]^{1/2}$ and $\omega = \sigma_F^{-2}$. A final difference Fourier synthesis map was flat to $\leq 1e/Å^3$ on atom sites and $\leq 0.5e/Å^3$ elsewhere.

Results and discussion

Structure description Final positional and thermal parameters for Sc_7Cl_{12} are listed in Table VI and important distances and angles are shown in Figure 7. Structure factor results are available in Appendix D. Figure 7 emphasizes the formulation of Sc_7Cl_{12} as a $M_6X_{12}^{3-}$ cluster anion with a scandium(III) counter cation if Cl3 in the center of the cluster is neglected. Figure 8 gives an alternative perspective of the structure in terms of close-packed halogen-metal layers with similarities to the simple NaCl structure.

In Figure 7 the orientation of the cluster is such that the 3-fold rotation axis runs diagonally from top right to lower left. The isolated scandium(III) cation lies on the axis and is coordinated in octahedral fashion to six chlorine atoms at a distance of 2.549(1)Å. The actual point symmetry is D_{3d} with a halogen-metal-halogen angle of 90.26(3)°. These particular six halogen atoms are also edge-bridging on the metal atom cluster. The bridge angle is 77.66(4)° with Sc-Cl bond distances of 2.566(1)Å and 2.591(1)Å. The triangles of metal atoms are drawn together through metal-metal interactions and occur in pairs to generate M_6 trigonal antiprisms. The distances are, respectively, 3.234(1)Å and 3.204(1)Å. The six shorter edges of the metal cluster are edge-bridged by six

Table VI. Crystallographic data for Sc_7Cl_{12}

Composition: Sc_7Cl_{12}, Z = 3

Cell: Trigonal, $R\bar{3}$ (No. 148)

Lattice Parameters: a = 12.959(2)Å, c = 8.825(2)Å

Refinement: R = 0.053, R_w = 0.064 (483 reflections $2\theta \leq 50°$)

Atom Positions:

	x	y	z	B_{11}[a]	B_{22}	B_{33}	B_{12}	B_{13}	B_{23}
Sc1	0.0	0.0	0.0	0.95(6) = B_{11}		6.52(17) = ½B_{11}	0.0	0.0	
Sc2	0.1725(1)	0.6232(1)	0.0191(1)	0.88(4)	0.79(4)	1.10(5)	0.41(3)	-0.01(1)	-0.02(1)
Cl1	0.0230(1)	0.4377(1)	0.1615(1)	0.94(6)	1.25(6)	1.49(7)	0.36(2)	-0.12(1)	0.23(3)
Cl2	0.1801(1)	0.0503(1)	0.1660(1)	1.42(5)	1.14(6)	1.37(7)	0.66(14)	0.24(3)	0.11(3)
Cl3[b]	0.0	0.0	0.5	1.25(19) = B_{11}		1.34(25) = ½B_{11}	0.0	0.0	

[a] $T = \exp[-\frac{1}{4}B_{11}h^2a^{*2} + B_{22}k^2b^{*2} + B_{33}\ell^2c^{*2} + 2B_{12}hka^*b^* + 2B_{13}h\ell a^*c^* + 2B_{23}k\ell b^*c^*)]$.

[b] Occupancy factor 0.46(1).

Figure 7. Sc_7Cl_{12} viewed as a M_6X_{12} cluster where solid ellipsoids represent scandium, open, chlorine, at 50% probability. The atom in the center of the six atom cluster represents residual electron density of unknown origin.

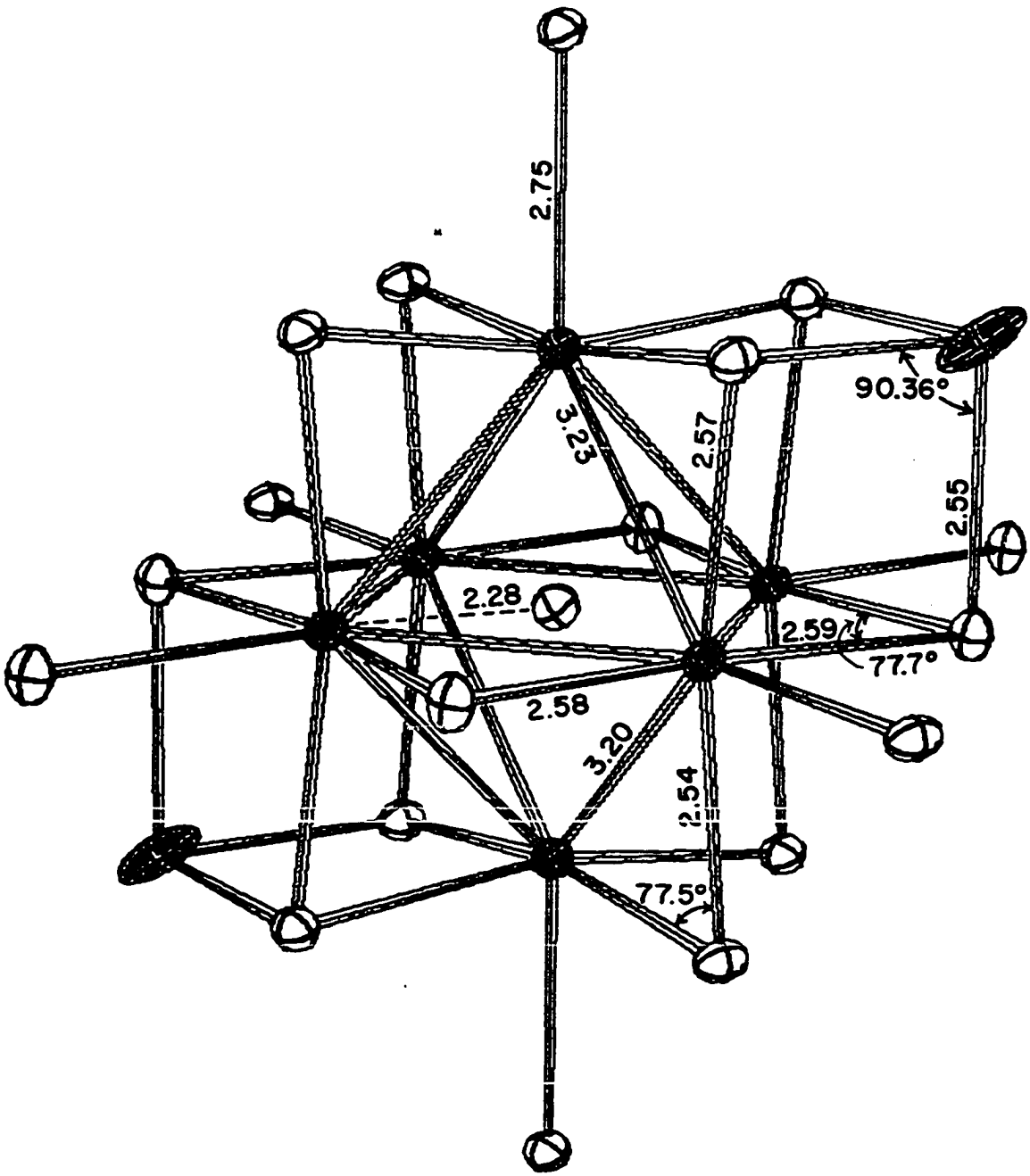
2.75
3.23
2.57
90.36°
2.55
2.28
2.59
77.7°
2.58
3.20
2.54
77.5°

Figure 8. A distorted close-packed halogen layer (C-layer) with ordered octahedral sites occupied by metal atoms. The thermal ellipsoids are scaled to 50% probability.

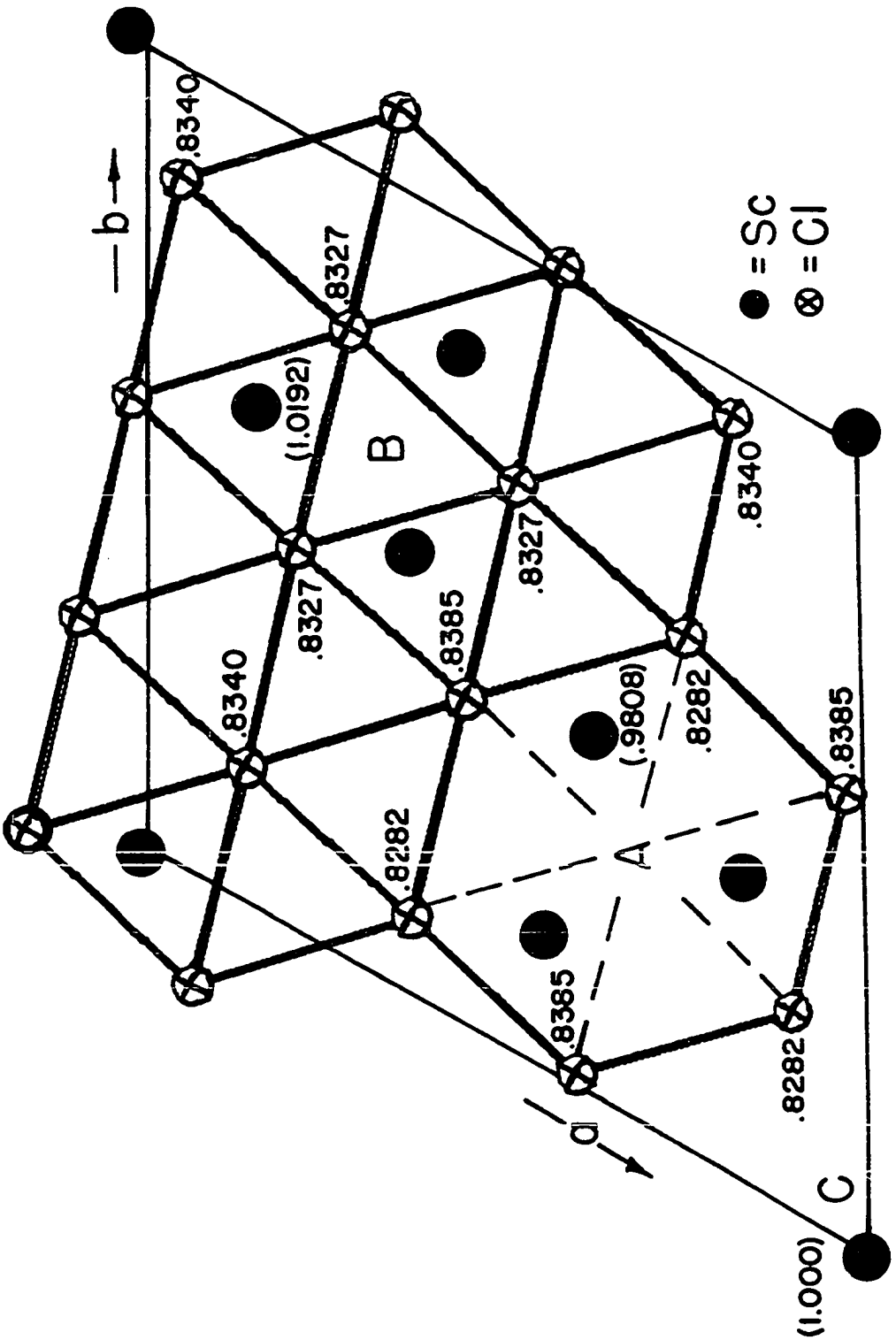
—b→
—a→
● = Sc
⊗ = Cl
.8340
.8327
(1.0192)
B
.8327
.8340
.8385
.8340
.8327
.8282
(.9808)
.8385
.8282
A
.8385
.8282
(1.000)
C

chlorine atoms alternating at 2.540(1)Å and 2.576(1)Å and with a bridge angle of 77.53(4)°. These particular six halogen atoms are also exo to a neighboring cluster at 2.755(1)Å. The six corresponding chlorine atoms edge-bridging in neighboring clusters and exo to this cluster are also shown. The nine electron anion $Sc_6Cl_{12}^{3-}$, isoelectronic with the Group IV zirconium cluster cation $Zr_6Cl_{12}^{3+}$ found in Zr_6Cl_{15} (56), represents the first example of a M_6X_{12} anion.

Two problems remain in this structure and refinement, both have been illustrated in Figure 7. First, the thermal parameter B_{33} for the isolated scandium(III) cation is abnormally large. In $R\bar{3}$ these atoms occur on the special position (0,0,0) and therefore are evenly spaced along the c axis and in the chains displaced by the R-centering operation. Neither the z parameter nor the large B_{33} changed significantly when the space group R3 and special position (0,0,z) were used. Therefore, if the large B_{33} term represents a systematic displacement and not just anisotropic thermal motion the distortion must be long range and at a minimum double the c axis. With the present data set this Peierls-like distortion cannot be verified.

The second problem is the large build up of electron density in the center of the cluster on the special position (0,0,1/2) which has been largely ignored up to now. This

same problem existed in the refinement of Zr_6Cl_{15} (56). Whether this represents a real foreign atom or termination effects awaits improvement of the synthetic routes to the point where larger and more useful quantities will allow additional analytical and physical characterization.

Figure 8 views the structure of Sc_7Cl_{12} from the viewpoint of close-packed atoms. In the figure a nearly close-packed layer of halogen atoms along with the metal atom arrangement in the octahedral sites is shown. The stoichiometry Sc_7Cl_{12} is determined by this pattern. All such halogen-metal layers are identical. The three dimensional lattice is simply built with these layers in a cubic-closest packed sequence, ABC•••. The layer shown in figure 8 has the symbol C since it is the third layer out the c axis, a fact also shown by the z coordinates listed next to the individual atoms. By translating the C layer so the atom at (1,0,1) is at the position (2/3, 1/3, 1 1/3) and then again to (1/3, 2/3, 1 2/3) the layers A and B, respectively, are generated and thus the entire sequence $\overline{ABCABC}$•••. In this way the alternating pattern of an isolated scandium(III) cation, Sc_6 cluster, scandium(III) cation, etc. along any one of the 3-fold axes is easily recognized. The R-centering operation positions each individual cluster relative one to the others.

If not already apparent, significant distortions from the ideal NaCl-type structure occur in addition to the gross defect nature of the metal sublattice. The metal atoms approach one another closer both in inter- and intralayer triangles than corresponding halogen atoms. The halogen sublattice distorts in a complementary fashion. For example, the six chlorine atoms around site A (Figure 8) alternate their z coordinates so the three halogens exo to the metal clusters on the C layer are raised. The remaining three halogens are exo to metal clusters below the C layer and have smaller z coordinates. One striking feature of the metal array is the intralayer minimization of coulomb repulsion between the scandium(III) ions and other metal near neighbors. A similar structure relationship exists between $NbF_{2.5}$ and a defect NaCl-like cell with the composition Nb_6F_{15} (62).

Cluster Condensation Reactions. The Synthesis and Structure of Pentascandium Octachloride (Sc_5Cl_8). An Infinite Chain Structure Derived by Cluster Condensation[1]

Introduction

Evidence that any rare-earth metal, yttrium, or scandium would reduce its corresponding trihalide to compositions with X:M < 2.0 has until very recently been limited to the single example of the unusual gadolinium compound Gd_2Cl_3 (3,4) where a remarkable infinite metal chain consisting of edge-shared octahedra is formed. Later McCollum and co-workers (5) were able to reduce scandium trichloride and tribromide to the composition $ScX_{1.5}$ with scandium foil at elevated temperatures when proper attention was paid to avoiding blockage of the metal surface by product, a condition which also allows the preparation of the monochloride ScCl which contains double metal layers (38). Recent applications of the technique of chemical transport along a temperature gradient above 880°C have now allowed kinetic accessibility to several additional scandium phases in the composition range 2.0 > Cl:Sc > 1.0. Among

---

[1]Accepted for publication: K. R. Poeppelmeier and J. D. Corbett, J. Am. Chem. Soc., 100, (1978).

these are Sc_7Cl_{10} (63), with infinite metal chains composed of double octahedra, Sc_7Cl_{12} (53), which contains discrete six-atom metal clusters, and the compound of interest in this work, Sc_5Cl_8. The chemistry of very reduced rare-earth metal halides (X:M < 2) has also recently been broadened substantially by Simon and co-workers (37) who have reported the formation of monochlorides for M = Gd, Tb, Er and Lu together with Tb_2Cl_3 which is isostructural with Gd_2Cl_3. This paper reports on the synthesis, single crystal x-ray structure, and electron paramagnetic resonance behavior of Sc_5Cl_8 and relates these results both in terms of architecture and electronic states to those of other polyscandium structures. The formation of Sc_5Cl_8 and other transported compositions is considered in terms of transport by the high temperature species $ScCl_2(g)$.

Experimental section

Synthesis All preparation and analyses of materials were as previously described in an earlier publication (38). The best metal available (99.998 atomic % purity) was used and as such had impurity levels in atomic ppm as follows: H, 401; C, 105; O, 118; F, 14; Fe, 50; Ni, 20; Cu, <20; Ta, 260; W, 160; Gd, <7; La, 6.4; Ho, <4; other rare-earths and other metals, <1 each. Typically, ca. 0.25 - 0.50 g of $ScCl_3$ was placed in one end of a 12 cm, 9 mm o.d. tantalum tube along with two 0.4 x 4 x 110 mm metal strips

and welded under a He atmosphere (0.8 - 0.9 atm). Typical reaction gradients were $T_1 \rightarrow T_2$ (850 → 1000 to 1050°C) and the time of the reaction ranged from four to six weeks. The temperatures were monitored by thermocouples attached to the outside of the evacuated fused silica jacket in which the tantalum reaction tube had been sealed. The transported phases were identified by powder x-ray diffraction and in addition microprobe analysis was performed on new phases in order to estimate their composition and to ensure absence of other metallic elements. In all cases the products were found condensed in the hotter regions of the reaction tube away from the cold end where the $ScCl_3$ had been originally placed.

Specifically, in one particular reaction where the gradient was $T_1 \rightarrow T_2$ (850 → 1010°C) three distinct phases were found in separate bands as crystallites loosely attached on both the metal strips and container walls and ordered in increasing degree of reduction. The most oxidized phase Sc_7Cl_{12} (as previously identified from a single crystal diffraction study (53)) was found in the coolest region of the tube followed by a band of $ScCl_{1.58}$ $ScCl_{1.58 \pm 0.04}(Sc_5Cl_8)$ and finally in the middle portion of the tube, a yet structurally uncharacterized compound $ScCl_{1.40 \pm 0.07}$. Microprobe examination of the latter two phases revealed no significant variation in composition in

a particular crystal or between crystals of the same phase and consistently detected only scandium and chlorine among elements beyond the second period. Standard deviations indicated for the compositions were calculated on the basis of 25 independent observations. These reduced scandium chloride compounds all react with water and evolve hydrogen gas in keeping with their reduced character.

The materials obtained under the above reaction conditions are crystalline but suffer profuse nucleation and growth and result in crystals of very small dimensions. In order to obtain crystals of adequate size for single crystal x-ray diffraction more control over reaction parameters was necessary. As such, the reaction conditions described in the previous paragraph contrast greatly with minimization of gradients and careful control of the overall stoichiometry necessary to prepare ScCl (38) or the careful control of the gradient in a narrow range necessary for good crystal growth of the Sc_7Cl_{10} (63) phase. Suitable monocrystals of Sc_5Cl_8 were subsequently obtained based on the observation that on several occasions a phase with a unique green hue to otherwise black crystals had been observed to form in small amounts while preparing ScCl (38). The phase identified above as $ScCl_{1.58 \pm 0.04}$ from the gradient experiment had the same unusual cast, and a comparison of the powder x-ray diffraction patterns from the two

experiments showed them to be the same. A composition Cl:Sc = 1.0 was prepared as before (38) except that no attempt was made to control the small natural gradient (∿940 → 960°C) across the tantalum reaction tube, positioning it within a sealed fused silica jacket in a 2 1/2 in. bore Marshall furnace without the benefit of a Inconel linear and radiation shields. The desired crystals condensed on the walls in the void end of the tube away from the major product which was a nonequilibrium mixture of metal plus several reduced phases including ScCl.

Crystal selection and data collection The crystals were of marginal size (.375 x .04 x .04 mm) for a single crystal study. Several possible candidates were chosen in the dry box with the aid of a stereozoom microscope and were mounted and sealed in 0.3 mm i.d. Lindemann glass capillaries under an inert atmosphere. Two possible crystals were chosen on the basis of oscillation and Weissenberg photographs and in the course of this study single crystal x-ray diffraction data were collected on each.

The data crystal in each case was mounted with the needle axis b nearly colinear with ϕ on a four circle diffractometer designed and built in the Ames Laboratory (29). All procedures used for indexing and orientation of the crystal were as previously described (64), although

the weak diffraction from the very small crystals made the task somewhat tedious. The preliminary film work and the automatic indexing routine both indicated monoclinic symmetry.

Data collection X-ray data were collected at ambient temperatures using Mo K_α radiation monochromatized with a graphite single crystal (λ 0.70954 Å). All reflections within a sphere defined by $2\theta \leq 50°$ in the octants HKL and $H\bar{K}L$ were examined using an ω-scan mode. The scan on the first crystal was over $\pm 0.5°$ in ω from the calculated center peak position, counting 0.5 seconds per measurement every 0.01° in ω and culminating when the count had reached the smaller of the two background count rates. Background was counted for four seconds 0.5° from the peak on each side. This mode proved less than satisfactory because the very small size of the data crystals resulted in a relatively large percentage of unobserved reflections. The data set for the second crystal from which all reported parameters were calculated was obtained by increasing the counting time to 1.0 seconds per step and setting a minimum requirement of either an integrated count of 2000 or a maximum of ten scans across the reflection.

As is customary, the peak heights of three standard reflections were remeasured every 75 reflections to check on instrument and crystal stability. These did not show

any change over the data collection period. The initial portion of the data was collected based on a primitive monoclinic cell but after sufficient data had been collected the condition for C-centering, $h + k = 2n$, was obvious and this Bravais lattice type was imposed. Final cell parameters and their estimated standard deviations were obtained from the same data crystal for which structure parameters are reported, utilizing a least-squares refinement with $\pm 2\theta$ values from 12 independent reflections for which $2\theta > 25°$. The results were $a = 17.78(2)$Å, $b = 3.523(8)$Å, $c = 12.04(1)$Å and $\beta = 130.10(6)°$.

Structure determination and refinement Programs for data reduction, structure solution and refinement, illustration, and the sources of atomic scattering factors for neutral atoms (including corrections for both real and imaginary parts of anomalous dispersion) were as referenced before (27, 32). Data reduction yielded 563 observed reflections ($I > 3\sigma(I)$), 85% of the total possible. Appropriate averaging of duplicate reflections yielded 513 independent data.

A trial structure was formulated using structural concepts gained from past work on similar phases, particularly Sc_7Cl_{10} (63). The observed monoclinic β angle of 130° and the same short $\underline{b}$ axis as in Sc_7Cl_{10} implied a possibly similar layered structure in space group C2/m with

all atoms at y = 0 and y = 0.5. If six atom metal clusters in a chain were again the structural skeleton, the β angle and the length of the c axis would indicate the metal array to be a single chain of metal octahedra which share edges parallel to the b axis. Preliminary metal atom coordinates were calculated with appropriate bond distances and with the cluster centered around (1/2, 1/2, 1/2) for two orientations of the cluster; that is, with the two apical atoms approximately parallel or perpendicular to the $(10\bar{1})$ plane (which includes the short diagonal of the ac face). With the correct choice (the former) an electron density map revealed all of the halogen atoms, and three subsequent cycles of full-matrix least-squares refinement varying the scale factor, positional parameters, and isotropic thermal parameters converged at R = 0.154 where $R = \Sigma||F_o|-|F_c||/\Sigma|F_o|$. Further refinement with anisotropic thermal parameters for all atoms gave convergence at R = 0.144 and R = 0.198 where $R_w = [\Sigma\omega(|F_o|-|F_c|)^2/\Sigma\omega|F_o|^2]^{1/2}$ and $\omega = \sigma_F^{-2}$. In this data set the weaker reflections were observed to have larger values of $\omega\Delta^2$ ($\Delta = |F_o|-|F_c|$) so the data set was reweighted in ten overlapping groups sorted according to F_o so that $\omega\Delta^2$ across the groups was constant, yielding converged values of R = 0.11 and R_w = 0.165. The occupation parameters refined to 1.00(3) at this stage for all atoms,

indicating no significant deviation from the ideal stoichiometry. Two moderately strong reflections were found to be in very poor agreement with the calculated values, with $||F_o|-|F_c||/|F_o| > 0.85$. These were remeasured and found to be in error. When this restriction was applied to all the reflections 25 additional reflections were eliminated, all with F_c less than 10% of F_o (max), corresponding to those reflections difficult to measure accurately on such a small crystal. Final agreement factors were $R = 0.115$ and $R_w = 0.136$, with a difference Fourier synthesis map flat to $\leq 1 e/Å^3$ in all regions. Some of the reason for the size of the residual secured here was that 64% of the observed reflections occurred at $2\theta > 33°$.

The first crystal examined (with a faster scan) gave an identical chemical structure with all parameters within 3σ of those described above and with the same inherently large residual at first glance, $R = 0.123$. Standard deviations obtained for final refined position and thermal parameters were systematically 30 - 50% greater than for the result described first, an expected result since the number of reflections per variable was lower for this data set because of the faster scanning mode. But there were no systematic trends suggesting a particular type of disorder or imperfection as was observed earlier with Sc_7Cl_{10}, where weak binding between infinite metal chains

composed of double octahedra evidently allowed marked differences in crystal perfection and even in cell volume. Refinement to a residual <10% was possible then but required favorable crystal growth and great patience in searching for that more nearly perfect crystal. We have no reason to suspect this would not be true with Sc_5Cl_8 but our search in this case was only marginally successful.

A comparison of the standard deviations for final positional and thermal parameters of Gd_2Cl_3 (4) and Sc_7Cl_{10} (63) with those reported here for Sc_5Cl_8 shows that the precision of the atom parameter refinement achieved for Sc_5Cl_8 is comparable.

Electron paramagnetic resonance The EPR spectrum was obtained at room temperature on a Varian Model E-3 spectrometer utilizing a 20 mg polycrystalline sample from the same reaction product used for the structural determination. This instrument has a frequency range of 8.8 - 9.6 GHz and a dial-selected magnetic field.

Results

Structure description Table VII provides final positional and thermal parameters for Sc_5Cl_8, and Table VIII lists important interatomic distances and selected angles. Structure factor results are available in Appendix E. The spatial arrangement of all atoms in the unit cell is shown in Figure 9 viewed down the short b axis, while Figure 10

Table VII. Crystallographic data for Sc_5Cl_8

Composition: Sc_5Cl_8, Z = 2

Cell: Monoclinic, C2/m (No. 12)

Lattice Parameters: a = 17.78(2)Å, b = 3.523(8)Å, c = 12.04(1)Å, β = 130.10(6)°

Refinement: R = 0.115, R_w = 0.136 (486 reflections, $2\theta \leq 50°$)

Atom Positions:

	x	y	z	B_{11} [a]	B_{22}	B_{33}	B_{13}
Sc1	0.0	0.0	0.0	1.22(19)	2.12(21)	0.97(17)	0.55(15)
Sc2	0.4882(2)	0.0	0.6136(3)	1.19(14)	0.96(14)	0.85(12)	0.47(10)
Sc3	0.3372(2)	0.5	0.3247(3)	0.87(12)	1.22(14)	0.74(12)	0.36(10)
Cl1	0.2987(3)	0.0	0.4324(4)	1.23(16)	1.35(16)	1.09(15)	0.83(13)
Cl2	0.1328(3)	0.5	0.1033(4)	1.18(17)	1.27(15)	1.39(16)	0.47(13)
Cl3	0.3277(3)	0.0	0.1625(4)	1.25(16)	1.27(17)	0.92(15)	0.49(13)
Cl4	0.5298(3)	0.5	0.2385(4)	1.86(17)	1.67(17)	0.31(17)	1.19(14)

[a] $T = \exp[-\frac{1}{4}(B_{11}h^2a^{*2} + B_{22}k^2b^{*2} + B_{33}\ell^2c^{*2} + B_{12}hka^*b^* + 2B_{13}h\ell a^*c^* + 2B_{23}k\ell b^*c^*)]$. $B_{12} = B_{23} = 0$ by symmetry.

Table VIII. Selected bond distances (Å) and angles (deg.) in Sc_5Cl_8

Distances		Angles	
		Metal Array	
Sc2 - Sc2a	3.021(7)	Sc2 - Sc3 - Sc2b	66.3(1)
Sc3 - Sc2a	3.213(5)	Sc3 - Sc2 - Sc2b	56.86(5)
Sc2 - Sc3	3.222(5)	Sc2a- Sc3 - Sc2c	66.5(1)
		Sc3 - Sc2a- Sc2c	56.75(6)
		Sc2 - Sc3 - Sc2a	56.0(1)
		Sc2 - Sc2a- Sc3	62.2(2)
		Sc3 - Sc2 - Sc2a	61.8(1)
		Chlorine Atoms on Metal Array	
Sc2 - Cl1	2.578(6)	Sc2 - Cl1 - Sc3	78.2(1)
Sc3 - Cl1	2.530(4)	Sc3 - Cl1 - Sc3d	88.3(2)
Sc3 - Cl2	2.799(6)	Sc3 - Cl3 - Sc2a	77.6(2)
Sc3 - Cl3	2.554(4)	Sc3 - Cl3 - Sc3d	87.2(2)
Sc2a- Cl3	2.572(6)	Sc2a- Cl4 - Sc2c	88.7(2)
Sc2a- Cl4	2.667(4)		
		Chlorine Atoms Around Isolated Metal Atoms	
Sc1 - Cl2	2.538(4)	Cl2 - Sc1 - Cl2d	87.9(2)
Sc1 - Cl4e	2.563(5)	Cl2 - Sc1 - Cl4e	89.7(1)

Table VIII. (Continued)

Nonbonded Distances < 3.6Å

Cl1 - Cl1f	3.517(7)	Sc1 - Cl2 - Sc3	133.96(8)
Cl1g- Cl4e	3.541(6)	Sc2a- Cl4 - Sc1h	136.16(9)
Cl1 - Cl2	3.528(6)		
Cl2 - Cl3	3.527(6)		
Cl3 - Cl3g	3.481(7)		
Cl3 - Cl4	3.551(6)		

a = 1 - x, y, 1 - z

b = x, 1 + y, z

c = 1 - x, 1 + y, 1 - z

d = x, y - 1, z

e = x - 1/2, y - 1/2, z

f = 1/2 - x, 1/2 + y, 1 - z

g = 1/2 - x, 1/2 + y, -z

h = x + 1/2, y + 1/2, z

i = -x, -y, -z

j = 1/2 - x, y, -z

k = -x, y, -z

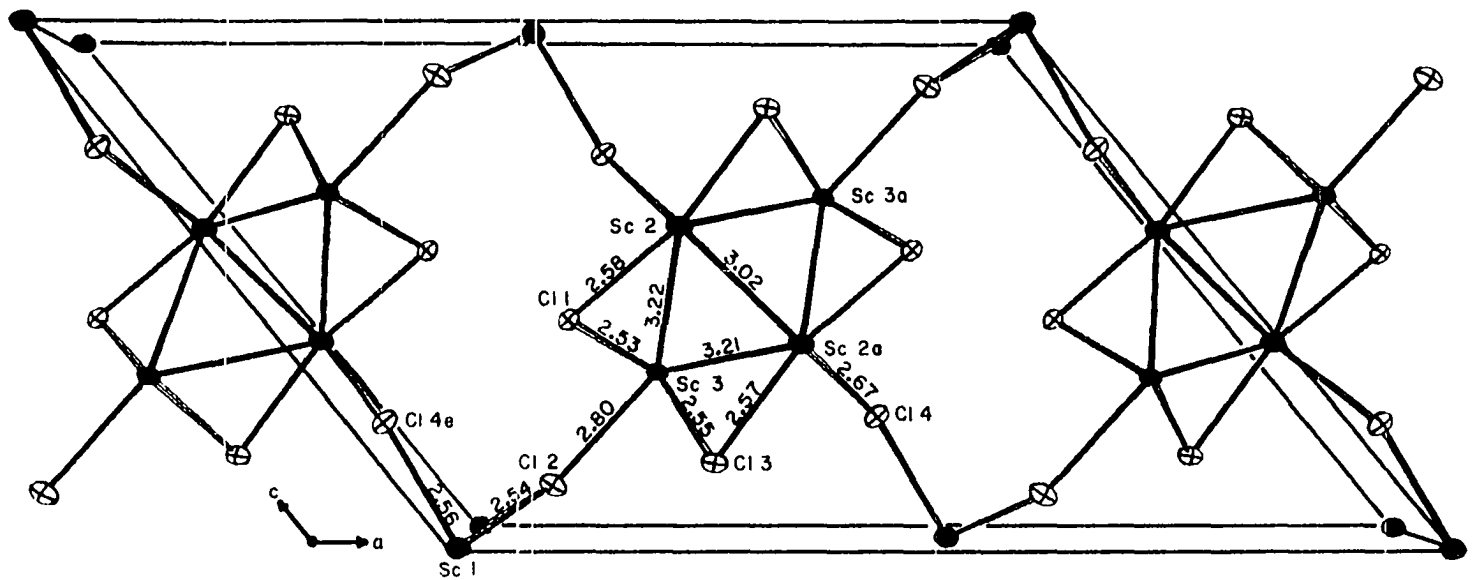

Figure 9. The Sc_5Cl_8 structure viewed down the short b axis. Scandium and chlorine atoms are represented by solid and open ellipsoids, respectively, at 50% probability. Atoms Sc3, Cl2 and Cl4 occur at y = 0.5; all others are at y = 0.

shows the principal features of the metal array and the chlorine atoms which surround the metal chain approximately from the [101] direction. As in Gd_2Cl_3 (4) the clustering of metal atoms forms distorted metal octahedra which then share trans-edges to form scandium chains parallel to the b axis. The distortion of the octahedra is principally in the waist (Sc2, 2a (65)) with two long edges at 3.53Å (the b axis length) and two short edges at 3.02Å which comprise those shared between adjacent octahedra. The apical metal sites (Sc3, 3a) at y = 0.5 are centered over the four waist atoms to within experimental error, 3.222(5) and 3.213(5)Å. The isolated Sc1 atom at (0,0,0) forms a chlorine-bridged chain of single metal atoms along b with the same 3.53Å repeat. Both the chlorine-bridged chain and the chain of metal octahedra are related to an adjacent chain by a displacement of b/2 in an alternating manner throughout the crystal.

As has been the case in all the scandium chloride phases investigated structurally to date (38,53,63), all halogen atoms have three metal neighbors. Chlorine atoms 1 and 3 cap the outward facing scandium triangles of the cluster but in a manner not seen before, occupying the metal triangles between apices of the octahedra (e.g., Sc2-Sc3-Sc3d, Figure 10). This allows a higher coordination of chains by chlorine than would result from capping outward

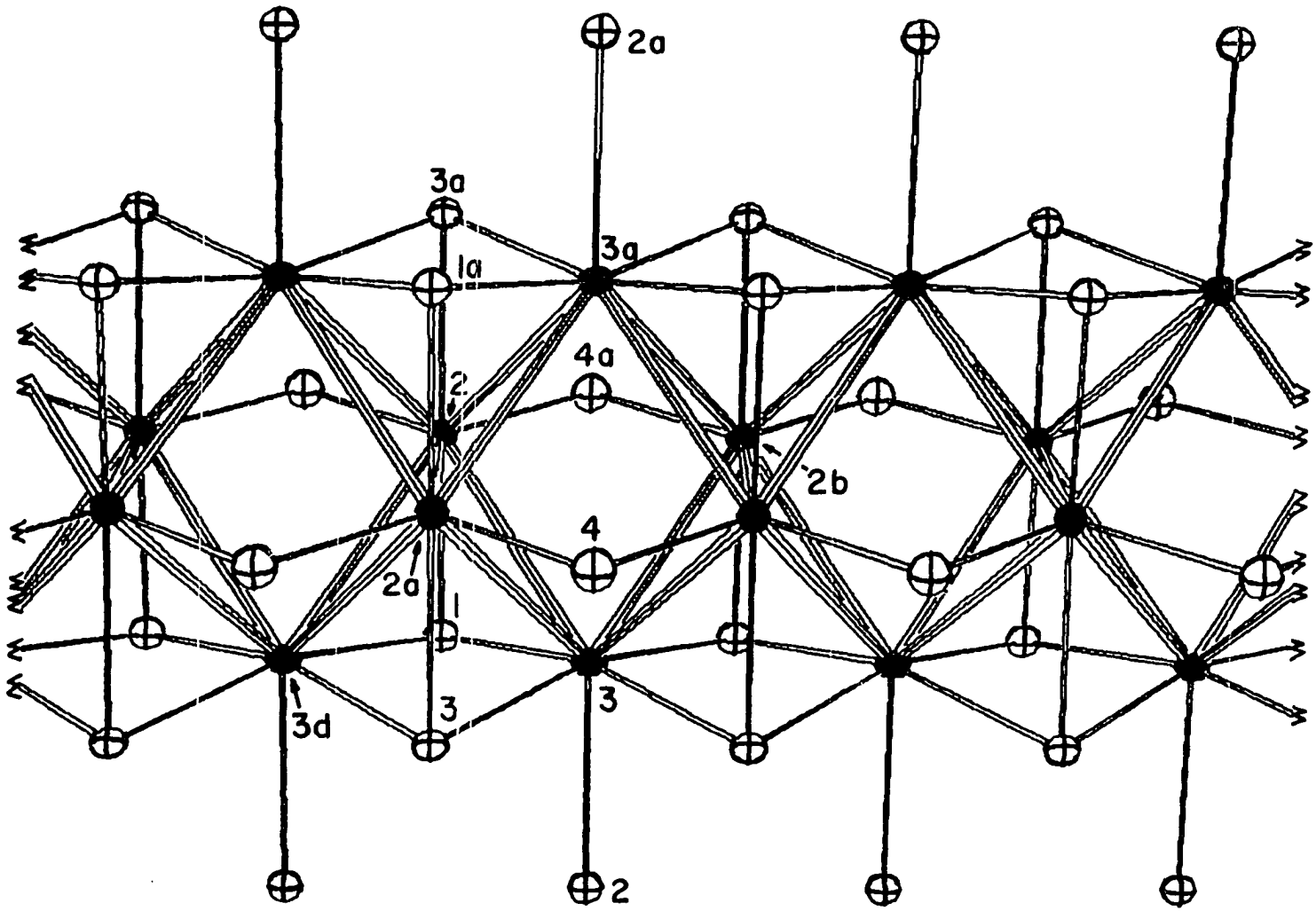

Figure 10. The anionic polymetal chain in Sc_5Cl_8 with the b axis horizontal. Solid ellipsoids represent scandium; open, chlorine. The letters in atom identifications refer to symmetry operations, Table VIII.

facing triangles of the octahedra (2-2b-3) which would thereby crowd the halogen atom Cl4 situated on the long waist edge of each octahedron. Finally, Cl2 bonds to the metal cluster at the apices in an exo-fashion at a distance which is somewhat longer, 2.80Å compared with 2.53 to 2.67Å for the other metal-chlorine bond distances. These are very typical scandium-chlorine distances relative to 2.58Å in $ScCl_3$ (34), 2.59Å in ScCl (38) and 2.44-2.70Å in Sc_7Cl_{10} (63), which again serves to emphasize the apparent disposition of the reduction electrons within the chains.

The isolated metal sites, Sc1, presumably consist of tripositive scandium based on both the scandium-chlorine distances and the absence of a detectable EPR transition. The Sc1 atoms are coordinated by chlorine atoms 2 and 4 to generate only slightly distorted octahedra of halogen atoms which share trans-edges parallel to b, as depicted in Figure 11. Chlorine atoms 2 and 4 serve to connect the two rather different structural environments of the isolated scandium atoms and metal chains and both appear somewhat more tightly bound to the scandium(III) atoms than to the chains based on distances.

Discussion

Single crystal x-ray diffraction has proven to be a valuable tool in unraveling the structural and compositional

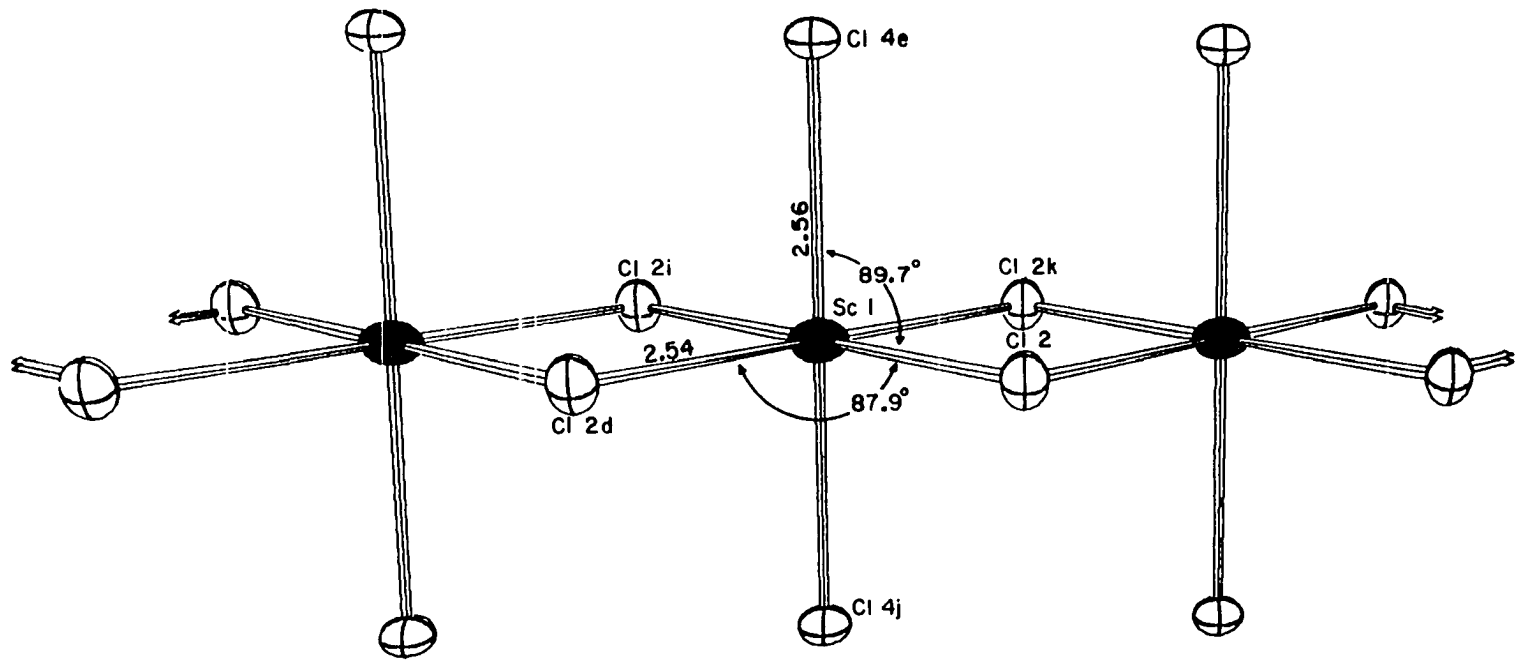

Figure 11. The chlorine-bridged chain about the isolated scandium(III) atoms.

relationships between the phases in the region 2.0 $\leq$ Cl:Sc $\leq$ 1.0 where the earliest studies (38, 63) indicated what appeared to be an unusually large number of distinct phases unrelated by simple structural principles. The remarkable variety in structure which is achieved with small changes in composition can best be appreciated and understood by considering first the metal sub-structure and then the arrangement of the halogen atoms around this metal array and the linkages which exist. The atom connectivity scheme developed before (11) for discrete clusters also provides a useful description of the Sc_5Cl_8 structure, viz.,

$$[Sc(Cl2)_{4/3}(Cl4)_{2/3}]_\infty[Sc_4Cl_4(Cl4)_{4/3}(Cl2)_{2/3}]_\infty ,$$

where the first portion represents the isolated Scl groups (Figure 11) and the second, the metal bonded chain of interest (Figure 10). In this assignment the one long Cl2-Sc3 distance, 2.80Å, is assumed to be equivalent to all other metal-halogen bonds in the sense of formal electron distribution. With consideration of all distances the simple distribution $(ScCl_2^+)_\infty(Sc_4Cl_6^-)_\infty$ seems appropriate and is in keeping with the anionic nature of the metal array also found in both Sc_7Cl_{10} (63) and Sc_7Cl_{12} (53).

The metal array found in Sc_5Cl_8 is very much like that in Gd_2Cl_3 where M_6 clusters have also linked through shortened trans-edges to form an infinite chain running parallel to the b crystal axis. The distance between the

scandium metal atoms on the shared edges, 3.021(7)Å, is the shortest metal-metal bond yet observed for scandium and compares with the shortest distance of 3.26Å in the metal (33), 3.216(6)Å in ScCl (38), 3.147(3)Å in Sc_7Cl_{10} (63) and 3.204(2)Å in Sc_7Cl_{12} (53). In Gd_2Cl_3 the analogous short distance is 3.349(1)Å vs. 3.604Å in the metal. In both compounds the presence of the especially short metal-metal bond on the shared trans-edge emphasizes the alternate description of the array in terms of parallel dimeric metal units bridged by capping metal atoms.

If two chlorines are formally allocated to the isolated scandium(III) the anion chain in this compound and the metal chain in Gd_2Cl_3 have the same X:M ratio (M_4X_6). But because of the presence of the isolated scandium(III) ion the average number of valence electrons per metal site in the chain in Sc_5Cl_8 is greater than in Gd_2Cl_3 even though the average oxidation state in the gadolinium compound is less. The simplest manifestation (11) of a greater effective reduction should be found in the $\Delta\underline{d}/\underline{d}$ ratio where $\Delta\underline{d}$ is the relative shortening of a bond compared with the average metal-metal distance $\underline{d}$ in the 12-coordinate metal. The $\Delta\underline{d}/\underline{d}$ value of 0.07 for the short bond in Gd_4Cl_6 compares with 0.08 for the corresponding bond in $(ScCl_2^+)(Sc_4Cl_6^-)$, a small difference which is at least in the right direction in terms of electron count. More strikingly,

the apical to waist atom distances in the gadolinium compound are both slightly longer than the average metal-metal distance, while in Sc_5Cl_8 these distances are less, $\Delta d/d = 0.02$.

Surprisingly, this sort of comparison may be extended fairly well to all of the reduced scandium compounds as well as to Gd_2Cl_3 in spite of the diversity of bonding arrangement and electronic structures. Table IX lists for the phases ScCl, Sc_7Cl_{10}, Gd_4Cl_6, Sc_5Cl_8 and Sc_7Cl_{12} the average number of bonding electrons per metal atom together with all significant metal-metal distances and their multiplicity per metal atom. Finally, the Pauling bond orders n (where $d_n = d_1 - 0.60 \log n$) summed over all distances are listed. As shown in Figure 12, the marked irregularities and contrasts now all disappear, and the total bond order per metal is seen to closely parallel the number of bonding electrons, including for Gd_2Cl_3! Even the status of Sc_7Cl_{10} is clarified. This compcund has been found to exhibit a sharp EPR signal and a magnetic moment which closely corresponds to two separate d^1 states per formula unit (Sc_7Cl_{10}) if Curie-Weiss behavior is assumed. The correlation shown in Figure 12 supports this in the sense that the bond order sum found appears too low when compared with that expected for all 11 electrons per repeating unit whereas fewer bonding electrons (but >9) would be more consistent.

Table IX. Stoichiometry and bonding electrons, bond distances and bond orders in scandium and gadolinium metal-metal bonded arrays

	ScCl	Sc_7Cl_{10}	Gd_4Cl_6	Sc_5Cl_8	Sc_7Cl_{12}
Cl:M	1.00	1.43	1.50	1.60	1.71
Bonding electrons per M in sheet, chain, or cluster	2.00	1.83[a] (1.50)[b]	1.50	1.75[a]	1.50[a]
M-M distances (Å) (Frequency per M)	3.22(x3) 3.47(x6)	3.15(x4/3) 3.26(x8/3) 3.41(x4/3)	3.35(x1/2) 3.74(x4)	3.02(x1/2) 3.22(x4)	3.20(x2) 3.23(x2)
Σ Pauling Bond Order[c]	1.70	1.51	1.37	1.63	1.32

[a]One isolated Sc(III) ion per formula unit is presumed to have donated 3 electrons to the metal-metal bonded unit.

[b]Alternate value assuming 2 of 11 electrons per six metal atoms in the metal-metal bonded repeating unit are localized and nonbonding.

[c]$d_n = d_1 - 0.60 \log n$, n = bond order; d_1(Sc) = 2.924Å, d_1(Gd) = 3.264Å (reference 33).

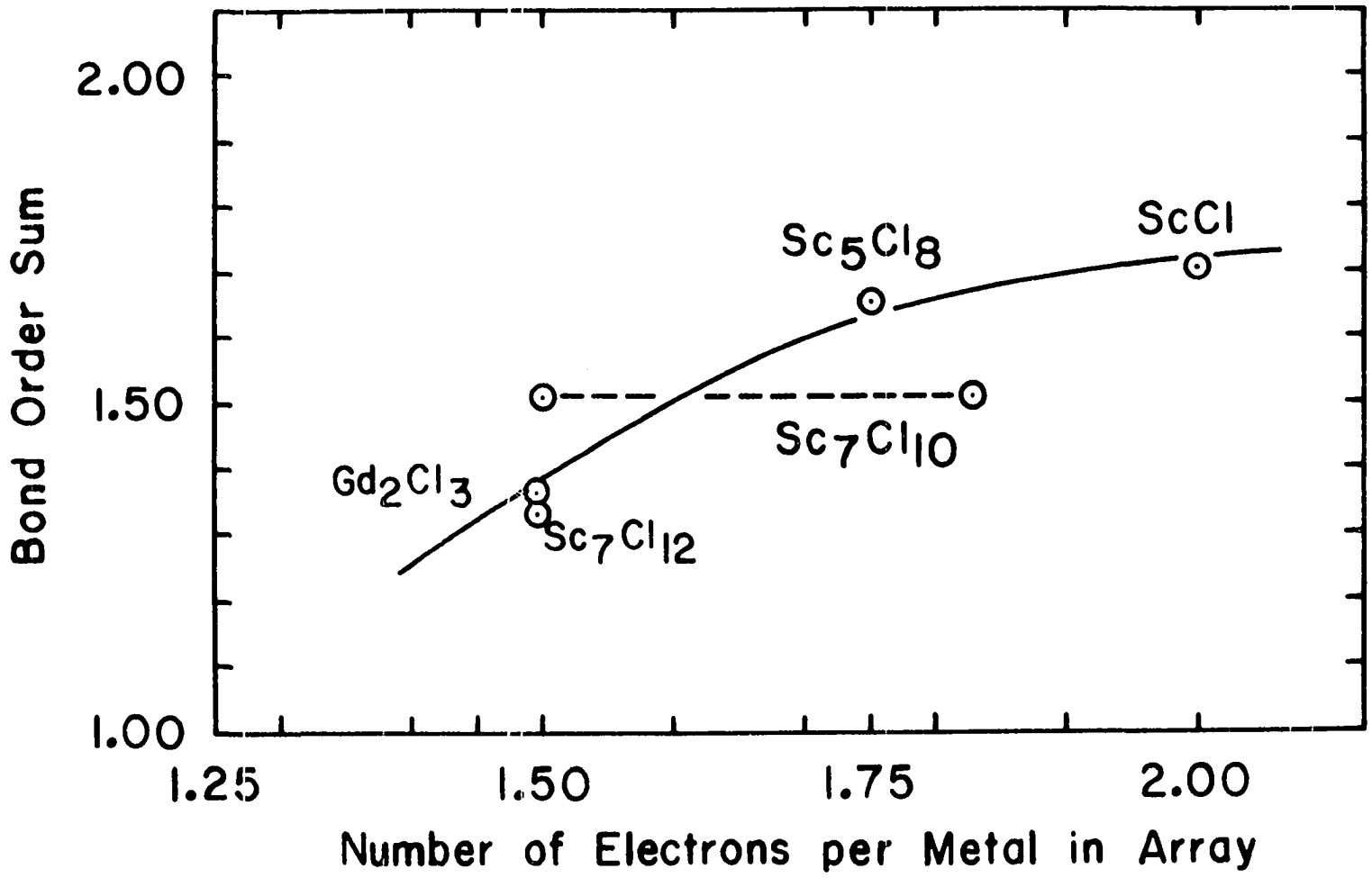

Figure 12. The number of electrons per metal atom in the cluster, chain, or sheet vs. the sum of Pauling bond orders for all metal-metal bonds. The dotted line for Sc_7Cl_{10} represents the range possible, corresponding to 11 (right) or 9 (left) electrons per repeating unit (see text).

In these chain structures the halogen atoms complete the structure in a remarkably versatile fashion and ultimately determine the traditional definition of the degree of reduction X:M. In order to generate the anionic chain in Sc_5Cl_8, octahedral sites for the isolated scandium(III) cation must be created in the anion sublattice. The M_4X_6 units in Sc_5Cl_8 have separated in relation to those in Gd_4Cl_6 so that half the halogen atoms on triangular faces of the chain are no longer exo to a waist metal atom in a neighboring M_6 chain cluster. Moreover, the capping halogen atoms occur over the triangular face situated between apices of the condensed clusters, and as such belong wholly to the chain. Now the exo positions are occupied by the apical Cl 2 and in a sense by Cl 4 bridging the long edge of the octahedra, both of which simultaneously complete the anion sublattice and create the octahedral interstice necessary for the isolated metal atom. Another important difference is the decrease in chlorine-chlorine repulsion relative to those in Gd_4Cl_6. There the shortest distances between face capping and bridging halogen atoms are 3.22 and 3.34Å vs. 3.48Å here, the rearrangement being dictated in part by the smaller size of the triangular faces with the scandium compound.

We now begin to understand the ways the metal and anion sublattices adapt to one another to create new

structures with slightly different compositions. There are clearly major electronic requirements in the metal bonded arrays as well, as witnessed by the strong proclivity to form anion states, but we are well short of understanding these. The versatility of scandium in creating these new structures certainly must depend at the very minimum on both its ability to readily form the relatively low charged scandium(III) counter-cation, thereby allowing the generation of anionic chains, and a sufficient radial extension of the valence orbitals to form shortened metal-metal bonds. To date neither titanium or zirconium appear capable of generating (or needing) isolated M(IV) cations, and we have not succeeded in generating strongly metal-metal bonded or metallic examples of titanium halide systems. Zirconium does form both ZrCl (27) analogous to ScCl and $(Zr_6Cl_{12})Cl_3$ (53) which is isoelectronic with Sc_7Cl_{12}.

The disposition of halogen in the anion chain in Sc_5Cl_8 (Figure 10), namely, edge bridging rather than face capping as found in the extended chains in Gd_2Cl_3 and Sc_7Cl_{10}, provides a new perspective for the <u>hypothetical</u> cluster condensation reactions. Edge-bridging by halide in isolated clusters such as $Ta_6Cl_{14}^{2+}$ is well known (11), and a structurally comparable anion is known in $Sc(Sc_6Cl_{12})$ (53). In all of these the presence of a polar solvent, a basic group, or condensation into the solid state invariably

causes occupation of secondary exo or outward pointing orbitals of the octahedron. A similar behavior is also observed in the present structure with Cl2 as well as in Sc_7Cl_{10} and in $Sc(Sc_6Cl_{12})$, where half of the bridging halide in one cluster occupy exo positions in neighboring clusters, that is $M_6X_6^{i}X_{12/2}^{i-a}$ (66). In Sc_5Cl_8 the particular arrangement of Cl1, Cl3 and Cl4 only over edges of the scandium chain seems particularly significant in that the anion $(Sc_4Cl_6^-)_\infty$ can be viewed as the first example of the condensation of edge-bridged M_6X_{12} polyhedra. The corresponding condensation of face-capped M_6X_8 clusters (as found in $MoCl_2$ and Nb_6I_{11}) to yield the infinite chain in Gd_2Cl_3 has been described by Simon (9), and Sc_7Cl_{10} also provides a further example. The cluster condensation to yield both the cation and anion chain in Sc_5Cl_8 can be accomplished in a particularly simple way from the phase $Sc(Sc_6Cl_{12})$, as depicted in Figure 13. Stoichiometrically the conversion amounts to the reaction where conceptually

$$Sc(Sc_6Cl_{12})(s) \rightarrow (ScCl_2)(Sc_4Cl_6)(s) + 2ScCl_2(g)$$

two $ScCl_2$ groups as well as two bridging chlorine atoms split off what will become the common face and shared metal edge, with the latter combining with the isolated scandium(III) ion to form the infinite $ScCl_2^+$ chain. To generate the rest of the structure one has only to pack these $(\bar{1}01)$ sheets (the short diagonal in Figure 9) together

Figure 13. A representation of the condensation of $Sc(Sc_6Cl_{12})$ to yield a section of the $(\bar{1}01)$ sheet in the structure of Sc_5Cl_8. The overall reaction is $Sc(Sc_6Cl_{12}) \rightarrow Sc_5Cl_8 + 2ScCl_2$; the $ScCl_2$ units removed at the condensation points are circled. The structure is completed by packing these sheets so that Cl4 atoms which bridge the long edges of the octahedra in the $(Sc_4Cl_6^-)_\infty$ chain also comprise the apices of the shared octahedra in the $(ScCl_2^+)_\infty$ chain (dashed circles).

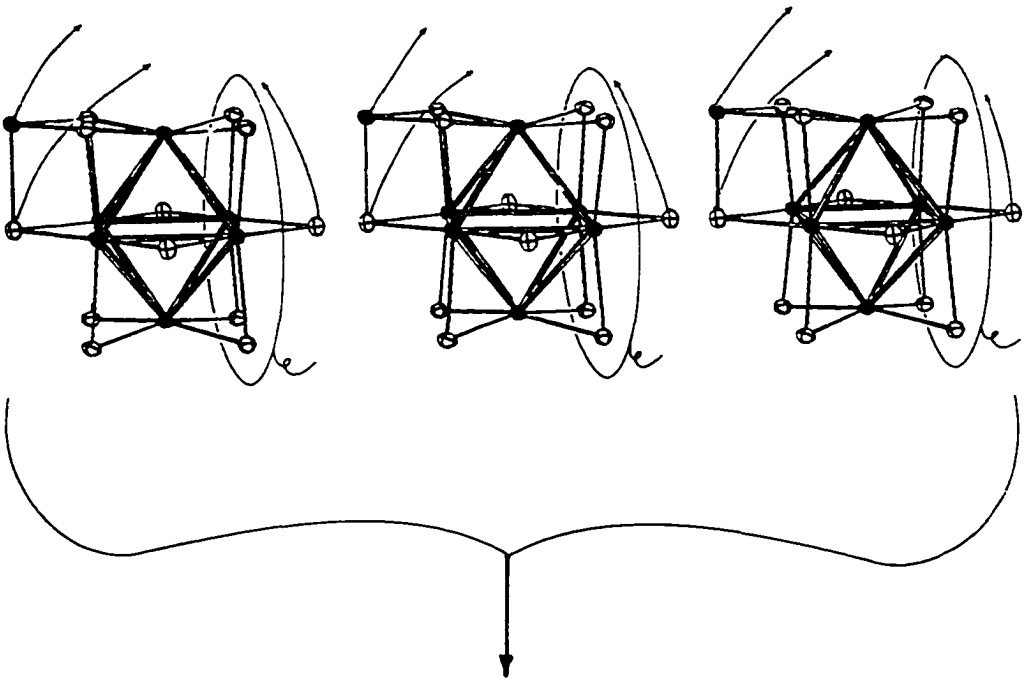

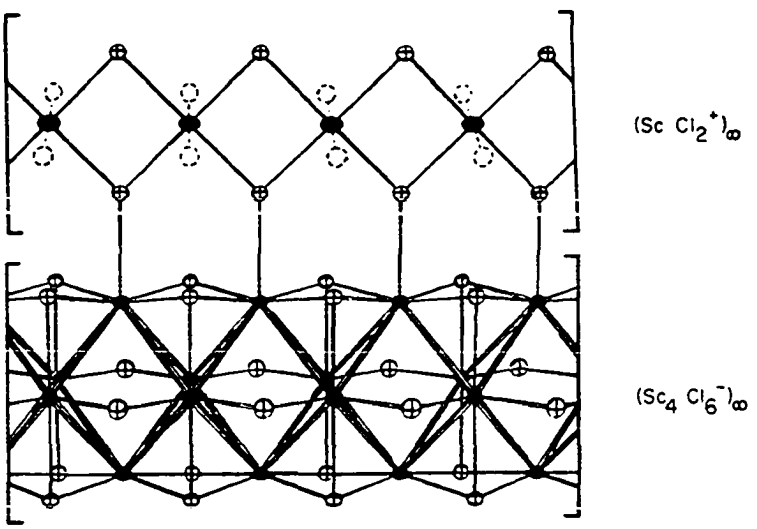

$$Sc\ (Sc_6Cl_{12}) \longrightarrow (ScCl_2)(Sc_4Cl_6) + 2ScCl_2$$

so that Cl4 atoms which edge-bridge the metal chain also form the apices of the chlorine octahedra in the $ScCl_2^+$ chain in another sheet (the dotted atoms in Figure 13).

The preparative methods available are only beginning to allow the characterization of phase-pure metal-rich scandium halides by methods other than x-ray crystallography. As a result, the nature of the electron distribution in these highly anisotropic materials is by no means clear and additional physical measurements are needed. The phase Sc_7Cl_{10} provides an interesting comparison with Sc_5Cl_8 where only the former gives a detectable EPR signal. This result clearly supports the assignment of scandium(III) to the isolated scandium atoms (0,0,0) contained in the edge-shared chloride octahedra which are found in both phases. This is consistent with the scandium-chlorine bond distances found for the isolated metal site and the resultant effective reduction of the metal array as shown by the relative shortening of the metal distances ($\Delta\underline{d}/\underline{d}$ ratios and Figure 12). The weak, temperature-dependent paramagnetism measured for Sc_7Cl_{10} (63) appears to arise from localized nonbonding paramagnetic centers associated with some but not all of the metal atoms in the metal array. Sc_2Br_3 (5) also has been found to have a similar susceptibility. Judging from its lack of a detectable EPR signal Sc_5Cl_8 may be expected to behave in a more conventional fashion, with a simple

temperature-independent Pauli paramagnetism, although this has not been verified to date experimentally.

One of the most fascinating aspects of the chemistry in the reduction of $ScCl_3$ has been the formation of the new solid state compounds Sc_7Cl_{10}, Sc_7Cl_{12} and, in particular, Sc_5Cl_8 by vapor phase transport. The molecular transporting species is probably $ScCl_2(g)$. Hastie and co-workers (67) have reported the formation of $ScCl_2(g)$ from reaction of gaseous $ScCl_3$ with Sc metal at 1450°C followed by isolation in a solid argon matrix and ir examination. In our synthesis work isothermal and stoichiometric reactions involving metal and $ScCl_3$ and solid-liquid or solid-gas conditions have all been unsuccessful routes to compositions Cl:Sc > 1.5. The formation of compounds which are very incongruent melting from either a melt or the metal by a reaction requiring substantial diffusion certainly is kinetically hindered although thermodynamically the compounds appear quite stable. The disproportionation of a lower valent vapor species such as $ScCl_2$ would, on the other hand, provide a direct and facile transport reaction, viz.,

$$7ScCl_2(g) = Sc_5Cl_8(s) + 2ScCl_3(g) \ .$$

Empirical evidence based on observation suggests that there are several competing processes and that, depending on conditions, compounds as oxidized as Sc_7Cl_{12} and as reduced as the metal itself will deposit. Simple condensation of

stable dichloride has not been observed. A possible structure for $ScCl_2(s)$ would be the neutral cluster $Sc_6Cl_6^{i}Cl_{12/2}^{i-a}$, isostructural with the recently characterized Zr_6I_{12} (53), and an energetically more favorable alternative to the layered CdI_2 or $CdCl_2$ types common to the majority of the transition metal dihalides. However, only the 9 electron cluster $[Sc^{3+}][Sc_6Cl_6^{i}Cl_{12/2}^{i-a}]^{3-}$ has been prepared to date, and the stoichiometric dichloride with only 6 bonding electrons may be too electron deficient to be stable.

Less Investigated $ScCl_x$ Compositions

Seven distinct phases have been recognized to date in the binary Sc-$ScCl_3$ system, four of which have been discussed extensively in the preceding sections. The remaining phases have all been identified by x-ray powder diffraction and analyzed either by chemical analysis or microprobe. These compositions are $ScCl_{1.50(3)}$, $ScCl_{1.45(3)}$, and $ScCl_{1.40(7)}$.

$ScCl_{1.50}$

Scandium sesquihalide was the first (5) reduced phase identified in the binary system and is conveniently prepared by the straightforward gas-solid reaction

$$Sc(s) + ScCl_3(g) \xrightarrow{800°C} 2ScCl_{1.5}(s) .$$

In this reaction 0.5 - 1.0 gram of scandium trichloride in one end of a tantalum reaction tube and metal foil (excess) in the other are equilibrated under isothermal conditions. The combination of a relatively low reaction temperature, moderate trihalide activity, limited metal surface area, and isothermal conditions maximize the conditions under which the compositionally intermediate phase $ScCl_{1.5}$ can be prepared.

Since compositions more reduced than Cl:Sc = 1.5 can be prepared, the combination of $ScCl_{1.5}$ on Sc must be a metastable system. The phase $ScCl_{1.5}$ itself probably is not metastable since thermal analysis indicates a quite ordinary peritectic decomposition at 877°C. The reaction is not completely reversible in the relatively short time period of a thermal analysis experiment. Upon cooling, the solidification process is supercooled by 20-30°C and, as expected, the recombination reaction is not complete and an eutectic halt near 800°C is observed. The solid products found on cooling are always amorphous or poorly crystalline so as to be difficult to recognize with x-rays. In general $ScCl_3$ can be identified which is consistent with the observed eutectic halt.

Unfortunately, $ScCl_{1.5}$ has never been observed to transport and satisfactory single crystals have yet to be prepared. A structure based on the composition $ScCl_{1.50}$ may be postulated to be $(ScCl_2^+)_\infty(Sc_5Cl_7^-)_\infty$. The five metal

atom anionic array would be intermediate between the four and six metal atom arrays found in the two compositions that bracket this phase. Several very plausible orientations are possible and each gives rise to a significant anisotropy in the metal array. The arrangement of five metal atoms would almost certainly be the fragment of hcp scandium metal itself:

In the direction of propagation the metal-bonded array perhaps would be stacked in a continuous sequence AA••• thereby creating three chains of shared prisms. An alternative hexagonal sequence AB••• would result in chains of face-sharing antiprisms. Or perhaps the metal array would resemble the distorted octahedra up to now always observed and the fifth metal atom will more or less simply be added onto the chain of octahedra. This can be seen quite easily in Figure 3. Here four of five metal atoms ($Sc2\text{-}3\text{-}4\text{-}4^{a}$) form the propagating chain of trans-edge shared octahedra and a fifth atom ($Sc3^{a}$) forms an M_4-type distorted tetrahedron ($Sc4\text{-}4^{b}\text{-}4^{a}\text{-}3^{a}$). Still yet another possibility may be the composition is determined by the nonmetal linkages between the metal fragments as in Gd_2Cl_3 but of a different mode since the two are not isostructural.

Additional effort in the determination of the structure of $ScCl_{1.5}$ would seem well worth the effort. The reaction

$$2ScCl_{1.5}(s) + ScCl_3(g) = 3ScCl_2(g)$$

may be possible if the reductant metal (foil) needed to generate the low valent vapor species is kept in a hot region (~900°C) and the gradient extends to lower temperatures (~800°C) than previously employed. Or perhaps a prepared reduced composition Cl:Sc = 1.5 could be placed in the hot end of a tube (>877°C) and allowed to disproportionate and reform via $ScCl_2(g)$ in a cooler region.

$\underline{ScCl_{1.45}}$

$ScCl_{1.45}$ can be prepared by the disproportionation of $ScCl_{1.5}$ at 877°C but <900°C. The growth habit of this material is similar to $ScCl_{1.5}$ and as a result whiskers with a sufficiently large cross section for single crystal work have never been observed. The powder x-ray diffraction pattern is unique among all the scandium chlorides and is striking in two respects. First, there is such a multitude of narrowly and more or less evenly spaced diffraction cones starting at very low angles that it becomes difficult to imagine how a simple binary compound could adopt a structure sufficiently complex to explain the observed pattern. Second, $ScCl_{1.45}$ is itself metastable, decomposing exothermically in the range 890-895°C. The solid product

of this decomposition is the better characterized phase $ScCl_{1.43}$ (Sc_7Cl_{10}). The prospect of single crystals of $ScCl_{1.45}$ considering its whisker growth, narrow stability range, and apparent metastability is not good. In the upcoming photoelectron section the x-ray p.e. spectra of this material will be compared with that of Sc_7Cl_{10} with some striking and interesting results.

$ScCl_{1.40}$

Of the seven known binary $ScCl_x$ phases, the one remaining to be discussed is $ScCl_{1.40}$. This phase is typically black, reflective and nicely crystalline. X-ray powder diffraction indicates a well ordered phase with a cell of reasonable dimensions. Based solely on the composition, the stoichiometry may be guessed to be $(ScCl_2^+)_\infty(Sc_7Cl_9^-)_\infty$ or $ScCl_{1.38}$. This model is consistent with the anionic metal unit found in Sc_7Cl_{10} (63) adding one more metal atom to the six atoms in the metal array. Very nice single crystals of the phase have been grown by chemical transport but unfortunately with dimensions too small for data collection. The transport reaction conditions have been described previously (59) and involved a large gradient over an equally long tantalum reaction container. These conditions have always given rise to small crystals and profuse nucleation and growth.

The disproportionation sequence $ScCl_{1.5}$ $\xrightarrow{877°C}$ $ScCl_{1.45}$ $\xrightarrow{890\text{-}5°C}$ $ScCl_{1.43}$ should be further tested using thermal analysis in order to determine the decomposition temperature of $ScCl_{1.43}$ and the solid product of this decomposition. If the preceding sequence is any gauge the temperature of decomposition will probably be in the 910-920°C range. Hopefully, the product will be the phase now identified as $ScCl_{1.40}$. If true, once the decomposition temperature of $ScCl_{1.43}$ is known a more controlled approach can be made to a gradient experiment. On the other hand careful equilibration of a Cl:Sc = 1.40 composition at or slightly above the decomposition temperature of $ScCl_{1.43}$ may yield crystals of $ScCl_{1.40}$.

$ScCl_x$

Two regions immediately apparent where little is known about the nature of x are: $1.40>x>1.0$ and $x<1.0$. Will $ScCl_{1.40}$ decompose at some still higher temperature to form yet another intermediate solid phase or will ScCl be the product? Are compositions with Cl:Sc < 1.0 stable and if so, how can this reduction be accomplished? Considering the role of kinetics in the formation of extended metal-bonded arrays this is not an easy question to answer. Perhaps Sc_2Cl can be prepared analogous to Hf_2S (68) or the more metal-rich composition Sc_6Cl like Ta_6S (69).

Photoelectron Study of Two Reduced Scandium Chlorides

As revealed through their structure determinations, the reduced scandium chlorides characteristically have contained extensive metal-metal bonded arrays. The regular and undistorted periodicity of the metal lattice indicates (70) the possibility of electronic conduction. Traditionally, studies of conductivity and magnetic susceptibility as a function of temperature have been used to characterize the metallic state. Since metallic properties are attributed to itinerant electrons in the valence shells, the metallic state may also be studied by the relatively new technique of photoelectron spectroscopy (71,72,73). For the metal-rich scandium chlorides photoelectron spectroscopy offers some distinct advantages over other methods. Most important the general sample handling techniques and high vacuum technology required for ESCA are well suited for the study of reactive materials. This combination makes UV-XP spectroscopy a valuable new technique.

The compositions $ScCl_{1.45}$ and $ScCl_{1.43}$ (Sc_7Cl_{10}) were studied because their synthesis reactions allowed phase pure samples to be prepared. They were prepared as previously described (63) in sealed tantalum reaction containers which were only opened in the dry box attached to the spectrometer, and were mounted and inserted into

the high vacuum chamber in a matter of minutes. Full scan x-ray spectra showed little or no oxygen and carbon contamination. In fact, in order to obtain UV results low power 0.5 kV - 5 ma etches for 15 minutes were sufficient to remove absorbed surface carbon and oxygen containing species. The spectra in Figures 14 and 15 are of remarkable quality compared with the uninterpretable spectra of surface contaminated samples which contained multiple and broad bands.

Electron binding energies for core and valence levels of $ScCl_{1.45}$ and Sc_7Cl_{10} were measured along with appropriate core levels for scandium metal and scandium trichloride needed for reference. Table X summarizes these results. $ScCl_{1.45}$ and Sc_7Cl_{10} were found to be good conductors in the sense no amount of charging could be detected.

For an electrically conducting sample in contact with a spectrometer (74), the photoionization process can be described by the equation:

$$E_{B_F} = h\nu - E_k - \phi_{sample}$$

In this equation the initial photon energy, $h\nu$, is conserved and partitioned among three terms: (1) E_{B_F}, the binding energy of the level of interest referenced to the Fermi level, (2) E_k, the kinetic energy of the photoelectron, and (3) ϕ_{sample}, the work function of the sample.

Figure 14. Valence band (VB) regions (raw data).

(a) Ultra-violet photoelectron spectrum from Sc_7Cl_{10} (25 volts-256 channels, 10 scan composite).

(b) X-ray photoelectron spectrum from Sc_7Cl_{10} (25 volts-256 channels, 175 scan composite).

(c) X-ray photoelectron spectrum from $ScCl_{1.45}$ (25 volts-256 channels, 65 scan composite).

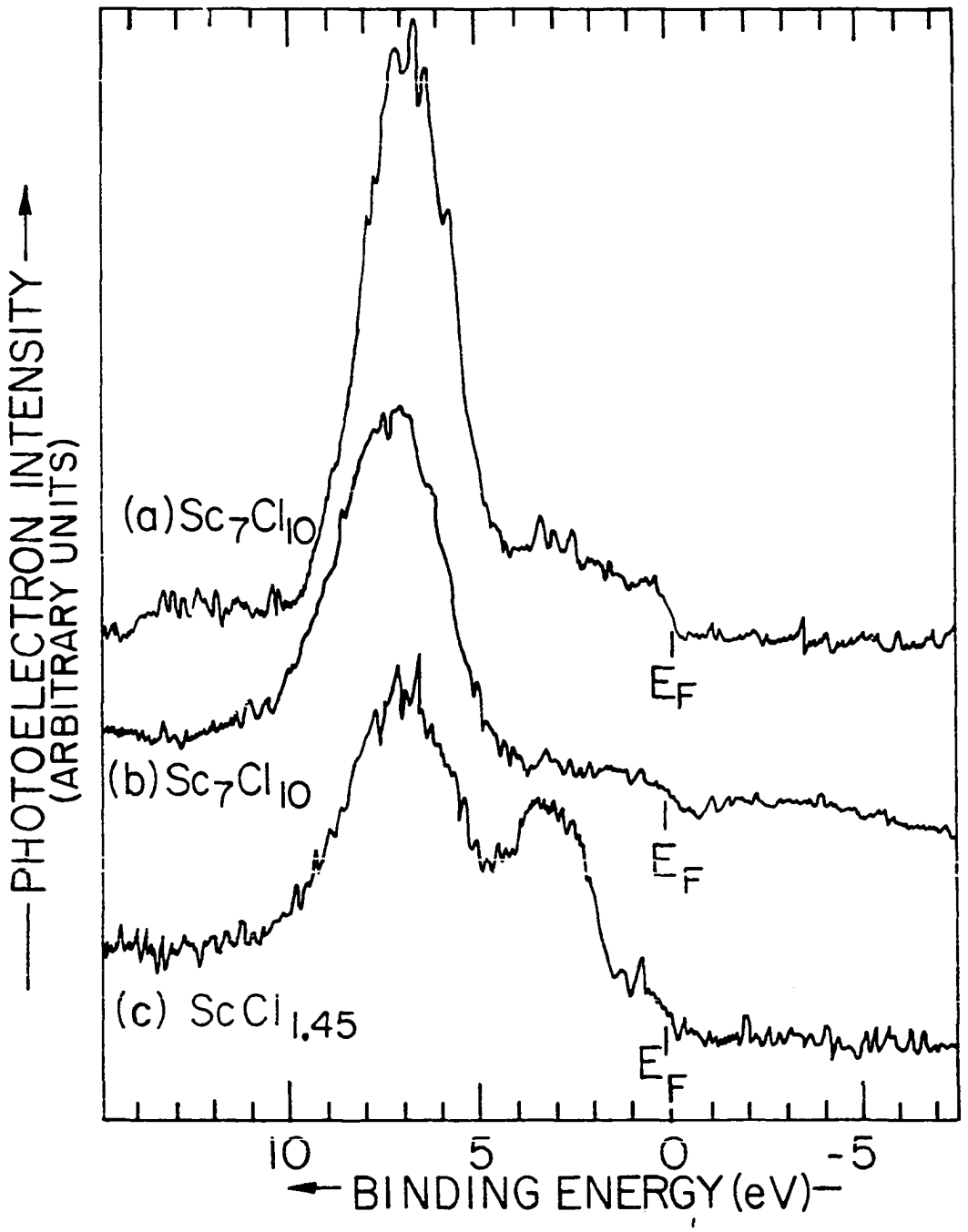
PHOTOELECTRON INTENSITY
(ARBITRARY UNITS)
(a) Sc_7Cl_{10}
(b) Sc_7Cl_{10}
(c) $ScCl_{1.45}$
E_F
E_F
E_F
10
5
0
-5
BINDING ENERGY (eV)

Table X. X-ray photoelectron binding energies for Sc, Sc_7Cl_{10}, $ScCl_{1.45}$ and $ScCl_3$ in eV[a]

	Level	Sc	Sc_7Cl_{10}	$ScCl_{1.45}$	$ScCl_3$[b]
Sc	VB(4s-3d)	X	0.0-5.0	0.0-5.0	X
Cl	3p	X	7.0	7.0	6.4
Sc[c]	$2p_{3/2}$	398.7	399.2	400.2	X
Sc[c]	$2p_{1/2}$	403.4	403.5	404.2	X
Sc[d]	$2p_{3/2}$	X	404.2	not observed	404.0
Sc[d]	$2p_{1/2}$	X	408.5	not observed	408.5
Cl	$2p_{3/2}$	X	200.2	200.2	200.1
Cl	$2p_{1/2}$	X	201.3	201.3	201.2

[a] All values ±0.2 eV.

[b] Au correction 1.4 eV.

[c] Metallic scandium.

[d] Ionic scandium(III).

The actual measured kinetic energy of the ejected electron will be E_k^*; however, since the photoelectron will be accelerated by an amount equal to the difference between the sample and spectrometer work functions. E_{B_F} can be calculated by the equation:

$$E_{B_F} = h\nu - E_k^* - \phi_{spectrometer}$$

The calibration term for the Ames Laboratory spectrometer was determined against the reported (75) absolute binding energies:

Ag $3p_{3/2}$	573.2	±	0.2 eV
Ag $3d_{5/2}$	368.0	±	0.2 eV
Au $4f_{7/2}$	84.0	±	0.2 eV
Pd $3d_{5/2}$	335.5	±	0.2 eV
Pt $4f_{7/2}$	71.3	±	0.2 eV

Based on the absolute assignment of the Ag $3d_{5/2}$ level at 368.0 eV all the other levels in the list were measured and found to be within ±0.2 eV (76) of those reported. The calibration term for the Argonne spectrometer was based on the Au $4f_{7/2}$ level at 84.0 eV (77).

In Table X the entries for scandium trichloride have an additional correction term for the mean steady state potential, Q_{CH}, commonly referred to as charging, that is rapidly established at the sample surface of insulating materials. No evidence for differential charging, such as

multiple or broadened peaks, was detected. Vacuum deposition of a small amount of gold (78) was used to calculate the magnitude of Q_{CH}.

In Figure 14, spectrum 14(a) is the valence region for the compound Sc_7Cl_{10} recorded with an ultraviolet He(I) photon source. Spectrum 14(b) is the valence region for the same sample but recorded with Al K_α x-rays and in 14(c) the x-ray VB region of $ScCl_{1.45}$ can be compared. In Figure 15, the Sc 2p core level for both Sc_7Cl_{10} (15(a)) and $ScCl_{1.45}$ (15(b)) are shown along with the Cl 2p level for each compound, respectively.

All x-ray spectra shown were recorded with an unmonochromatized source. Monochromatization was used on occasion when the better resolution possible may have added detail to a spectrum. One such case was the Cl 2p band for Sc_7Cl_{10} in Figure 15(c). In this compound there are five crystallographically unique chlorine atoms and differentiation of these sites was considered a possibility, but none could be resolved.

Based on the data in Table X and Figures 14 and 15, the following comparisons and conclusions can be made:

(1) The metallic nature of $ScCl_{1.45}$ and Sc_7Cl_{10} can be attributed to the free valence electrons filling the valence band up to the Fermi level (E_F=0) resulting in the photoelectron intensity, PI(E), observed. The

Figure 15. Core levels (raw data).

(a) X-ray photoelectron spectrum of the Sc 2p region of Sc_7Cl_{10} (25 volts-256 channels, 100 scan composite).

(b) X-ray photoelectron spectrum of the Sc 2p region of $ScCl_{1.45}$ (25 volts-256 channels, 50 scan composite).

(c) X-ray photoelectron spectrum of the Cl 2p region of Sc_7Cl_{10} (12.5 volts-256 channels, 200 scan composite).

(d) X-ray photoelectron spectrum of the Cl 2p region of $ScCl_{1.45}$ (12.5 volts-256 channels, 33 scan composite).

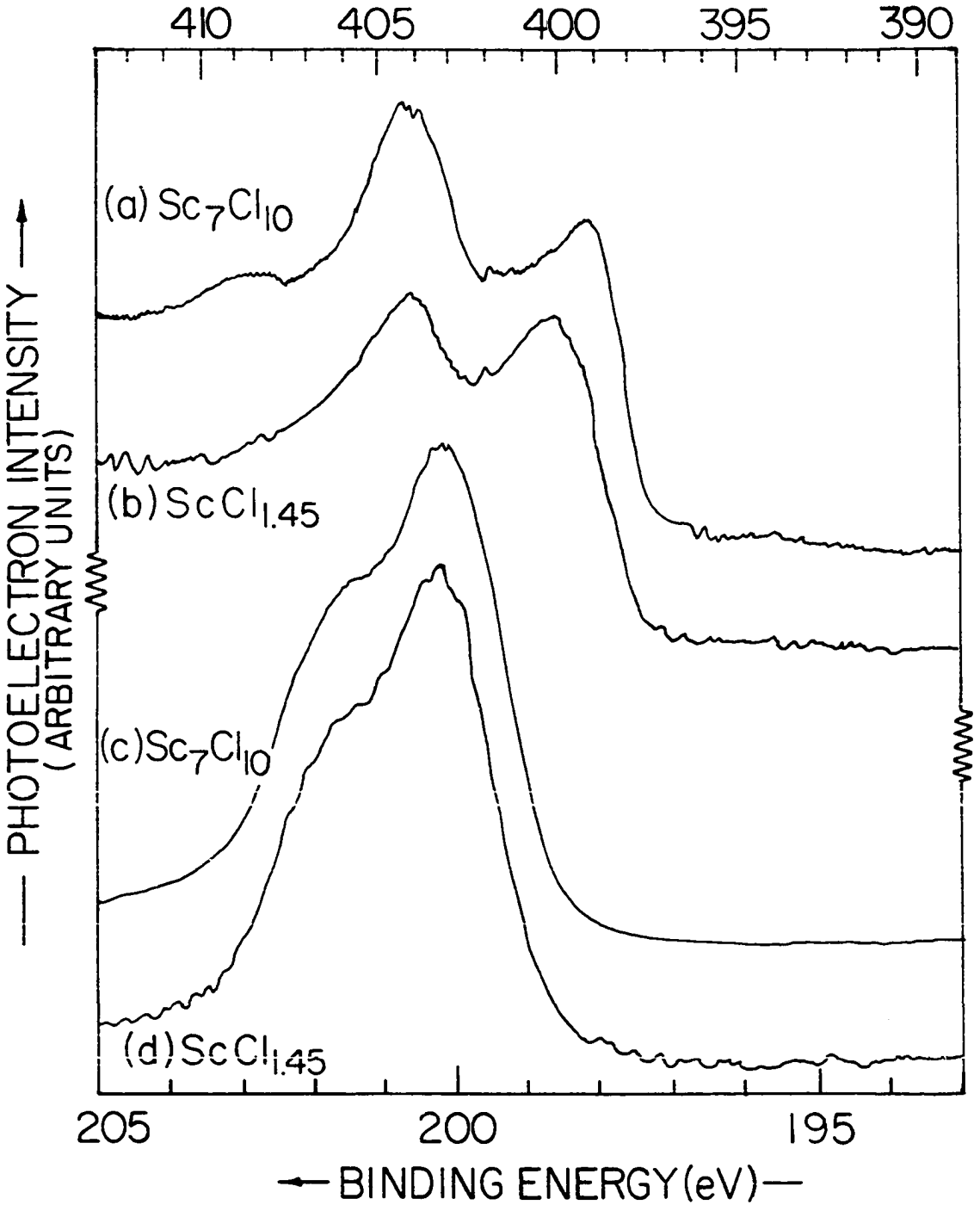
410
405
400
395
390
(a) Sc_7Cl_{10}
(b) $ScCl_{1.45}$
(c) Sc_7Cl_{10}
(d) $ScCl_{1.45}$
PHOTOELECTRON INTENSITY
(ARBITRARY UNITS)
205
200
195
BINDING ENERGY (eV)

difference between their valence band spectra is most pronounced at 3 eV where $ScCl_{1.45}$ has a more intense peak compared with the Cl 3p band at 7 eV than does Sc_7Cl_{10}. This difference probably represents a change in the relative 4s, 3d, (4p?) orbital character of their valence bands. Although all photoelectron spectra are modulated by cross-section effects as well as others (79), these factors would only serve to accentuate any change in band character between $ScCl_{1.45}$ and Sc_7Cl_{10}.

(2) A comparison of Sc 2p core level binding energies for the reduced compounds vs. scandium metal and scandium trichloride clearly show substantial chemical shifts to intermediate binding energies. In contrast the Cl 2p core level binding energies of the reduced phases are not significantly different from those of scandium trichloride. The five independent chlorine atoms in Sc_7Cl_{10}, even though their connectivity functions differ widely, are not isolable in spectrum 15(c). The variety of chlorine environments does, however, broaden the Cl $2p_{3/2-1/2}$ band for Sc_7Cl_{10} (3.0 eV full-width at half-maximum) compared with the same band in scandium trichloride (2.5 eV FWHM). The similar broadening of the Cl $2p_{3/2-1/2}$ band for $ScCl_{1.45}$ in spectrum 15(d) may indicate a variety of chlorine atoms are present which are very similar structurally to those in Sc_7Cl_{10}.

(3) The Sc 2p spectrum 14(a) of Sc_7Cl_{10} clearly contains a low intensity peak at 408.5 eV. Although this could be caused by any number of energy loss phenomena or simply surface oxidation, this peak has been assigned as a Sc $2p_{1/2}$ peak from the ionic scandium(III) centers present in Sc_7Cl_{10}. An argon-ion etch for two hours at maximum power, 5 kV - 25 ma, with rastering, did not change the spectrum in any fashion, reasonably ruling out surface oxidation. Other possible sources of the multi-line structure such as electron shake-up transitions or exchange splitting from unpaired electrons, both intrinsic in nature, are extremely difficult to rule out unambiguously. Extrinsic energy loss processes can account for the large increase in background to the lower kinetic energy region (greater apparent binding energy) of spectra 15(a,b). No other discrete peaks at lower kinetic energies, except the one at 408.5 eV, were observed. Therefore, bulk plasma oscillations in Sc_7Cl_{10} can be ruled out since several peaks of successively lower intensities and separated by the energy of oscillation would be expected. The most convincing evidence <u>for</u> mixed oxidation states as the cause of the high binding energy peak, the crystal structure notwithstanding, is the intensity and shape of the peak centered near 404 eV in spectrum 15(a) compared with the corresponding peak in 15(b). The corresponding spin-orbit

Sc $2p_{3/2}$ peak from the scandium(III) sites would come at approximately four electron volts lower binding energy which would place it under the large peak at 404 eV. The near superposition of the Sc $2p_{3/2}$ (ionic) and Sc $2p_{1/2}$ (metallic) peaks broadens and increases the intensity of the peak at 404 eV in spectrum 14(a) compared to the corresponding peak in 14(b). The asymmetry of the peak toward lower binding energy suggests the presence of a shoulder at 403.5 eV corresponding to the Sc $2p_{1/2}$ (metallic) peak and a second peak at 404.2 eV arising from the Sc $2p_{3/2}$ (ionic) photoemission. Based on the Sc 2p spectrum of $ScCl_{1.45}$ (14(b)) isolated scandium(III) centers are evidently lacking or there are fewer than the one out of seven present in Sc_7Cl_{10} and these go undetected. The substantial shift of the Sc $2p_{3/2}$ (metallic) peak for $ScCl_{1.45}$ to a higher binding energy vs. Sc_7Cl_{10} is consistent with a more oxidized metal array in $ScCl_{1.45}$ compared to Sc_7Cl_{10}, but the magnitude of the shift of 1.0 eV does not seem attributable to the small change in composition alone.

(4) In Figure 14(a,b), the ultra-violet and x-ray photoemission spectra of the valence band region, 0.0-5.0 eV, for Sc_7Cl_{10} show only small differences in their measured density of ionization potentials, PI(E). Some difference is detectable in the region centered near 3.0 eV and may be attributed to conduction band modulation (80)

with the UV source combined with cross-section modulation effects between UPS and XPS. The core-like Cl 3p band at 7 eV is not influenced by conduction band modulation and, as expected, the Cl 3p band in spectrum 14(a) is more intense than in 14(b) because of the increase in UV photoionization probability.

Any attempt to interpret PI(E) for Sc_7Cl_{10} in terms of a theoretical density of states, N(E), must at the present time await a suitable band-structure calculation. Recently, the metal-rich compound ZrCl (27,28) has been shown by Marchiando, Harmon, and Liu (81) to have a theoretical density of states, N(E), well represented by the experimental data, PI(E). Likewise, early first row transition metals, including scandium, have PI(E) ≈ N(E) (79). For this relationship to hold, the valence orbitals must retain their atomic wavefunction character in the condensed state to the extent that any difference in x-ray photoionization probability for these orbitals does not modulate PI(E) vs. N(E).

The phase $ScCl_{1.45}$ has been shown to be distinctly different from Sc_7Cl_{10} based on x-ray diffraction, thermal analysis, chemical analysis and now UV-XP spectroscopy. Combined, these results can be used to speculate about the differences and similarities between them.

The most obvious similarity between $ScCl_{1.45}$ and Sc_7Cl_{10} ($ScCl_{1.43}$) is composition. Up until now, all differences between $ScCl_{1.45}$ and Sc_7Cl_{10} have been attributed to the small difference in their compositions but, in fact, their compositions may not be different. Assume for the present the composition of each "phase" is the same or, at least, not an important factor. A very reasonable assumption to make would be to assume the spatial arrangement of atoms in Sc_7Cl_{10} and $ScCl_{1.45}$ is nearly the same. The large unit cell of $ScCl_{1.45}$ may result from a distortion of the lattice brought on by electron transfer from the chains of metal octahedra to the single atom chains. Localization of electrons on the single atoms would almost certainly result in bond formation along these chains with alternating long and short bonds. The effect would be to double the crystal axis parallel to chain propagation. Interchain correlations brought on by the reduction of the scandium(III) centers and partial oxidation of the metal array would likewise result in changes in the crystal lattice planes perpendicular to the propagation of the chains.

The metastability of the $ScCl_{1.45}$ phase is also consistent with it being the distorted low temperature phase and Sc_7Cl_{10} the high temperature undistorted form. It should be pointed out, however, this transformation

has never been observed to be reversible on cooling to room temperature and thus does not appear to be solely a function of temperature.

These speculations are consistent with the XPS data where for $ScCl_{1.45}$: (1) isolated scandium(III) centers, as such, were not evident, (2) all metal atoms appeared to have about the same reduced character and (3) the metal array did not appear to be as anionic, or as reduced compared with Sc_7Cl_{10}. Although the XPS data are encouraging, much more work needs to be done. Still not known is the answer to the important question of composition. Certainly techniques such as magnetic susceptibility, EPR and ^{45}Sc NMR together with structural data for $ScCl_{1.45}$ would help define the relationship between $ScCl_{1.45}$ and Sc_7Cl_{10}, which is now only speculative.

RESULTS: PART II. THE TERNARY $Cs_3Sc_{2+x}Cl_9$; $0 \leq x \leq 1.0$ SYSTEM

Preparation and Characterization of $Cs_3Sc_2Cl_9$ and $CsScCl_3$

Introduction

As a class, the ternary phases with the general formula $A_xB_yX_{3x}$ include hundreds of compounds related by simple structure concepts. At the same time, these compounds have widely different properties ranging from ferroelectric behavior, as typified by $BaTiO_3$ (82), to metallic conductivity, as found for $BaVS_3$ (15). The basic structural concepts of sphere packing, polyhedra and nets have been thoroughly covered by A. F. Wells in his book Structural Inorganic Chemistry (12, pp. 56-155). The following introduction is a brief summary based on his text.

The formation of complex ternary phases containing K^+ and F^- or Cs^+ and Cl^- in the ratio of 1:3 is related to the fact that these pairs of ions are of similar size and can form essentially close-packed (c.p.) A+3X layers. With two kinds of atoms, two c.p. arrangements are possible if only X atoms are around A atoms:

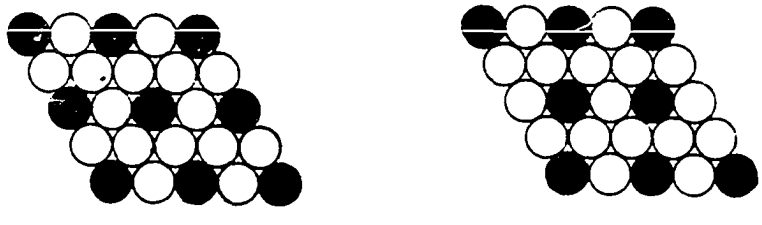

(a) (b)

The two A+3X layers (a) and (b) differ in one important respect, namely, (b) layers cannot be superimposed to generate octahedral sites surrounded only by 6X atoms without bringing A cations into direct contact. For this reason only layers of type (a) are important for complex halides and oxides. Type (b) layers are important in binary AX_3 intermetallic compounds and ternary hydroxyhalides $M_2X(OH)_3$ where, for the latter, the c.p. layers are composed entirely of halide and hydroxyl anions.

Figure 16 depicts several common packing sequences of A+3X layers with not more than six layers in the repeat unit. The A+3X layers are represented by the horizontal lines and are identified by capital letters. The particular packing sequence of the A+3X layers determines where the octahedral sites with only X anions at the vertices occur. These sites occur between the layers AB, AC, and BC, respectively, in the first, second and third columns. The particular formula depends on the number of B atoms (dark spheres) found between the A+3X layers and is dictated by the necessity to maintain an electrically neutral $A_xB_yX_{3x}$ crystal. For example, if $A = Cs^+$ and $X = Cl^-$ (a) through (d) represent cesium chlorometallate(II) compounds ABX_3 and (e) through (g) metallate(III) compounds $A_3B_2X_9$.

The ionic bonding model with particular emphasis on the importance of electrostatic repulsion and anion polarization

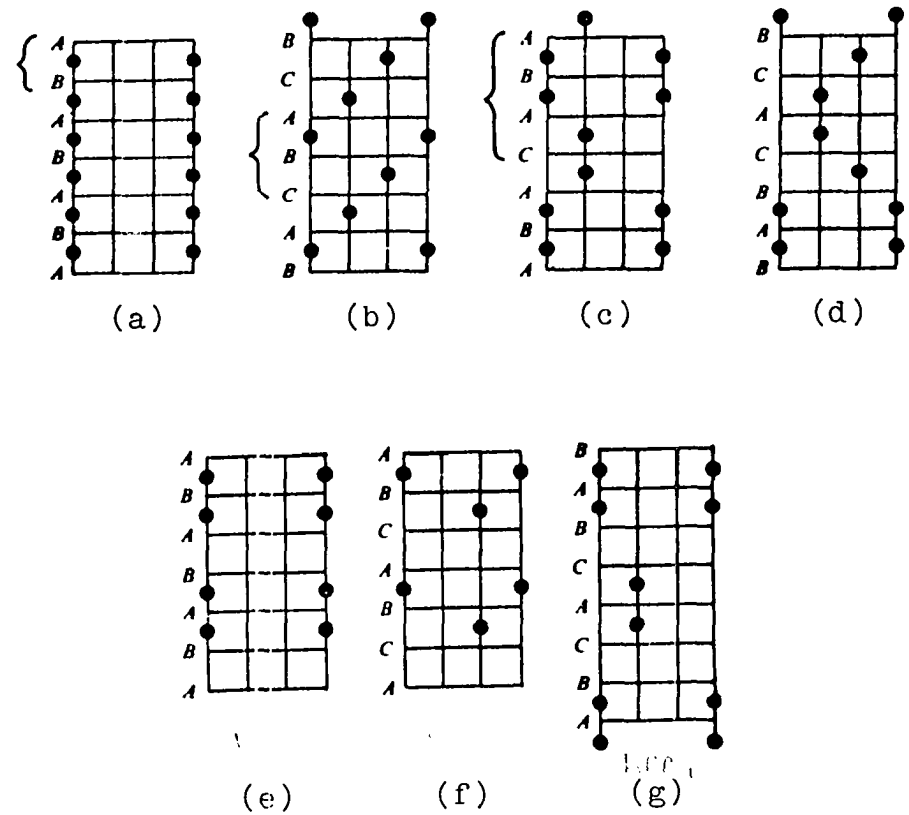

Figure 16. Closest packed structures $A_xB_yX_{3x}$. In these structures there is octahedral coordination of B by 6X atoms: (a)-(d) ABX_3 and (e)-(g) $A_3B_2X_9$.

has been widely used to explain the bonding in most $A_xB_yX_{3x}$ compounds. As can be seen in Figure 16, an increase in electrostatic repulsion between B ions is expected when the structure is based on hexagonal packing AB··· (face shared octahedra) compared with cubic stacking ABC··· (corner shared octahedra). Van Arkel (83) and Blasse (84) have emphasized that cation-cation repulsions between B ions is opposed by a more favorable anion polarization in the hexagonal structure. This effect can be rationalized with a simple comparison of the anion coordination by the B ions. In the cubic environment the B-X-B angle is ideally 180° and does not allow anion polarization, but with the favored hexagonal stacking the angle is 90° and the lattice can be stabilized by anion polarization. In general, the cubic stacking is favored more by the fluorides and oxides while the hexagonal sequence is often found for chlorides, roughly reflecting the polarizibility of these anions.

The energy differences between the hexagonal and cubic structures can be small and a common feature of $A_xB_yX_{3x}$ compounds is polytypism (a compound crystallizes in more than one structure). Quantitative electrostatic energy calculations (85) have shown energy differences between polytypes to be only a few kilocalaries per mole, which in turn makes qualitative predictions on the stable polytype difficult. In recent years, the use of high pressure

synthesis techniques (86) has resulted in the preparation of many metastable polytypes of both oxides and halides.

$Cs_3Sc_2Cl_9$

When Gut and Gruen (87) first prepared $Cs_3Sc_2Cl_9$, they reasonably assumed it would be isostructural with $Cs_3Cr_2Cl_9$ (88) since most first row transition metal $Cs_3M_2Cl_9$ compounds adopt the six layer structure, represented in Figure 16(g). Other structures are possible for compounds having the same composition and several are shown in Figure 16 (e) and (f). Using the Jagodzinski-Wyckoff symbols (89), the stacking sequence of the A+3X layers in Figure 16 (e-g) are, respectively, $(h)_2$, $(c)_3$ and $(hcc)_2$. In particular, the $(hcc)_2$ packing sequence with face shared BX_6 groups satisfies the need for anion polarization and reduction of electrostatic repulsion between the B ions. The $(h)_2$ sequence (Figure 16 (e)) does not satisfy the latter requirement, the $(c)_3$ sequence (Figure 16 (f)) does not satisfy the former and no examples of either are known. A distorted $(c)_3$ type is found in $Cs_3As_2Cl_9$ (90) and in β-$Cs_3Fe_2Cl_9$ (91) where the BX_6 groups are distorted to resemble discrete BX_3 molecules. $Cs_3Tl_2Cl_9$ (92,93) is the only example of a hexagonal sequence of the A+3X layers similar to that shown in Figure 16 (e). Figure 17 depicts the relationship between the $(h)_2$ structure of Figure 16 (e) and the actual six layer

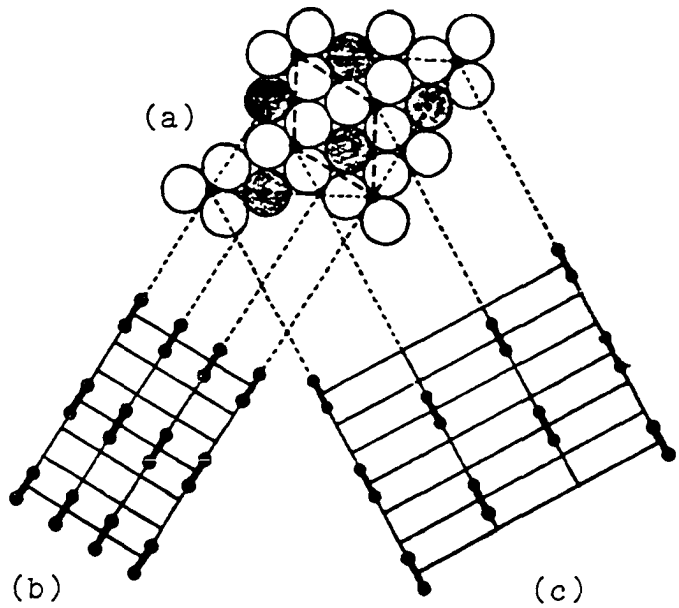

(a) Closest packed A+3X layer parallel to (0001) plane of the trigonal cell

(b) This arrangement (e in Figure 16) has not been observed for $A_3B_2X_9$ salts

(c) The actual spatial arrangement (c) of $Cs_3Sc_2Cl_9$ is closely related to (b) but has a more uniform spatial distribution of $B_2X_9^{3-}$ ions

Figure 17. The crystal structure of $Cs_3Sc_2Cl_9$.

$(h)_6$ rhombohedral variant caused by the spatial arrangement of the $Tl_2Cl_9^{3-}$ ions.

When the A+3X layers adopt the $(hcc)_2$ packing sequence, there are two alternative arrangements of the BX_6 units besides face shared $B_2X_9^{3-}$ ions. $Cs_3Bi_2Cl_9$ (94) is the only known example where BX_6 groups are joined by a common vertex, and mixed face and vertex shared BX_6 groups, while in principle possible, have not been found. When BX_6 groups share a common face and B = W or Mo, the B centers are displaced from the centers of the octahedra towards one another forming metal-metal bonds as was first shown for the compound $K_3W_2Cl_9$ (95). The question of metal-metal bonding in general for compounds with the same or similar composition has motivated many workers in this area of research.

In a surprising result, using Guinier x-ray powder diffraction, $Cs_3Sc_2Cl_9$ has been determined to be isostructural with $Cs_3Tl_2Cl_9$. Table XI compares experimental and calculated (96) lattice spacings and intensities for $Cs_3Sc_2Cl_9$ based on the $Cs_3Tl_2Cl_9$ model ($R\bar{3}c$) with good results and no discrepancies. There can be absolutely no doubt tha A+3X layers are stacked in hexagonal, $(h)_2$, fashion. The idealized atomic coordinates used to calculate the powder pattern in space group $R\bar{3}c$ (hexagonal setting) were:

Table XI. Guinier powder diffraction data for $Cs_3Sc_2Cl_9$

hkℓ	$d_{obs.}$	$d_{calc.}$	$I_{obs.}$[a]	$I_{calc.}$
012[b]	6.990	6.994	w	2.7
110[b]	6.350	6.354	vw	1.4
202[b]	4.700	4.703	vw	1.0
113	4.390	4.377	s	43.4
104	4.190	4.188	vw	0.8
122[b]	3.780	3.780	vw	1.2
300	3.667	3.668	ms	34.0
220	3.180	3.177	wm	12.9
006	3.019	3.020	m	20.6
223	2.812	2.812	vs	100.0
116	2.729	2.727	wm	12.1
036	2.332	2.331	wm	5.4
143	2.231	2.231	m	15.7
226	2.189	2.189	m	25.0
330	2.117	2.118	wm	8.0
146	1.880	1.880	wm	8.8
600	1.835	1.834	ms	47.0
229	1.700	1.700	m	22.0
253	1.691	1.692	wm	7.6
066	1.567	1.568	m	18.1

[a] s = strong, m = medium, w = weak and v = very.

[b] Reflections not used in the calculation of the lattice constants.

18Cs in (e), $x \simeq 2/3$

12Sc in (c), $z \simeq 1/6$

18Cl in (e), $x \simeq 1/6$

36Cl in (f), $x \simeq 1/6$, $y \simeq 1/2$, $z \simeq 1/4$.

No distortions from ideal atomic positions were used for this comparison although certainly the scandium(III) ions repulse one another and are displaced outward from the center of the octahedron ($z<1/6$). While it is doubtful $Cs_3Sc_2Cl_9$ would be in a noncentrosymmetric space group, the polar space group R3c cannot be ruled out. The lattice constants $a = 12.707(2)$Å and $c = 18.177(4)$Å were obtained from 16 reflections (see Table XI) by least-squares refinement using the program LATT (42). In contrast to the results in Table XI major differences between the observed and calculated powder pattern were found using the $Cs_3Cr_2Cl_9$ model.

As a practical matter, the powder pattern of $Cs_3Sc_2Cl_9$ is similar to one based on an alternate hexagonal cell with one-ninth the volume and the following relationships: $a_{new} = a_{old}/\sqrt{3}$ and $c_{new} = c_{old}/3$. The ab plane of the smaller cell is shown in Figure 17 by the dashed line but because of the vacancies on the B positions the larger cell ($R\bar{3}c$) is, of course, the correct one. The low angle and weak reflections in Table XI, 012, 110, 202, 104 and 122, cannot be indexed based on the smaller cell. Since these five reflections are easily missed or simply not detectable

on Debye-Scherrer films, the only suitable camera for this work is the Guinier XDC-700.

$Cs_3Sc_2Cl_9$, like $Cs_3Cr_2Cl_9$, maintains face sharing chlorine octahedra for maximum anion polarization while at the same time minimizes cation-cation repulsion between the B-chains with adoption of the R-centered cell. The rhombohedral $(h)_6$ structure can be rationalized as the favored structure for moderately large B ions. Locally, the distortions around the $B_2X_9^{3-}$ ion must be very similar with either the $(h)_6$ or $(hcc)_2$ layer sequence where repulsion between the B ions results in a shortening of the edges of the shared face of the complex ion and lengthening of the others. This has been verified by single crystal x-ray diffraction for $Cs_3Cr_2Cl_9$ (88) and suggested for $Cs_3Tl_2Cl_9$ (92). The distortion is limited, in part, by the presence of Cl-Cl nonbonded contacts on the shared face and the resistance of B-Cl bonds to stretching. The crystal structure of $Cs_3Cr_2Cl_9$ contains two crystallographically distinct cesium ions which become less equivalent as the ideal structure becomes increasingly distorted. The charge distribution (chloride ions) around the cesium ions also becomes increasingly less isonomous. Based on the ionic radii of Shannon and Prewitt (97) both scandium(III) ($r = 0.730$Å) and thallium(III) ($r = 0.880$Å) would result in substantial distortion of the $M_2X_9^{3-}$ ion which can be better

accommodated in the $(h)_6$ structure where all the cesium ions are equivalent vs. the $(hcc)_2$ structure of $Cs_3Cr_2Cl_9$. Empirically, Pauling's fifth rule (98) expresses this rationalization much more succintly: "The number of essentially different kinds of constituents in a crystal tends to be small." Schippers, Brandwijk and Gorter (99) have gone even further to state: "The same ions will prefer to have the same coordination, as regard number and polyhedron shape, of oppositely charged ions, ··· , chemically identical ions prefer to occupy an identical crystallographic position." Interestingly, no justification from electrostatic theory or elsewhere has been found for this widely used concept. Consistent with this rationalization is the structure of $Cs_3Bi_2Cl_9$ (94) where only $BiCl_6$ octahedra joined by a single vertice are found. The large size of the bismuth(III) (radius = 1.02Å) ion makes face sharing of even distorted $Bi_2Cl_9^{3-}$ ions impossible. If chloride is replaced by iodide, the $Cs_3Cr_2Cl_9$ structure $(hcc)_2$ with double octahedral $Bi_2I_9^{3-}$ groups is stabilized (100), as expected.

In the $CsCl$-$ScCl_3$ pseudo binary system, Gut and Gruen (87) found a congruent melting 3:1 compound Cs_3ScCl_6 (m.p. 814°) and the 3:2 compound $Cs_3Sc_2Cl_9$ with a peritectic at 691°C. Two eutectics occur at 6.5 and 56.5 mole % $ScCl_3$ at 613°C and 569°, respectively. Accordingly, the synthesis of $Cs_3Sc_2Cl_9$ was quite straightforward. A $3CsCl:2ScCl_3$ mole

ratio was heated in a sealed tantalum reaction container to 700°C (one liquid condensed phase) and mixed by shaking. The sample was cooled slowly through the slightly incongruent peritectic at 691°C at 1.25°/hr to 650°C. The sample was annealed at this temperature for several days, the power to the Marshall furnace turned off, and the sample allowed to cool to room temperature over the period of several hours inside the furnace. The sample was white, crystalline and single phase melting at 692°C ± 3° with no evidence for unreacted starting materials or a second phase in either the x-ray powder pattern (Guinier) or DTA results. Careful handling and storage of $Cs_3Sc_2Cl_9$ is important since the compound is hygroscopic.

Opposed to the powder x-ray and DTA results are the ^{45}Sc (I = 7/2) NMR data obtained on the same sample. The $Cs_3Sc_2Cl_9$ NMR data were a small part of the larger study of the $Cs_3Sc_{2+x}Cl_9$; $0 \leq x \leq 1$, system undertaken by Tom McMullen in Solid State Physics with Dr. R. G. Barnes (101). The understanding of the ^{45}Sc NMR results for the simple compound $Cs_3Sc_2Cl_9$ is fundamental if NMR is to be used as a guide to the synthesis and characterization of the reduced compounds $Cs_3Sc_{2+x}Cl_9$; $0 \leq x \leq 1.0$. McMullen detected two types of scandium atoms as major components in $Cs_3Sc_2Cl_9$, contrary to what is expected for a homogeneous, stoichiometric sample in which all the scandium sites are equivalent.

In contrast, the NMR spectrum of $ScCl_3$ contained a single central transition ($m = 1/2 \leftrightarrow m = -1/2$) characteristic of isolated and chemically equivalent scandium(III) ions.

The NMR data on $Cs_3Sc_2Cl_9$ can be explained by a variety of mechanisms, i.e., the sample was not single phase, non-stoichiometry of the type $Cs_3Sc_{2-x}Cl_{9-3x}$, or intrinsic disorder along the BX_6 chain ($B_nX_{3n+3}^{3-}$, n = 1,2,3 etc.). Of these, only the first explanation would appear to be reasonable under the conditions used for the synthesis of $Cs_3Sc_2Cl_9$. In all likelihood, the sample segregated on slow cooling forming a dense layer of scandium trichloride-deficient Cs_3ScCl_6 (solid phase) covered by a molten scandium trichloride rich liquid phase. On cooling through the peritectic to the annealing temperature (650°C) some recombination probably took place on the interface but mostly $Cs_3Sc_2Cl_9$ precipitated, as the liquid phase cooled, leaving a layer of solid Cs_3ScCl_6 covered by solid $Cs_3Sc_2Cl_9$. Subsequently, the system was prevented from reaching equilibrium because the Cs_3ScCl_6 could not react with the melt since they no longer were in physical contact and presumably the melt reduces the activity of scandium trichloride in the gas phase to such an extent any solid-vapor mechanism for equilibration was not effective at the annealing temperature.

In order to prepare several grams of single phase $Cs_3Sc_2Cl_9$, the synthesis must be carried out differently. The $3CsCl \cdot 2ScCl_3$ composition should be heated to 700°C where the entire system is a homogeneous liquid phase as before. The slow cooling in the earlier synthesis should be replaced by rapid cooling (quench) to room temperature to prevent segregation and to guarantee a homogeneous mixture with the composition of the melt ($3CsCl \cdot 2ScCl_3$). Reequilibration of the mixture below the pentectic at 691°C should result in the recombination of all the components to make a homogeneous sample of $Cs_3Sc_2Cl_9$. Slow cooling might also help with possible disorder. Should a sample prepared in this fashion result in a single NMR central transition, these techniques should be applied and tested for the reduced compositions $Cs_3Sc_{2+x}Cl_9$; $0 \leq x \leq 1.0$. If this synthesis is not successful, other techniques should be tried. One possible alternative would be to grind the $3CsCl \cdot 2ScCl_3$ sample to make an intimate mixture and then to heat the mixture until the CsCl melts (646°C). The reaction may go to completion under these relatively mild conditions and be the preferred synthesis.

$CsScCl_3$

All first row transition metals are known to form halometallate(II) ABX_3 compounds with the exception of scandium (14,84). The large majority crystallize with the $(h)_2$ structure favored by anion polarization. The presence

of d electrons on the B site, although not a necessary condition for a compound to crystallize with the $(h)_2$ structure, can be an important stabilizing factor. Large B cations such as calcium or strontium, cations which do not effect polarization as well and have no d electrons, crystallize in the perovskite $(c)_3$ structure. Although $CsScCl_3$ is expected to be isostructural with other first row transition metal ABX_3 compounds, the properties derived from what are formally scandium(II) d^1 ions make $CsScCl_3$ a new and unusual material.

Pseudo binary phase studies between $ScCl_2(s)$ and Group I chlorides have not been studied since $ScCl_2(s)$ does not exist. The reduction of $Cs_3Sc_2Cl_9$ with scandium metal to $CsScCl_3$ is an alternative reaction and quite simple to imagine, occurring along the pseudo binary $Cs_3Sc_2Cl_9$-Sc line in the ternary system. $CsScCl_3$ lies at the point in the composition plane where the binary sections $CsCl$-$ScCl_2$ and $Cs_3Sc_2Cl_9$-Sc intersect.

$CsScCl_3$ was prepared by the following reaction in a sealed tantalum tube:

$$3CsCl + 2ScCl_3 + Sc \xrightarrow[9d]{700\text{-}850^\circ C} 3CsScCl_3 .$$

The reaction product was cooled to room temperature by turning the power to the Marshall furnace off and allowing the sample to cool with the furnace. The reaction temperature (range) was chosen to be above the decomposition

temperature of $Cs_3Sc_2Cl_9$ (692°C ± 3°). Powdered scandium metal (100 mesh) was used. The product was a lustrous, black crystalline material and no white $Cs_3Sc_2Cl_9$ or unreacted scandium could be detected with microscopic examination or powder x-ray diffraction. When ground to a powder $CsScCl_3$ has a deep blue color. The material evolves hydrogen gas when reacted with water but at a moderate rate compared with reduced binary scandium chlorides.

The Guinier x-ray powder diffraction patterns of blue-black $CsScCl_3$ and $Cs_3Sc_2Cl_9$ are very similar but they have one important difference. The powder pattern of $CsScCl_3$ does not contain the five weak reflections described in the $Cs_3Sc_2Cl_9$ section and subsequently all observed reflections for $CsScCl_3$ can be indexed on the smaller hexagonal cell with a = 7.350(2)Å and c = 6.045(3)Å based on 15 reflections. The similar powder patterns and the length of the c axis for $CsScCl_3$ are consistent with the A+3X layers stacked in $(h)_2$ fashion in $CsScCl_3$ as in $Cs_3Sc_2Cl_9$. The absence of the five weak reflections indicates all the B sites are now equivalent, that is, no ordered vacancies occur along the columns of face shared chloride octahedra as they did in $Cs_3Sc_2Cl_9$. The distance between what are now formally scandium(II) centers is c/2 or slightly more than 3.02Å. This spacing corresponds to a shortened bond distance of over 0.2Å as compared with the average distance in the 12-coordinate element. Likewise, the spacing found is

equivalent within 1σ to the metal-metal distance for the trans-edges of the octahedral chain in Sc_5Cl_8 of 3.021(7)Å which is the shortest Sc-Sc distance yet observed among the binary compounds.

A single crystal x-ray study was undertaken to define the spatial arrangement of the atoms in a more precise fashion and to verify the powder results. A small crystal fragment, reasonably isotropic in dimension (0.075 mm), was chosen to avoid absorption effects. Crystal data were collected on the Ames Laboratory four-circle diffractometer using graphite monochromatized Mo K_α radiation (λ 0.70954Å). The data were collected based on a hexagonal cell with a = 7.345(2)Å and c = 6.045(2)Å which match those obtained from the Guinier powder data. All reflections within a sphere defined by $2\theta \leq 50°$ in octants HKL and $H\bar{K}L$ were examined with an ω-scan mode. The 649 pieces of data collected were treated as described previously to yield 513 reflections with $I > 3\sigma(I)$. The data were averaged in Laue 6/mmm symmetry to yield 108 unique reflections. Only one weak reflection was eliminated in the averaging step based on $|F_0-F_A|/F_A > 0.20$.

The systematic absence hh2$\bar{h}$l, l≠2n limits the choice of space group to three: $P6_3mc$ (No. 186), $P\bar{6}2c$ (No. 188) and $P6_3/mmc$ (No. 194). Since $CsScCl_3$ was expected to be isostructural with $CsNiCl_3$ (102), the centrosymmetric space

group $P6_3/mmc$ with atoms in the following positions was chosen:

Atom	Wyckoff notation, point symmetry	Position
Cs	c, $\bar{6}m2$	1/3, 2/3, 3/4
Cl	h, mm	x, $\bar{x}$, 1/4
Sc	a, $\bar{3}m$	0, 0, 0

The chlorine positional parameter was initially chosen to be the ideal c.p. value x = 1/6. After three cycles to least-squared refinement with a scale factor, chlorine positional parameter, and isotropic thermal parameters as variables the refinement converged at R = 0.099 and R_w = 0.122 where R and R_w have their usual definition and $\omega = \sigma_F^{-2}$. Variation of occupation parameters for all atoms at this stage of the refinement indicated the scandium position was not fully occupied. An electron density map was computed with the observed data and the occupation parameter determined by peak integration scaled to a chlorine peak. The occupancy of the scandium site was determined to be 0.82 and was constrained to this occupancy until the final stage of the refinement. With anisotropic temperature factors for all atoms, the structure refined to an R = 0.057 and R_w = 0.065 in three cycles of least-squares refinement. The occupation parameter was included as a variable in the refinement at this stage and in two cycles led to a final occupation parameter of 0.79(3) and a final R value of

0.055 and R_w = 0.064. The maximum shift in a variable was less than 1% of the estimated standard deviation in the final refinement cycle. If the scandium site was fixed at unit occupancy, a final R_w of 0.079 was obtained with anisotropic temperature factors for all atoms. This model can be rejected at the 0.005 significance level based on Hamilton's (103) significance test of the crystallographic R_w-factor.

The final positional and thermal parameters are listed in Table XII. Figure 18 is an ORTEP drawing of the $(11\bar{2}0)$ section of the unit cell with the atoms behind the mirror plane included. Important distances and angles are also shown in this figure. Final calculated and observed structure factors are available in Appendix F.

The crystallographic model for $CsScCl_3$ in Figure 18 is based on slightly distorted A+3X layers with the shared face of the chlorine octahedra slightly compressed from the ideal (x (ideal) = 0.1667, x (actual) = 0.1611). The Sc sites are occupied roughly 80% of the time. No evidence for ordering of the vacancies could be found based on Guinier films of the bulk sample. Likewise, no anomalous diffraction intensity could be detected with the single crystal using 2θ-ω step scans (ω = 0.05°) over axial and nonaxial directions. In particular, the (100) reflection for the single crystal, which corresponds to the (110) reflection in the related $Cs_3Sc_2Cl_9$ cell, was not observed. Therefore,

Table XII. Position and thermal parameters for $CsScCl_3$

Atom	Position	x	y	z	β_{11}[a]	β_{22}[b]	β_{33}	β_{12}	β_{13}	β_{23}
Cs	c	1/3	2/3	3/4	174(5)[c]	β_{11}	298(9)	$\frac{1}{2}\beta_{11}$	0.0	0.0
Cl	h	0.1611(3)	-0.1161	1/4	155(9)	β_{11}	205(13)	87(9)	0.0	0.0
Sc	a[d]	0.0	0.0	0.0	101(15)	β_{11}	376(34)	$\frac{1}{2}\beta_{11}$	0.0	0.0

[a]The general form of the anisotropic thermal ellipsoid is $\exp[-(\beta_{11}h^2 + \beta_{22}k^2 + \beta_{33}\ell^2 + 2\beta_{12}hk + 2\beta_{13}h\ell + 2\beta_{23}k\ell)]$.

[b]Restrictions on the thermal parameters were:

(1) Cs and Sc, $\beta_{11} = \beta_{22} = 2\beta_{12}$; $\beta_{13} = \beta_{23} = 0$, and

(2) for Cl, $\beta_{11} = \beta_{22}$; $\beta_{13} = \beta_{23} = 0$.

[c]All β's x 10^4. Numbers in parentheses are estimated standard deviations.

[d]Occupation parameter = 0.79(3).

Figure 18. The $(11\bar{2}0)$ section of $CsScCl_3$.

Important distances and angles are:

(a) Sc-Cl 2.548(3)Å
Cl-Sc-Cl 91.60(8)°

(b) Cs-Cl intralayer 3.6759(2)Å
Cs-Cl interlayer 3.734(2)Å

(c) Cl-Cl nonbonded, shared face 3.552(7)Å
Cl-Cl nonbonded, between faces 3.654(2)Å.

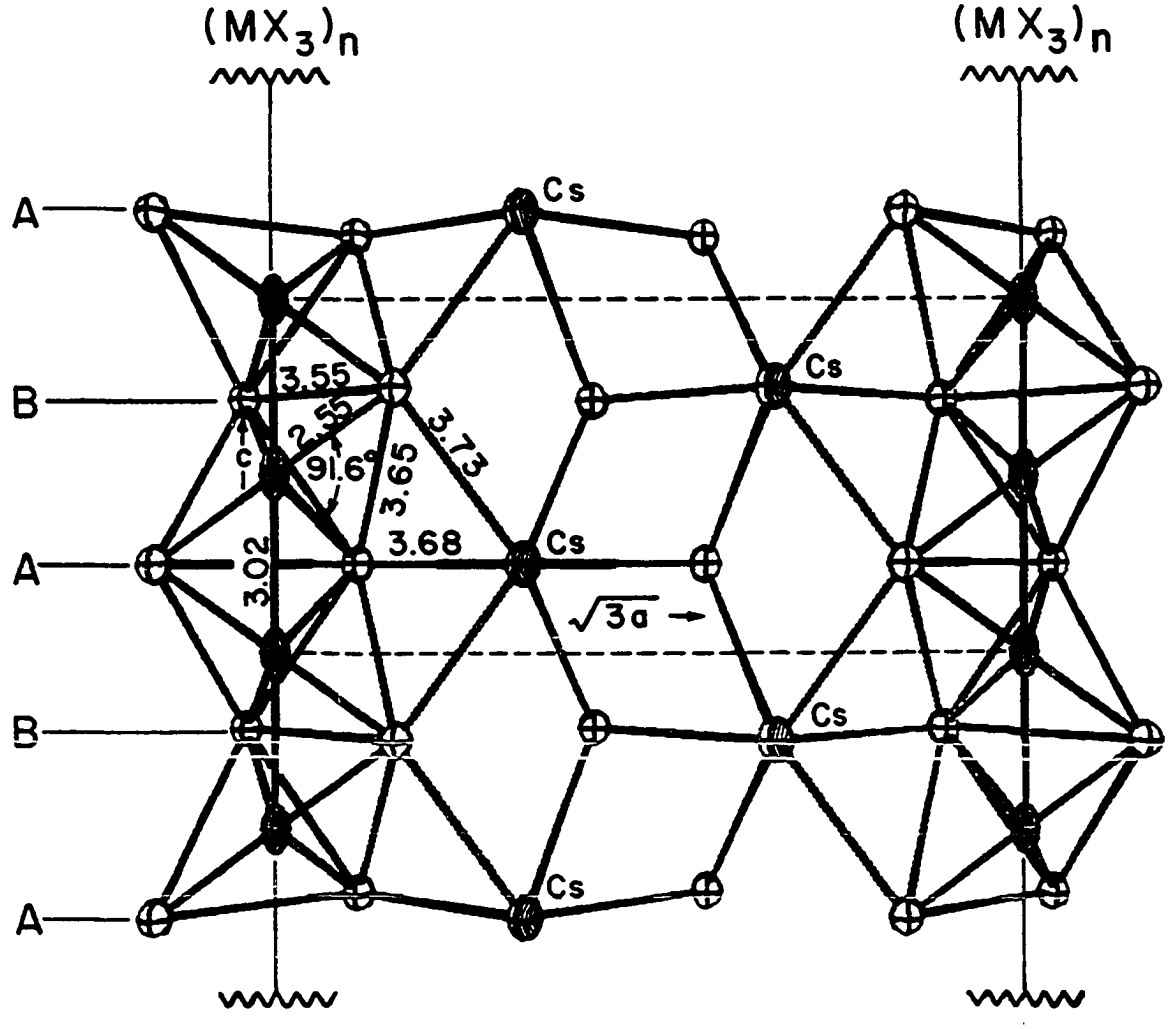
$(MX_3)_n$
$(MX_3)_n$
A
B
A
B
A
Cs
Cs
Cs
Cs
3.55
2.55
c
91.6°
3.65
3.73
3.02
3.68
$\sqrt{3}a$

the particular model based on $Cs_3Sc_2Cl_9$ with partial occupancy of the (0,0,0) and (0,0,1/2) sites in $R\bar{3}c$ can be ruled out. The vacancies are therefore assumed to be random in both the bulk sample and single crystal to the investigating radiations. The scandium and cesium sites appear to have some anisotropy in their thermal parameters but careful examination of electron density contours did not reveal any preferred displacements. The lack of anisotropic motion on the chlorine sites is a strong indication the scandium atoms are evenly spaced in, and randomly occupy, the octahedral voids along the c axis.

Nonstoichiometry is an unusual circumstance for ABX_3 solids since B cation voids and mixed B oxidation states result. McPherson and Henling (104) have been studying the effect of diluent amounts of paramagnetic B(III) species in host ABX_3 phases, for instance gadolinium(III) or chromium(III) doped $CsMgCl_3$. They have found the B(III) ions form a pair around the cation void as expected based on local lattice effects. The mixed valence character of grossly nonstoichiometric $CsSc_{1-x}Cl_3$ is, by comparison, difficult to rationalize based on a substitutional model. An alternative model of electron delocalization over small and smaller fragments of the linear metal chain as $CsSc_{1-x}Cl_3$ becomes increasingly nonstoichiometric would seem equally improbable. Logically, $CsSc_{1-x}Cl_3$ would be expected, as x becomes greater than several percent, to order the vacancies

as the nonperiodic coulomb potentials increased. In other words a new phase, or phases, would be expected such as $Cs_5Sc_4Cl_{15}$. In the next section the region $Cs_3Sc_{2+x}Cl_9$; $0 \leq x \leq 1.0$, will be examined where the end members are the idealized scandium(III) and scandium(II) compounds.

Preliminary investigations using the techniques of resistivity, ^{45}Sc NMR, EPR and DTA have been completed on the same sample of $CsScCl_3$ with the following results:

(1) Conductivity-resistivity measurements were made with a simple two probe dc method on various fragments of $CsScCl_3$ as they initially came from the reaction tube. Approximately 10% of the fragments examined were found to have resistivities of less than 10 ohms. By microscopic and x-ray examination these fragments were not sintered bits of unreacted scandium metal but were $CsScCl_3$. The conclusion is some of the material is a good conductor.

(2) Tom McMullen (101) thoroughly examined the ^{45}Sc NMR and came to the conclusion the main features of the spectra closely paralleled those found for $Cs_3Sc_2Cl_9$. In addition, a resonance with a signal barely above noise levels was detected which exhibited a Knight shift characteristic of elemental scandium. The implication is the sensitivity of detection is greater with NMR or the free scandium particle size is too small to be detected with x-rays. If the latter is the case, the metal must have been precipitated after undergoing some chemical reaction. This is made clear by

the results of a similar reaction with ScF_3, NaF and powdered Sc metal. At a reaction temperature of 1000°C, no reduction occurred and the unreacted scandium was in the same physical form as before the reaction. The unreacted metal in the fluoride reaction was easily recognized visually, microscopically and by its characteristic x-ray powder pattern. The NMR results indicate the bulk $CsScCl_3$ sample contains some free metal and the remaining phase, or mixture of phases, contain a variety of scandium species.

(3) Room temperature EPR detected a broad resonance centered near 3400G (g-factor ≈ 2.0) with resolved hyperfine splitting characteristic of a nucleus with I = 7/2. An EPR spectrum is shown in derivative form in Figure 19. Evidently some of the scandium species can be described as scandium(II) d^1 ions with a localized electron. In the past, detection of paramagnetic scandium(II) d^1 ions has been limited to scandium doped host crystals at liquid helium temperatures.

Since disproportionation may have been a problem in the original synthesis of $CsScCl_3$, the sample was annealed at 700°C for several days and cooled as before. The sample appeared unchanged to NMR after this treatment. The process was repeated but with slow cooling from 700°C to room temperature at 1.25°/hr. Again no change could be detected in the sample with NMR.

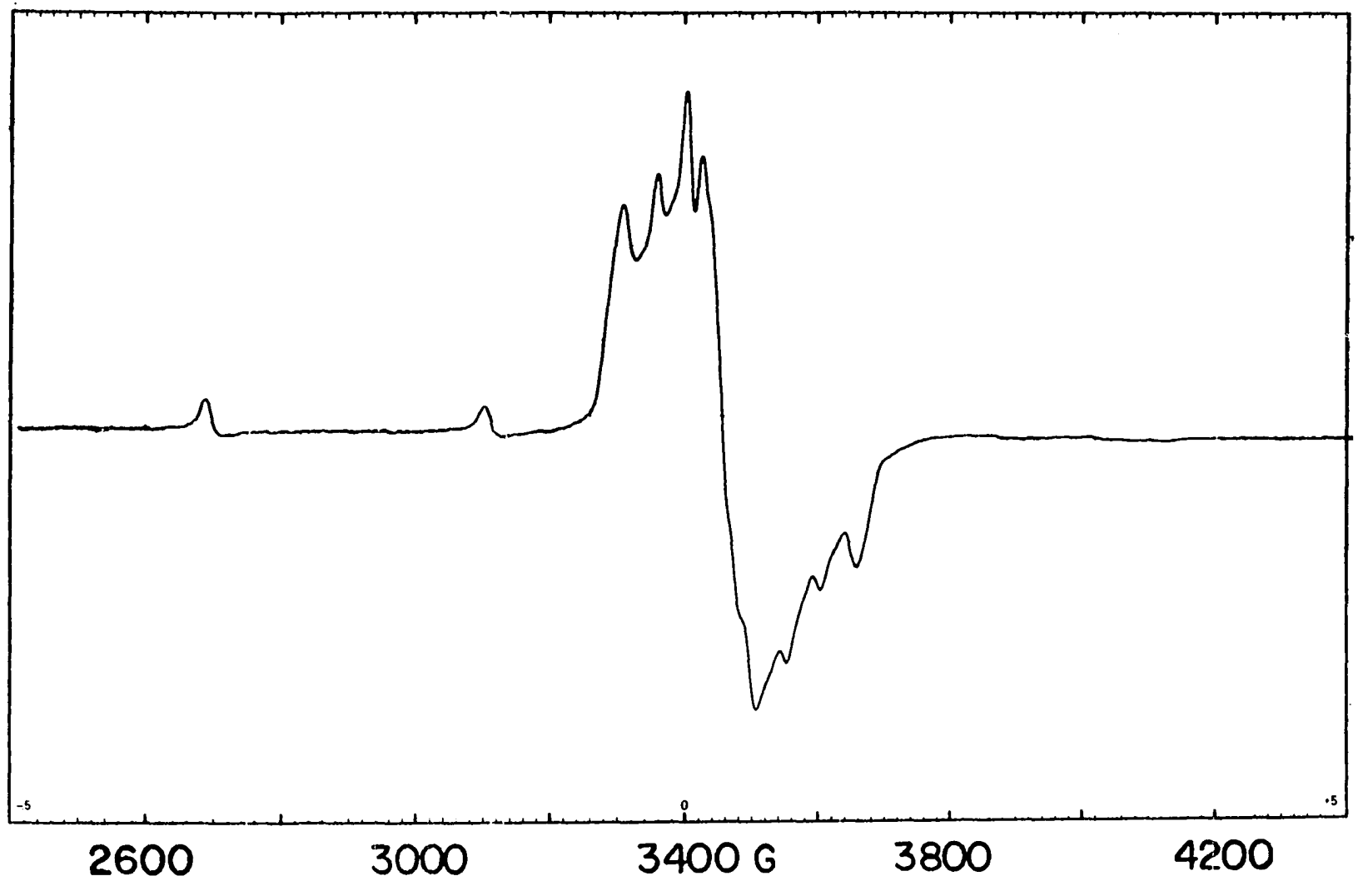

Figure 19. The room temperature EPR spectrum (derivative) of powdered $CsSc_{0.750}Cl_3$.

(4) After the NMR work, the well-annealed and slowly cooled sample was next studied by DTA. The sample was found to melt at 704°C±3°. No $Cs_3Sc_2Cl_9$ could be detected (m.p. 692°C) in the sample and no other transitions could be found from room temperature to 850°C on heating and cooling at a rate of 4° per minute.

Combined, these studies indicate the sample of $CsScCl_3$ is best described as $CsSc_{1-x}Cl_3$ and unreacted metal. The particular single crystal removed from the bulk sample had $x = 0.2$ but the NMR evidence indicates the bulk sample is a more complicated mixture of scandium species. Some of the material is highly conducting while at the same time the bulk sample contains an appreciable concentration of localized Sc d^1 ions, again, probably a reflection of the variable stoichiometry and/or multi-phase character of the bulk sample. A systematic synthetic approach coupled with DTA, x-ray analysis, EPR and especially ^{45}Sc NMR of the entire $Cs_3Sc_{2+x}Cl_9$; $0 \leq x \leq 1.0$, system is necessary to define and characterize this region. The simple notion of two compounds $Cs_3Sc_2Cl_9$ ($x = 0$) and $CsScCl_3$ ($x = 1.0$) is not correct. The first attempt at this characterization is reported in the next section, a Guinier x-ray powder diffraction study of the region as a function of composition.

$Cs_3Sc_{2+x}Cl_9$; $0 \leq x \leq 1.0$

The compositions listed in Table XIII were prepared by the reaction:

$$3CsCl + 2ScCl_3 + ySc \longrightarrow 3CsSc_xCl_3$$

where $x = (2+y)/3$.

The samples were heated to slightly obove 692°C for several hours to melt any $Cs_3Sc_2Cl_9$ but held below 700°C to avoid disproportionation. Next, the samples were slowly cooled at 1.25°/hr to 300°C and finally cooled to room temperature by turning the power to the furnace off. All the samples with the exception of $Cs_3Sc_2Cl_9$ ($y = 0$) were black and upon grinding appeared blue. Lattice constants for each composition were determined by measuring each Guinier film five times, averaging the film readings and computing (56) *a* and *c*. An internal silicon standard was added to all samples. If the larger $R\bar{3}c$ cell of $Cs_3Sc_2Cl_9$ fit the data, the lattice constants were reduced to the smaller hexagonal cell. The results are tabulated in Table XIII and are graphed in Figure 20. For discussion, Figure 20 has been divided into three regions:

(1) Region I: $CsSc_{0.6667-0.80}Cl_3$. A two phase region between white $Cs_3Sc_2Cl_9$ and black $Cs_3Sc_{2+x}Cl_9$ was not evident and the lattice constants reveal only smooth changes up until $x = 0.8$. The rate of change of the lattice constant *c* as a function of composition is linear whereas *a* shows an initial

Table XIII. Guinier data for the $Cs_3Sc_{2+x}Cl_9$; $0 \leq x \leq 1.0$, system

Composition	a	c
$CsSc_{0.6667}Cl_3$	7.336(2)	6.039(3)
$CsSc_{0.706}Cl_3$	7.340(1)	6.040(1)
$CsSc_{0.750}Cl_3$	7.342(1)	6.042(2)
$CsSc_{0.800}Cl_3$	7.342(3)	6.044(4)
$CsSc_{0.816}Cl_3$	7.350(1)	6.045(2)
$CsSc_{0.870}Cl_3$	7.355(2)	6.048(3)
$CsSc_{0.900}Cl_3$	7.344(1)	6.041(1)
$CsSc_{0.950}Cl_3$	7.346(1)	6.042(2)
$CsSc_{1.0}Cl_3$	7.350(2)	6.045(3)

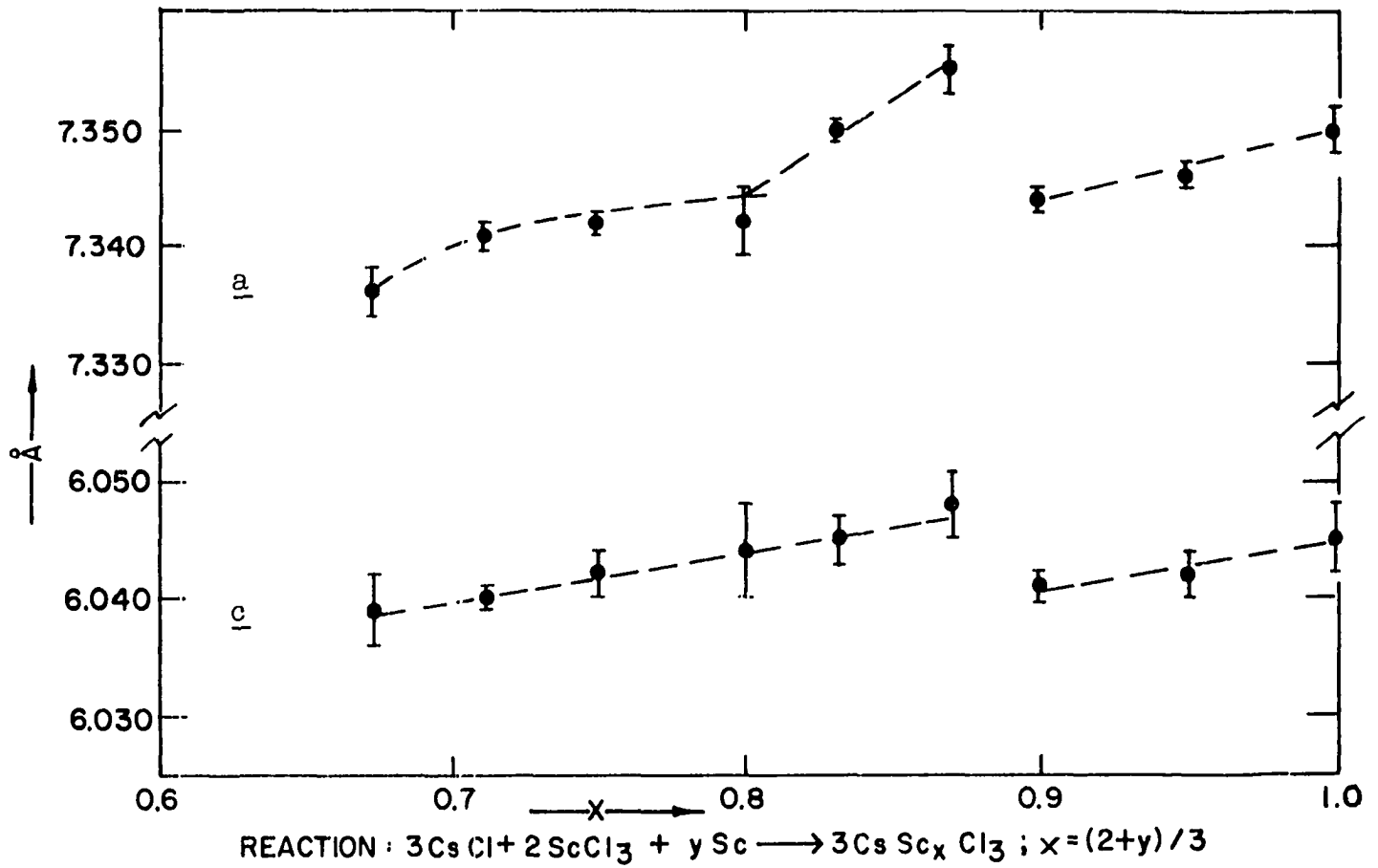

Figure 20. Lattice constants vs. composition for the $Cs_3Sc_{2+x}Cl_9$; $0 \leq x \leq 1.0$, system.

large increase followed by a slower rise. Across the region all the powder patterns have the five characteristic lines of the $R\bar{3}c$ cell of $Cs_3Sc_2Cl_9$ and these become gradually less intense as x increases so that at x = 0.8 they are very weak in some films and not visible in others. No line broadening or splitting of individual reflections was observed. Thus, it appears the vacant scandium sites in $Cs_3Sc_2Cl_9$ (at 0,0,0 and 0,0,1/2 plus R-centering) are filled statistically up to about 40% while the $Sc_2Cl_9^{3-}$ ions remain spatially unchanged.

At least some of the reduction electrons appear to be localized since all the reduced compositions in Region I give similar powder EPR spectra at room temperature to the one shown in Figure 19. The sample chosen for this figure at x = 0.75 was the only sample to show the weak low field transitions to the left of the main resonance. These transitions may result from spin states (S > 1/2) of coupled electrons.

(2) Region II. $CsSc_{0.8-0.9}Cl_3$. The c lattice constant in this region continues to vary in a linear fashion up to at least x = 0.87. The large and nonlinear changes in a indicate strong interchain coupling predominates. No reflections are evident to differentiate B sites and therefore all the B sites appear equivalent to the investigating radiation.

(3) Region III: $CsSc_{0.9-1.0}Cl_3$. If the break in a and c between Region II and III is real, then there exists the possibility no two phase region exists between them if the transition is second order. No change in symmetry between Region II and III could be detected.

The lattice constants obtained from the single crystal study; a = 7.345(2)Å and c = 6.045(2)Å, correspond to those predicted by Figure 20 for the crystallographic composition x = 0.79(3) where a = 7.344Å and c = 6.044Å are within one standard deviation. The double value near x = 1.0 can be ruled out based on the significance of R_w values as described earlier in the single crystal study.

The three compositions x = 0, 0.816, 1.0 were studied briefly by XPS. The results are inconclusive and problematical since the effects of charging, mixed-valence character and chemical shifts, multiplet splitting and others must be taken into consideration (60). The Cs and Cl core levels are unaffected by nature of their chemical role in the solid and reveal little about the material. The scandium core levels, Sc 2p and 3s mainly, give complex spectra. The prominent peaks are often asymmetric and multiple energy loss peaks are found. The two compositions $Cs_3Sc_2Cl_9$ and $CsSc_{0.816}Cl_3$ suffered severe charging to the degree that any attempt to use the monochromator resulted in broad and unrecognizable bands. In contrast, the sample thought to be nearly x = 1.0 did not have a severe charging

problem and spectra could be obtained with the monochromator. XP spectroscopy may be a valuable investigative tool for the ternary system if the charging problems can be either controlled or eliminated.

The data presented in this Result section represent an initial step in understanding the nature of the reduced ternary system. These data are presented as a starting point for future investigations and not as completed or fully understood results. An understanding of the mechanism of nonstoichiometry, electron localization vs. delocalization and structural interrelationships will not be easily attained. However, if recent activities in the general area of one-dimensional conductors (15) is any indication, these investigations should be worthwhile and interesting.

FUTURE WORK

The lack of knowledge in compounds formed by early transition elements is more the result of difficult preparative requirements than any fundamental instability. Certainly compounds made from transition metals early in each series will be intrinsically no less interesting than, for example, those of tungsten or molybdenum, or ruthenium and rhodium. Specifically, new compounds like Sc_7Cl_{10}, ZrCl and Gd_2Cl_3 provide models for studying the metallic state which are presently unique to early transition metals and some rare-earth elements.

The choice of what to do in future projects is not only to prepare every possible $ScCl_x$ phase but also to improve on their syntheses so their properties can be measured and evaluated. The most discouraging aspect of the experimental work has been the inability to prepare larger quantities of the new materials for more complete characterization and testing. Alternative preparative schemes which increase the yields need to be developed.

The relatively low melting (700°C) ternary $3CsCl:2ScCl_3$:Sc system may be used to improve on the syntheses of binary scandium chlorides. The presence of nascent scandium(II) species and finely divided metal (metal crystallites) may provide a kinetically tractable preparation for reduced binary scandium chlorides by the addition of

excess scandium trichloride and scandium. For example, $CsTiCl_3$ can be prepared by the reaction of CsCl and $TiCl_2$, likewise, the unknown $ScCl_2(s)$ could be investigated by the addition of the molar quantities $2ScCl_3$:Sc to the ternary system. In this particular case all products would have the same oxidation state, i.e.,

$$3CsCl + 4ScCl_3 + 2Sc \xrightarrow{\sim 700°C} 3CsScCl_3 + 3ScCl_2.$$

The composite nature of the product would complicate isolation of $ScCl_2(s)$ but should not interfere with its identification. Other more reduced scandium chlorides may also be prepared by adjusting the stoichiometry to favor more metal-rich compositions.

The easiest binary compound to prepare, $ScCl_{1.5}$, can be used in a reaction similar to the one described in the previous paragraph to aid in the synthesis of $CsScCl_3$. The reaction is an oxidation with $ScCl_3$, i.e.,

$$3CsCl + 2ScCl_{1.5} + ScCl_3 \xrightarrow{\sim 650°C} 3CsScCl_3.$$

In this reaction elemental scandium is avoided as a reactant and the temperature required for reaction probably would not be any greater than the melting point of CsCl.

Preliminary experimental observations by their very nature are often synonymous with unusual observations which generally become clear with additional work. In any case

these observations can be valuable and are included here for the benefit of future students.

As expected, other reduced phases exist in the $ScBr_3$-Sc system besides the sesquibromide. What is unusual though, are the powder patterns of the $ScBr_x$ phases which, with the exception of $ScBr_{1.5}$, show no correspondence with the $ScCl_x$ phases. Apparently the change to bromide ion changes the structures as well. This may reflect the importance of halogen-halogen nonbonded contacts vs. metal-metal bonding between the layers perpendicular to chain propagation ([010] in the monoclinic structures).

In the Result section for the $ScCl_3$-Sc system seven reduced $ScCl_x$ phases were identified and characterized to varying degrees. Powder patterns have also been obtained for two products observed only once each in milligram quantities. In the disproportionation of $ScCl_{1.45}$ to make $ScCl_{1.43}$ a small amount of a second phase was obtained with a powder pattern typical of a hcp structure with $\underline{a}$ = 3.06Å and $\underline{c}$ = 4.92Å. This pattern is like hcp scandium metal except the lattice parameters for the element are ∿8% larger! The pattern has never been observed a second time. The other powder pattern resembled the pattern of ScCl where several prominent diffractions had nearly the same d-spacing. This material had been obtained from a transport reaction in a zone near 1000°C. Various reasonable polytypes for ScCl

were used as models but the pattern was never indexed and like the first pattern has never been observed a second time. There can easily be more than seven $ScCl_x$ phases and these may well be two examples but since they were never observed more than once they should be viewed with a degree of skepticism.

Preliminary studies of the three ternary systems $3CsCl:2MCl_3:xM$ where M = Y, La, Gd have indicated metal is consumed and reduction occurs for M = Y, La but not Gd. For M = Y, La the products are not highly colored like $CsScCl_3$ but are a flat gray color. Debye-Scherrer patterns of the yttrium product indicate it is isostructural with $CsScCl_3$ however. Two distinct patterns have been observed for the lanthanum system but there are no apparent similarities to the scandium and yttrium products. One of the phases may be Cs_3LaCl_6 which is the only lanthanum(III) compound in the $CsCl-LaCl_3$ system.

REFERENCES AND NOTES

1. D. A. Johnson, "Some Thermodynamic Aspects of Inorganic Chemistry," Cambridge University Press, New York, N.Y., 1968, p. 7.

2. J. A. Wilson and A. D. Yoffe, Adv. Phys., 18, 193 (1969).

3. J. E. Mee and J. D. Corbett, Inorg. Chem., 4, 88 (1965).

4. D. A. Lokken and J. D. Corbett, Inorg. Chem., 12, 556 (1973).

5. B. C. McCollum, M. J. Camp, and J. D. Corbett, Inorg. Chem., 12, 778 (1973).

6. O. G. Polyachenok and G. I. Novikov, Zh. Neorg. Khim., 8, 2819 (1963).

7. J. D. Corbett and B. N. Ramsey, Inorg. Chem., 4, 260 (1965).

8. M. Barber, J. W. Linnett, and N. H. Taylor, J. Chem. Soc., 3323 (1961).

9. A. Simon, Chem. Unserer Zeit, 10, 1 (1976).

10. H. F. Franzen, "Progress in Inorganic Chemistry," John Wiley and Sons, Inc., New York, N.Y., 1978, to be published.

11. H. Schäfer and H. G. Schnering, Angew. Chem., 76, 833 (1964).

12. A. F. Wells, "Structural Inorganic Chemistry," 4th ed., Clarendon Press, Oxford, England, 1975, p. 151.

13. L. Katz and R. Ward, Inorg. Chem., 3, 205 (1964).

14. J. F. Ackerman, G. M. Cole, and S. L. Holt, Inorganica Chimica Acta, 8, 323 (1974).

15. G. D. Stucky, A. J. Schultz, and J. M. Williams, Ann. Rev. Mater. Sci., 7, 301 (1977).

16. W. Fischer, K. Brunger, and H. Grieneisen, Z. Anorg. Chem., 231, 54 (1937).

17. U. Löchner, Diplomarbeit, Universitat Karlsruhe, Karlsruhe, West Germany, 1973.

18. J. Korbl and R. Pribil, Chemist-Analyst, 45, 102 (1956).

19. M. J. Buerger, "X-ray Crystallography," John Wiley and Sons, Inc., New York, N.Y., 1942, pp. 221-295.

20. J. G. Converse, Ph.D. Thesis, Iowa State University, Ames, Iowa, 1968.

21. B. C. McCollum and J. D. Corbett, Chem. Commun., 1666 (1968).

22. A. Hamnett and A. F. Orchard, "Electronic Structure and Magnetism of Inorganic Compounds," Vol. 1, P. Day, Ed., (Specialist Periodical Reports) The Chemical Society, London, 1971, p. 40.

23. Work performed for the U. S. Energy Research and Development Administration under Contract No. W-7405-eng-82.

24. D. T. Peterson and E. N. Hopkins, "Electropolishing the Rare Earth Metals," Report IS-1036, Iowa State University, Ames, Iowa, 1964.

25. M. L. Lieberman and P. G. Wahlbeck, J. Phys. Chem., 69, 3515 (1965).

26. At this stage of the experimental work all the $ScCl_x$ phases were thought to have Cl:Sc $\leq$ 1.5 based on the work of McCollum and co-workers (5). Therefore, when a composition such as Cl:Sc = 1.58(4) was determined by microprobe analysis, it was assumed under the conditions of electron bombardment and high vacuum the sample suffered disproportionation. Later it will be shown these compounds do not disproportionate under these conditions.

27. D. G. Adolphson and J. D. Corbett, Inorg. Chem., 15, 1820 (1976).

28. R. Daake and J. D. Corbett, Inorg. Chem., 16, 2029 (1977).

29. W. J. Rohrbaugh and R. A. Jacobson, Inorg. Chem., 13, 2535 (1974).

30. S. L. Lawton and R. A. Jacobson, Inorg. Chem., 7, 2124 (1968).

31. N. V. Belov, The Structure of Ionic Crystals and Metal Phases, Akademicâ Nauk SSSR, Inst. Kristalographii, Moscow, 1947.

32. D. G. Adolphson, J. D. Corbett, and D. J. Merryman, J. Am. Chem. Soc., 98, 7234 (1976).

33. L. Pauling, "The Nature of the Chemical Bond," 3rd ed., Cornell University Press, Ithaca, N.Y., 1960, p. 410.

34. W. Klemm and E. Krose, Z. Anorg. Allg. Chem., 253, 218 (1942).

35. J. D. Corbett, D. L. Pollard, and J. E. Mee, Inorg. Chem., 5, 761 (1966).

36. F. J. Keneshea and D. Cubicciotti, J. Chem. Eng. Data, 6, 507 (1961).

37. A. Simon, Hj. Mattausch, and N. Holzer, Angew. Chem., Int. Ed. Engl., 15, 624 (1976).

38. K. R. Poeppelmeier and J. D. Corbett, Inorg. Chem., 16, 294 (1977).

39. J. G. Converse and R. E. McCarley, Inorg. Chem., 9, 1361 (1970).

40. L. F. Bates, "Modern Magnetism," 3rd ed., Cambridge University Press, Cambridge, England, 1951, pp. 133-136.

41. R. A. Jacobson, "An Algorithm for Automatic Indexing and Bravais Lattice Selection. The Programs BLIND and ALICE," U. S. Atomic Energy Commission Report IS-3469, Iowa State University, Ames, Iowa, 1974.

42. F. Takusagawa, Ames Laboratory, Ames, Iowa, personal communication, 1975.

43. P. Main, M. M. Woolfson, and F. Germain, "MULTAN, A Computer Program for the Automatic Solution of Crystal Structures," University of York Printing Unit, York, England, 1971.

44. J. D. Scott, Queen's University, Kingston, Ontario, personal communication, 1971.

45. "International Tables for X-ray Crystallography," Vol. III, 2nd ed., Kynoch Press, Birmingham, England, 1962.

46. $X_M^* = X_g \cdot M \cdot \frac{7}{6}$ where M equals the formula weight of $ScCl_{1.43}$, and the factor $\frac{7}{6}$ accounts for the difference in types of metal atoms.

47. A. Guinier, "X-ray Diffraction In Crystals, Imperfect Crystals, and Amorphous Bodies," W. H. Freeman, London, 1963.

48. R. J. Clark and J. D. Corbett, Inorg. Chem., 2, 460 (1963).

49. J. D. Corbett, R. A. Sallach, and D. A. Lokken, Adv. in Chem. Series, 71, 56 (1967).

50. J. D. Greiner, J. F. Smith, J. D. Corbett, and F. J. Jellinek, J. Inorg. Nucl. Chem., 28, 971 (1966).

51. F. H. Spedding and J. J. Croat, J. Chem. Phys., 58, 5514 (1973).

52. The temperature dependence of the magnetic susceptibility of Sc was originally interpreted (51) in terms of a single localized 3d electron. However, the polarized neutron diffraction behavior of scandium is an applied magnetic field, W. C. Koehler and R. M. Moon, Phys. Rev. Lett., 36, 616 (1976), is not consistent with this interpretation.

53. J. D. Corbett, R. L. Daake, K. R. Poeppelmeier, and D. H. Guthrie, J. Am. Chem. Soc., 100, 652 (1978).

54. J. C. Sheldon, Aust. J. Chem., 17, 1191 (1964).

55. J. E. Ferguson, Prep. Inorg. React., 7, 93 (1971).

56. R. L. Daake, Ph.D. Thesis, Iowa State University, Ames, Iowa, 1976.

57. D. H. Guthrie, Ames Laboratory, Ames, Iowa, personal communication, 1977.

58. H. Schäfer, "Preparative Methods in Solid State Chemistry," Academic Press, Inc., New York, N.Y., 1972, p. 266.

59. K. R. Poeppelmeier and J. D. Corbett, J. Am. Chem. Soc., 100, accepted (1978).

60. K. R. Poeppelmeier and J. D. Corbett, Inorg. Chem., 16, 1107 (1977).

61. C. C. Evans, "Whiskers," Mills and Boon Limited, London, 1972.

62. H. Schäfer, H. G. Schnering, K. J. Niehues, and H. G. Nieder-Vahrenholz, J. Less-Common Metals, 9, 95 (1965).

63. K. R. Poeppelmeier and J. D. Corbett, Inorg. Chem., 16, 1107 (1977).

64. R. A. Jacobson, J. Appl. Crystallogr., 9, 115 (1976).

65. The superscript letters on atom numbers index the generating symmetry operations, Table VIII.

66. Following the nomenclature introduced in ref. 11, i = inner and a (äusser) = exo (outer) halogen atoms which are nonlinking and therefore belong only to one metal cluster. Those forming links between two clusters are X^{i-i}, X^{i-a}, or X^{a-a} depending on the mode.

67. J. W. Hastie, R. H. Hauge, and J. L. Margrave, High Temp. Sci., 3, 257 (1971).

68. H. F. Franzen and J. Graham, Z. Kristallogr., 123, 134 (1966).

69. H. F. Franzen and J. G. Smeggil, Acta Cryst., B26, 125 (1970).

70. J. M. Ziman, "Electrons in Metals," Taylor and Francis LTD, London, 1966.

71. S. B. M. Hagström, C. Nordling, and K. Siegbahn, Z. Physik, 178, 433 (1964).

72. S. Evans and A. F. Orchard, "Electronic Structure and Magnetism of Inorganic Compounds," Vol. 2, P. Day, Ed., (Specialist Periodical Reports) The Chemical Society, London, 1973, p. 1.

73. A. Hamnett and A. F. Orchard, "Electronic Structure and Magnetism of Inorganic Compounds," Vol. 3, P. Day, Ed., (Specialist Periodical Reports) The Chemical Society, London, 1975, p. 218.

74. R. S. Swingle and W. M. Riggs, Crit. Rev. Anal. Chem., 5, 267 (1975).

75. M. F. Ebel, J. Electron Spectrosc. Related Phenomena, 8, 213 (1976).

76. H. F. Franzen and J. Anderegg, Ames Laboratory, Ames, Iowa, personal communication, 1978.

77. R. J. Thorn and J. R. McCreary, Argonne National Laboratory, Argonne, Illinois, personal communication, 1977.

78. D. J. Hnatowich, J. Hudis, M. L. Perlman, and R. C. Ragaini, J. Appl. Phys., 42, 4883 (1971).

79. S. P. Kowalczyk, Ph.D. Thesis, Lawrence-Berkeley Laboratory and Department of Chemistry, University of California, Berkeley, California, 1976.

80. D. A. Shirley, Adv. Chem. Phys., 23, 85 (1973).

81. J. Marchiando, B. N. Harmon, and S. H. Liu, Ames Laboratory, Ames, Iowa, unpublished calculations, 1977.

82. C. Kittel, "Introduction to Solid State Physics," 4th ed., John Wiley and Sons, Inc., New York, N.Y., 1971, p. 475.

83. A. E. Van Arkel, "Moleculen Kristallen," W. P. Van Stockum, 's-Gravenhage (The Hague), 1961, p. 274.

84. G. Blasse, J. Inorg. Nucl. Chem., 27, 993 (1965).

85. J. W. Weenk and H. A. Harwig, J. Phys. Chem. Solids, 38, 1055 (1977).

86. J. B. Goodenough, J. A. Kafalas, J. M. Longo, "Preparative Methods in Solid State Chemistry," Academic Press, Inc., New York, N.Y., 1972, p. 2.

87. R. Gut and D. M. Gruen, J. Inorg. Nucl. Chem., 21, 259 (1961).

88. G. J. Wessel and D. J. W. Ijdo, Acta Cryst., 10, 466 (1957).

89. H. Jogodzinski, Acta Cryst., 7, 17 (1954).

90. J. L. Hoard and L. Goldstein, J. Chem. Phys., 3, 117 (1935).

91. H. Yamatera and K. Nakatsu, Bull. Chem. Soc. Jpn., 27, 244 (1954).

92. H. M. Powell and A. F. Wells, J. Chem. Soc., 1008 (1935).

93. J. L. Hoard and L. Goldstein, J. Chem. Phys., 3, 199 (1935).

94. K. Kihara and T. Sudo, Acta Cryst., B30, 1088 (1974).

95. W. H. Watson and J. Waser, Acta Cryst., 11, 689 (1958).

96. K. Yvon, W. Jeitschko, and E. Parthé, "A Fortran IV Program for the Intensity Calculation of Powder Patterns," Laboratory for Research on the Structure of Matter, University of Pennsylvania, Philadelphia, Pennsylvania, 1969.

97. R. D. Shannon and C. T. Prewitt, Acta Cryst., B25, 925 (1969).

98. L. Pauling, J. Am. Chem. Soc., 51, 1010 (1929).

99. A. B. A. Schippers, V. Brandwijk, and E. W. Gorter, J. Solid State Chem., 6, 479 (1973).

100. B. Chabot and E. Parthé, Acta Cryst., 1334, 645 (1978).

101. T. P. McMullen, Master's Thesis, Iowa State University, Ames, Iowa, 1978.

102. G. N. Tischemko, Tr. Inst. Kristallogr. Acad. Nauk SSSR, 11, 93 (1955).

103. W. C. Hamilton, Acta Cryst., 18, 502 (1965).

104. G. L. McPherson and L. M. Henling, Phys. Rev. B, 16, 1889 (1977).

ACKNOWLEDGEMENTS

The author would like to thank Professor John D. Corbett for his guidance and constructive criticism throughout these investigations.

He is particularly thankful to B. Helland, J. Benson and Dr. R. A. Jacobson for their support in the use of the diffractometer and in all aspects of the structure determinations.

F. Laabs is thanked for the microprobe analyses.

J. Anderegg and Dr. H. F. Franzen are acknowledged for their assistance in the collection and interpretation of the UPS-XPS data.

B. Beaudry and P. Palmer kindly provided the scandium for this work. L. Reed is thanked for the preparation of the scandium foil. Dr. D. T. Peterson is thanked for the hydrogen analysis of the scandium powder.

T. McMullen and Dr. R. G. Barnes are thanked for the NMR study.

He also wishes to thank all group members, past and present, for their help and friendship.

Last and most important he thanks his wife, Maria, for her patience and understanding.

APPENDIX A. OBSERVED AND CALCULATED STRUCTURE FACTORS (X10) FOR ScCl

H = 0

K	L	FO	FC
0	3	319	306
0	6	591	716
0	9	47	73
0	12	761	866
0	15	471	485
0	18	625	625
0	21	325	304
0	27	174	135
0	30	207	134
1	2	771	702
1	5	1567	1508
1	8	281	228
1	11	595	595
1	14	133	128
1	17	482	515
1	20	72	84
1	23	526	480
1	26	135	118
2	1	252	242
2	4	50	58
2	7	650	619
2	10	724	699
2	13	393	392
2	16	350	364
2	19	36	49
2	22	221	240
2	25	43	71
3	3	115	112
3	6	267	278
3	12	387	407
3	15	256	255

H = 1

K	L	FO	FC
0	1	415	387
0	4	135	112
0	7	897	873
0	10	934	955
0	13	487	508
0	16	412	461
0	19	73	68
0	22	258	280
0	25	61	82
0	28	401	320
1	0	1571	1263
1	3	232	197
1	6	384	424
1	9	80	73
1	12	506	597
1	15	420	352
1	18	456	475
1	21	262	234
1	27	109	112
2	2	379	349
2	5	855	762
2	8	134	124
2	11	273	331
2	14	52	60
2	17	349	321
2	20	45	58

H = 2

K	L	FO	FC
0	2	510	481
0	5	1089	1019
0	8	158	156
0	11	438	428
0	14	86	83
0	17	409	396
0	20	72	70
0	23	396	388
0	26	93	94
1	1	179	183
1	7	517	453
1	10	524	526
1	13	297	301
1	16	263	277
1	19	26	35
2	0	705	600
2	6	195	211

H = 3

K	L	FO	FC
0	0	934	788
0	3	101	110
0	6	276	273
0	12	354	393
0	15	230	245

APPENDIX B. PRELIMINARY MICROPROBE RESULTS FOR YCl_x AND LaO_xCl

Reduced Yttrium Chlorides

The reaction of powdered yttrium metal and yttrium trichloride in the temperature range 800-1000°C yields a mixture of reduced phases which react with water and evolution of hydrogen. In one particular reaction between yttrium and yttrium trichloride near 1000°C the original yttrium metal was recovered as a sintered mass of material. Preliminary Debye-Scherrer powder patterns indicated reaction had occurred. By microprobe analysis the composition was found to change in a predictable fashion with the surface region the most chlorine rich, the middle region more reduced and the interior still more reduced. The compositions determined were $YCl_{1.2-1.3}$, $YCl_{1.0}$ and $YCl_{0.7-0.8}$. The analyses were repeated several times and an indication of the variability of the results is reflected in the range of compositions given. One probe detected a region near the interior of unreacted yttrium.

Reduced Lanthanum Chlorides

Reaction of lanthanum metal with lanthanum trichloride at temperatures above and below the melting point of the metal resulted in black crystals which were first thought to

be a reduced binary $LaCl_x$ phase. Two crystals were mounted together in a microprobe spectrometer and were found to contain 5.8 and 7.3 wt % oxygen. The theoretical amount for LaOCl is 8.4 wt %. Evidently, the black color of the crystals is caused by the oxygen deficiency. The results also indicate the nonstoichiometry of $LaO_{1-x}Cl$ may be variable. The powder pattern of the bulk material matched the ASTM 8-478 listing for LaOCl.

The original goal of preparing a reduced binary $LaCl_x$ phase failed and it remains to be seen if reduced compounds can be prepared. The greater reactivity of lanthanum metal to oxygen compared with scandium or yttrium makes any synthesis with lanthanum metal that much more difficult.

APPENDIX C. OBSERVED AND CALCULATED STRUCTURE FACTORS (X10) FOR Sc_7Cl_{10}

K = 0			
H	L	FO	FC
-22	1	95	107
-22	2	164	152
-20	3	1113	1056
-20	4	922	881
-20	5	84	116
-20	6	361	367
-18	1	600	601
-18	3	672	627
-18	4	141	133
-18	8	1277	1296
-16	1	326	335
-16	2	743	799
-16	3	404	400
-16	4	712	718
-16	5	214	229
-16	6	325	275
-16	7	240	236
-16	8	351	369
-16	9	599	620
-16	10	661	632
-14	2	299	301
-14	3	286	320
-14	4	440	430
-14	5	373	355
-14	6	426	402
-14	7	1092	1018
-14	8	643	639
-14	9	213	202
-14	11	312	357
-12	1	582	621
-12	2	963	957
-12	3	202	204
-12	4	1562	1611
-12	5	685	646
-12	6	329	312
-12	8	655	625
-12	9	613	645
-12	10	244	275
-12	12	866	914
-10	3	638	654
-10	4	1149	1180
-10	5	563	575
-10	6	822	794
-10	7	334	316
-10	8	65	87
-10	9	626	648
-10	11	161	171
-10	12	770	804
-10	13	621	682
-8	1	235	267
-8	2	556	571
-8	3	1134	1241
-8	4	613	639
-8	5	977	902
-8	6	363	370
-8	7	504	507
-8	8	515	485
-8	9	529	489
-8	10	182	253
-8	11	756	737
-8	12	333	364
-6	1	982	1032
-6	2	1112	1169
-6	3	379	369
-6	4	2798	2957
-6	5	1151	1098
-6	6	1063	1032
-6	7	419	428
-6	8	682	675
-6	10	482	511
-6	11	800	837
-6	13	174	226
-6	14	202	259
-4	1	834	843
-4	2	643	637
-4	3	84	87
-4	4	263	209
-4	5	942	897
-4	6	788	774
-4	7	593	576
-4	8	1792	1713
-4	9	1205	1135
-4	11	165	195
-4	12	317	302
-4	13	846	812
-4	14	128	168
-2	1	724	714
-2	2	814	863
-2	3	460	429
-2	4	269	309
-2	5	391	419
-2	7	385	379
-2	8	531	492
-2	9	145	181
-2	10	428	457
-2	12	725	736
-2	13	1177	1159
-2	14	242	260
0	1	196	161
0	2	316	303
0	3	320	343
0	4	634	606
0	5	896	880
0	7	1137	1041
0	8	1406	1402
0	9	458	435
0	10	56	55
0	11	84	131
0	12	369	351
0	13	108	135
2	0	605	579
2	1	746	769
2	2	1009	1036
2	3	1007	1027
2	4	2142	2078
2	5	2204	2210
2	7	724	660
2	8	124	125
2	9	769	724
2	10	569	527
2	11	87	129
2	12	137	163
2	13	387	374
2	14	92	162
4	0	822	883
4	1	807	883
4	2	291	320
4	4	888	932
4	5	559	536
4	6	473	470
4	7	547	552
4	8	1201	1244
4	9	1221	1114
4	10	427	393
4	11	235	242
4	12	280	235
4	13	70	84
4	14	351	393
6	0	265	281
6	1	1068	1157
6	2	1499	1671
6	3	170	178
6	4	2084	2025
6	5	354	367
6	6	1015	1090
6	7	802	771
6	8	746	736
6	9	74	147
6	10	664	642
6	12	252	230
6	13	1047	975
8	0	1332	1452
8	1	1447	1618
8	2	360	382
8	3	155	144
8	4	256	219
8	5	833	781
8	6	492	459
8	8	260	260
8	9	1063	1054
8	10	162	165
8	11	270	298
8	12	435	409
8	13	341	315
10	0	1466	1484
10	1	795	814
10	2	503	540
10	3	366	360
10	4	639	685
10	5	566	548
10	6	501	509
10	7	426	422
10	8	114	144
10	9	670	651
10	10	156	205
10	11	476	463
10	12	348	337
12	0	561	639
12	1	614	596
12	2	980	1056
12	3	1380	1375
12	5	869	850
12	6	970	971
12	7	412	429
12	9	570	505
12	10	284	284
12	11	412	422
12	12	170	196
14	0	583	614
14	1	1279	1309
14	2	364	363
14	3	197	220
14	4	264	273
14	5	895	812
14	6	89	118
14	7	77	120
14	8	564	521
14	9	263	274
14	10	473	476
14	11	83	112
16	0	256	252
16	1	250	246
16	2	65	50
16	3	382	372
16	4	741	697
16	5	871	833
16	6	501	470
16	7	305	293
16	9	142	162
18	0	421	428
18	1	1067	1019
18	2	206	217
18	4	357	338
18	5	191	184
18	7	193	247
18	8	296	302
20	1	392	362
20	3	259	286
20	4	169	182
20	5	111	129
22	0	407	447
22	1	779	817

K = 1			
H	L	FO	FC
-21	1	423	432
-19	1	332	355
-19	2	72	88
-19	3	71	92
-19	4	356	395
-19	5	520	536
-19	7	442	464
-17	1	1003	930
-17	2	1087	1052

-17	3	380	368	-5	6	55	52	5	10	508	468	17	8	219	265
-17	5	111	117	-5	7	1048	995	5	11	491	472	19	0	442	450
-17	6	334	330	-5	8	268	265	5	12	444	427	19	2	374	373
-17	7	93	159	-5	9	255	270	5	13	551	535	19	3	1081	1022
-17	9	356	390	-5	10	68	106	7	0	307	315	19	4	449	404
-15	1	1093	1053	-5	11	111	142	7	1	511	547	19	5	81	79
-15	2	72	109	-5	13	313	333	7	2	672	698	19	6	246	311
-15	3	666	627	-3	1	308	311	7	3	1266	1266	21	2	423	421
-15	4	691	634	-3	2	3341	3664	7	6	617	609				
-15	5	387	352	-3	3	1318	1329	7	7	1197	1126		K =	2	
-15	6	1239	1187	-3	4	1432	1472	7	8	135	169	H	L	FO	FC
-15	8	330	331	-3	5	1044	1026	7	10	384	422	-18	1	503	492
-15	9	163	230	-3	6	361	381	7	11	622	602	-18	3	529	528
-13	1	925	922	-3	7	834	789	7	13	263	300	-16	1	199	272
-13	2	748	751	-3	9	655	630	9	0	1723	1898	-16	2	663	649
-13	3	462	475	-3	10	298	278	9	1	970	1064	-16	3	351	335
-13	4	580	580	-3	12	495	528	9	2	753	776	-16	4	627	581
-13	6	1210	1093	-3	13	418	437	9	3	547	551	-16	5	179	194
-13	7	298	267	-3	14	224	236	9	4	822	825	-16	6	222	238
-13	8	490	464	-1	1	506	565	9	5	803	792	-16	7	134	189
-13	10	454	456	-1	2	773	796	9	6	818	774	-14	2	134	228
-13	11	145	183	-1	4	358	370	9	7	64	81	-14	3	200	237
-11	1	351	333	-1	5	358	347	9	8	1282	1213	-14	4	342	339
-11	2	1344	1278	-1	6	2254	2285	9	9	523	525	-14	5	272	274
-11	3	166	194	-1	7	1106	1094	9	10	82	116	-14	6	337	325
-11	5	827	785	-1	8	490	481	9	11	619	590	-14	7	853	834
-11	6	1001	946	-1	9	893	836	9	12	69	79	-14	8	517	540
-11	7	150	171	-1	11	512	493	11	1	390	373	-14	9	110	160
-11	8	160	195	-1	12	92	113	11	2	744	777	-12	1	523	490
-11	9	894	823	-1	13	208	251	11	3	626	614	-12	2	799	755
-11	10	232	244	-1	14	335	348	11	5	581	569	-12	3	156	158
-11	11	451	461	1	2	704	766	11	6	626	628	-12	4	1181	1242
-9	1	1013	1054	1	3	392	406	11	7	722	697	-12	5	547	511
-9	2	681	642	1	4	425	415	11	8	405	394	-12	6	300	249
-9	3	443	445	1	5	465	454	11	9	438	424	-12	8	463	498
-9	4	285	298	1	6	104	76	11	10	228	244	-12	9	535	539
-9	5	281	294	1	7	548	504	11	11	620	579	-12	10	226	243
-9	6	1022	956	1	8	66	99	13	0	319	304	-10	3	531	471
-9	7	1280	1253	1	10	670	685	13	3	721	693	-10	4	973	904
-9	8	1064	973	1	11	1452	1481	13	4	60	83	-10	5	472	433
-9	9	530	527	1	14	295	319	13	5	111	133	-10	6	652	616
-9	10	632	602	3	1	232	268	13	6	140	190	-10	7	275	238
-9	11	294	322	3	2	1145	1084	13	7	1089	1024	-10	9	543	522
-9	13	329	356	3	3	1548	1710	13	11	333	342	-10	11	106	152
-7	1	290	288	3	4	1410	1362	15	0	75	124	-8	1	183	176
-7	2	1699	1653	3	6	1445	1385	15	1	714	676	-8	2	442	406
-7	4	113	143	3	9	152	147	15	3	776	737	-8	3	888	875
-7	5	370	355	3	10	952	935	15	4	985	902	-8	4	516	475
-7	6	198	193	3	11	189	206	15	5	578	580	-8	5	667	656
-7	7	430	390	3	12	538	482	15	6	567	538	-8	6	259	269
-7	9	235	212	5	0	54	62	15	7	117	162	-8	7	438	406
-7	10	1536	1528	5	2	1964	2228	15	9	209	209	-8	8	417	376
-7	11	528	498	5	3	1413	1463	17	1	370	338	-8	9	443	405
-7	13	81	141	5	4	329	312	17	2	391	357	-8	10	151	204
-5	1	289	275	5	5	922	916	17	3	256	239	-8	11	600	612
-5	2	1176	1180	5	6	478	486	17	4	307	338	-6	1	650	645
-5	3	374	357	5	7	193	208	17	5	409	406	-6	2	744	731
-5	4	76	75	5	8	91	143	17	6	132	162	-6	3	265	231
-5	5	639	625	5	9	217	220	17	7	259	263	-6	4	2199	2066

-6	5	881	793	4	11	173	195	18	0	362	356	1	2	334	379	0	3	92	120
-6	6	858	786	4	12	192	201	18	1	855	843	1	3	179	209	0	4	159	208
-6	7	357	340	6	0	271	251	18	2	137	188	1	4	211	201	2	0	148	193
-6	8	516	509	6	1	787	771	18	4	296	287	1	5	201	236	2	1	186	222
-6	9	74	97	6	2	957	1106					1	7	274	281	2	2	331	321
-6	10	425	414	6	3	122	115		K =	3		1	8	62	72	2	3	271	293
-6	11	675	688	6	4	1420	1416	H	L	FO	FC	1	10	458	470	2	4	752	741
-4	1	554	515	6	5	256	261	-15	1	678	705	3	2	535	516	4	0	253	295
-4	2	436	411	6	6	768	809	-15	3	379	421	3	3	891	898	4	1	171	216
-4	4	99	99	6	7	562	585	-13	1	588	588	3	4	811	746	6	1	379	418
-4	5	673	632	6	8	606	588	-13	2	517	506	3	6	960	865	6	2	570	613
-4	6	626	556	6	9	79	101	-13	3	283	299	3	10	609	631				
-4	7	434	418	6	10	549	534	-13	4	373	383	5	2	1154	1182				
-4	8	1431	1330	6	12	154	192	-11	1	221	210	5	3	799	819				
-4	9	940	878	8	0	1062	1019	-11	2	837	768	5	4	94	166				
-4	11	145	169	8	1	1134	1129	-11	3	110	120	5	5	550	535				
-4	12	185	249	8	2	256	263	-11	4	78	64	5	6	252	271				
-2	1	443	422	8	3	64	116	-11	5	515	531	5	7	90	132				
-2	2	541	515	8	4	83	170	-11	6	612	621	5	8	87	118				
-2	3	267	270	8	5	546	570	-11	7	81	120	5	9	103	135				
-2	4	178	192	8	6	341	351	-9	1	676	600	7	0	64	158				
-2	5	283	294	8	8	253	218	-9	2	420	384	7	1	298	287				
-2	7	288	278	8	9	914	851	-9	3	315	298	7	2	395	409				
-2	8	363	360	8	10	119	143	-9	4	181	216	7	3	648	713				
-2	9	103	146	8	11	239	256	-9	5	179	157	7	6	358	385				
-2	10	357	356	10	0	1146	1070	-9	6	663	620	7	7	680	716				
-2	12	581	603	10	1	622	602	-9	7	861	812	7	8	70	122				
0	0	3067	3546	10	2	432	389	-9	8	674	665	9	0	1175	1124				
0	2	206	207	10	3	258	269	-7	1	201	164	9	1	641	626				
0	3	182	201	10	4	493	501	-7	2	999	923	9	2	455	484				
0	4	349	320	10	5	446	424	-7	4	112	104	9	3	285	313				
0	5	648	615	10	6	357	389	-7	5	204	210	9	4	537	542				
0	7	811	759	10	7	316	327	-7	6	66	82	9	5	513	526				
0	8	1121	1073	10	8	69	107	-7	7	227	261	9	6	494	490				
0	9	359	341	10	9	535	539	-7	9	132	140	9	8	812	824				
0	11	71	117	10	10	113	165	-5	1	152	163	11	0	58	42				
0	12	280	297	12	0	505	474	-5	2	651	621	11	1	200	222				
2	0	372	380	12	1	470	463	-5	3	196	203	11	2	443	469				
2	1	514	486	12	2	791	812	-5	5	348	351	11	3	375	392				
2	2	696	642	12	3	1115	1064	-5	7	597	623	11	5	348	365				
2	3	632	624	12	5	679	667	-5	8	100	154	11	6	370	412				
2	4	1474	1391	12	6	839	796	-5	9	132	204	11	7	482	490				
2	5	1648	1523	12	7	359	365	-3	1	133	151	13	0	202	216				
2	7	517	505	12	9	399	415	-3	2	2142	1889	13	3	409	442				
2	8	80	97	14	0	526	489	-3	3	748	681	13	5	78	100				
2	9	549	554	14	1	994	1019	-3	4	888	808	15	0	75	99				
2	10	495	424	14	2	288	287	-3	5	612	575	15	1	456	472				
2	11	64	102	14	3	187	184	-3	6	239	234								
2	12	137	144	14	4	202	225	-3	7	535	472		K =	4					
4	0	529	532	14	5	676	654	-3	9	434	434	H	L	FO	FC				
4	1	487	519	14	8	399	427	-3	10	235	211	-6	1	324	328				
4	2	195	211	16	0	175	189	-1	1	228	255	-6	2	353	378				
4	4	665	638	16	1	187	201	-1	2	420	401	-4	1	260	249				
4	5	392	389	16	2	61	52	-1	4	242	223	-4	2	141	193				
4	6	363	331	16	3	303	298	-1	5	214	201	-2	1	148	166				
4	7	455	414	16	4	581	567	-1	6	1427	1333	-2	2	232	235				
4	8	968	947	16	5	720	696	-1	7	680	675	-2	3	106	126				
4	9	855	889	16	6	399	386	-1	8	329	294	0	0	1849	1734				
4	10	298	309	16	7	243	247	-1	9	545	549	0	2	103	128				

APPENDIX D. OBSERVED AND CALCULATED STRUCTURE FACTORS FOR Sc_7Cl_{12}

L = 0

H	K	FO	FC
1	1	138	147
1	4	97	102
1	7	43	45
1	10	6	9
2	2	71	75
2	5	50	48
2	8	36	34
2	11	69	69
3	0	68	72
3	3	12	10
3	6	58	58
3	9	307	321
4	1	19	19
4	4	75	74
4	7	5	3
4	10	107	114
5	2	521	584
5	5	14	14
5	8	66	69
6	0	87	82
6	3	141	141
6	6	65	62
6	9	6	8
7	1	142	143
7	4	5	5
7	7	19	20
8	2	4	6
8	5	41	37
9	0	11	10
9	3	23	21
9	6	14	16
10	1	70	64
10	4	259	258
11	2	23	22
12	0	24	27

L = 1

H	K	FO	FC
-12	14	20	18
-11	12	9	11
-10	13	28	28
-9	11	41	40
-8	9	141	136
-8	12	19	17
-8	15	93	94
-7	10	185	172
-7	13	9	9
-6	8	111	110
-6	11	47	46
-5	6	34	35
-5	9	108	107
-5	12	23	22
-4	7	46	45
-4	10	25	24
-4	13	9	10
-3	5	40	37
-3	8	38	36
-3	11	62	58
-3	14	17	19
-2	3	26	25
-2	6	17	17
-2	12	141	133
-1	4	141	139
-1	7	66	64
-1	10	116	105
-1	13	59	60
0	2	99	105
0	5	191	179
0	8	5	1
0	11	143	133
1	0	76	82
1	3	160	157
1	6	32	32
1	9	62	57
2	1	108	119
2	4	192	197
2	7	16	15
2	10	17	17
3	2	173	169
3	5	24	23
3	8	19	20
3	11	23	23
4	3	5	6
4	6	28	28
4	9	42	42
5	1	52	51
5	4	5	4
5	7	87	85
5	10	23	24
6	2	69	68
6	5	113	105
6	8	31	32
7	0	63	62
7	3	18	17
7	6	148	144
8	1	9	7
8	4	118	113
8	7	5	4
9	2	12	13
9	5	52	50
10	0	19	18
10	3	14	14
11	1	6	4
12	2	22	22
13	0	95	93

L = 2

H	K	FO	FC
-12	13	12	13
-11	14	13	15
-10	12	7	5
-9	10	51	49
-9	13	11	10
-8	11	40	38
-8	14	7	7
-7	9	117	111
-7	12	59	56
-7	15	10	12
-6	7	34	34
-6	10	49	43
-6	13	111	106
-5	8	49	45
-5	11	343	360
-5	14	27	27
-4	6	145	138
-4	9	4	2
-4	12	103	96
-3	4	550	737
-3	7	9	9
-3	10	33	33
-3	13	5	7
-2	5	140	136
-2	8	39	38
-2	11	68	68
-1	3	67	66
-1	6	31	28
-1	9	29	29
-1	12	65	63
0	1	46	52
0	4	119	117
0	7	46	42
0	10	47	45
0	13	221	227
1	2	94	99
1	5	38	37
1	8	86	84
1	11	13	13
2	0	75	78
2	3	127	129
2	6	439	480
2	9	14	11
2	12	33	39
3	1	43	46
3	4	34	34
3	7	129	139
3	10	34	33
4	2	34	33
4	5	96	96
4	8	17	18
5	0	125	138
5	3	37	37
5	6	24	22
5	9	5	9
6	1	14	13
6	4	29	26
6	7	48	45
7	5	85	82
7	8	219	229
8	0	12	12
8	3	6	7
8	6	5	4
9	1	366	362
9	4	22	22
10	2	102	101
11	0	107	107
11	3	19	20
12	1	22	23

L = 3

H	K	FO	FC
-11	13	73	78
-10	11	9	11
-10	14	124	126
-9	12	99	100
-8	10	13	13
-8	13	43	44
-7	8	45	44
-7	11	8	11
-7	14	24	24
-6	9	4	4
-6	12	45	44
-5	7	10	11
-5	10	7	7
-5	13	25	27
-4	5	105	103
-4	8	107	100
-4	11	48	49
-4	14	98	98
-3	6	29	25
-3	9	165	153
-3	12	9	10
-2	4	102	101
-2	7	121	116
-2	10	57	58
-2	13	23	24
-1	2	138	145
-1	5	42	39
-1	8	134	127
-1	11	13	11
0	0	163	166
0	3	33	33
0	6	87	85
0	9	7	6
1	1	140	146
1	4	21	21
1	7	29	28
1	10	33	32
2	2	4	2
2	5	38	40
2	8	27	29
2	11	88	90
3	0	54	58
3	3	66	66
3	6	89	88
3	9	110	106
4	1	30	28
4	4	93	93
4	7	18	17
4	10	110	114
5	2	106	115
5	5	23	22
5	8	70	69
6	0	58	57
6	3	145	143

6	6	22	22	7	3	15	13	8	3	35	33	-7	10	85	84
7	1	153	145	7	6	97	100	9	1	101	105	-6	8	118	113
7	4	9	6	8	1	35	34	10	2	73	81	-6	11	53	55
8	2	23	22	8	4	77	74	11	0	91	102	-5	6	34	32
8	5	14	16	9	5	5	1					-5	9	19	21
9	0	36	35	10	0	19	19		L =	6		-4	7	26	25
9	3	16	15	11	1	5	7	H	K	FO	FC	-4	10	5	5
10	1	65	65					-10	11	48	50	-3	5	55	55
10	4	94	95		L =	5		-9	12	229	224	-3	8	74	72
11	2	13	14	H	K	FO	FC	-8	10	24	26	-3	11	28	29
12	0	15	17	-10	12	44	47	-7	8	20	18	-2	3	35	35
				-9	13	22	19	-7	11	4	5	-2	6	35	34
	L =	4		-8	11	19	19	-6	9	32	31	-2	9	35	33
H	K	FO	FC	-7	9	84	85	-6	12	96	99	-1	4	60	56
-11	12	10	12	-7	12	53	51	-5	7	20	20	-1	7	88	87
-10	13	90	95	-6	7	15	17	-5	10	18	18	-1	10	108	108
-9	14	60	61	-6	10	11	14	-4	5	142	140	0	2	16	16
-8	9	80	89	-6	13	104	108	-4	8	67	62	0	5	62	65
-8	12	5	10	-5	8	76	70	-4	11	42	43	0	8	7	9
-7	10	95	94	-5	11	110	107	-3	6	60	58	1	0	99	96
-7	13	4	1	-4	6	125	122	-3	9	50	48	1	3	134	127
-6	8	399	404	-4	9	10	11	-2	4	104	102	1	6	46	43
-6	11	18	15	-4	12	58	58	-2	7	355	337	1	9	43	45
-6	14	11	17	-3	4	125	127	-2	10	15	16	2	1	29	29
-5	6	36	34	-3	7	65	59	-1	2	18	17	2	4	67	63
-5	9	81	77	-3	10	38	37	-1	5	35	35	2	7	57	57
-4	7	17	14	-2	5	83	79	-1	8	83	79	3	2	65	68
-4	10	26	24	-2	8	41	39	-1	11	18	19	3	5	27	26
-3	8	126	121	-2	11	36	37	0	0	434	449	3	8	5	8
-3	11	38	36	-1	3	70	64	0	3	13	11	4	0	66	65
-2	3	17	16	-1	6	5	7	0	6	31	32	4	3	38	39
-2	6	58	58	-1	9	8	10	1	1	79	84	4	6	35	36
-2	9	73	75	-1	12	42	43	1	4	28	26	5	1	61	57
-2	12	66	66	0	1	49	47	1	7	92	86	5	4	20	19
-1	4	79	90	0	4	83	83	1	10	26	26	6	2	98	96
-1	7	80	91	0	7	59	56	2	2	22	20	6	5	102	105
-1	10	318	308	0	10	69	71	2	5	39	41	7	0	7	8
0	2	8	8	1	2	82	80	2	8	67	75	7	3	25	24
0	5	67	63	1	5	13	12	3	0	94	93	10	0	28	32
0	8	7	4	1	8	101	92	3	3	50	52				
0	11	100	96	1	11	25	26	3	6	108	104		L =	8	
1	0	147	146	2	0	66	67	3	9	207	213	H	K	FO	FC
1	3	490	564	2	3	117	118	4	1	30	29	-7	9	113	110
1	9	50	49	2	6	124	117	4	7	6	6	-6	7	48	42
2	1	79	77	2	9	42	42	5	2	314	338	-5	8	53	50
2	4	133	129	3	1	64	58	5	5	14	14	-4	6	16	17
2	10	44	47	3	4	7	6	6	0	41	38	-4	9	24	25
3	2	76	80	3	7	104	100	6	3	89	85	-3	4	285	282
3	5	12	10	4	2	22	22	6	6	8	10	-3	7	22	21
3	8	14	17	4	5	93	86	7	1	63	57	-2	5	50	48
4	3	72	71	4	8	11	12	7	4	29	32	-2	8	44	42
4	6	24	24	5	0	107	103	8	2	25	28	-1	9	10	12
4	9	71	69	5	3	51	51	9	0	23	21	0	1	34	34
5	1	62	62	5	6	8	4	9	3	31	34	0	4	111	101
5	4	44	49	6	1	26	27	10	1	102	107	0	7	45	44
5	7	23	22	6	4	29	30					1	2	74	70
6	2	133	132	6	7	29	31		L =	7		1	5	66	61
6	5	313	311	7	2	35	35	H	K	FO	FC	2	0	51	50
7	0	23	26	7	5	80	80	-8	9	51	52	2	3	114	109

2	6	213	226
3	1	33	31
3	4	10	15
4	2	5	3
4	5	25	27
5	0	61	59
5	3	31	32
6	1	42	40
7	2	40	42
8	0	22	20

L = 9

H	K	FO	FC
-5	7	7	13
-4	5	83	80
-4	8	25	28
-3	6	14	11
-2	4	73	72
-2	7	115	113
-1	2	30	30
-1	5	5	9
0	0	130	127
0	3	50	52
0	6	31	34
1	1	28	28
1	4	63	68
2	2	45	47
2	5	28	26
3	0	53	50
3	3	32	34
4	4	19	23
5	2	111	112
6	0	6	6

L = 10

H	K	FO	FC
-2	3	10	19
-1	4	38	42
0	2	41	37
1	0	85	80
1	3	188	190
2	1	24	28
4	0	32	36

APPENDIX E. OBSERVED AND CALCULATED STRUCTURE FACTORS FOR Sc_5Cl_8

K = 0

H	L	FO	FC
-20	6	32	28
-20	8	18	16
-20	9	33	33
-20	10	26	29
-20	11	52	49
-18	3	72	74
-18	6	104	87
-18	7	6	11
-18	9	49	47
-18	12	24	26
-18	13	16	28
-16	1	78	67
-16	2	61	61
-16	5	52	43
-16	6	9	12
-16	8	36	27
-16	11	84	81
-16	12	61	64
-16	13	47	44
-16	14	46	45
-14	1	12	15
-14	2	12	15
-14	3	56	54
-14	4	87	88
-14	5	72	72
-14	6	24	24
-14	7	43	41
-14	8	61	54
-14	9	42	39
-14	10	49	48
-14	11	43	41
-14	12	17	23
-14	13	66	60
-14	14	41	35
-12	1	15	21
-12	2	69	66
-12	3	32	34
-12	5	24	28
-12	6	201	189
-12	7	25	25
-12	9	18	16
-12	10	17	16
-12	11	9	11
-12	12	25	29
-12	13	75	69
-12	14	10	16
-10	1	88	83
-10	2	91	85
-10	3	23	28
-10	4	6	8
-10	5	58	65
-10	7	17	27
-10	8	8	10
-10	9	12	6
-10	10	29	27
-10	11	17	19
-10	12	52	50
-10	13	69	64
-10	14	88	79
-8	1	49	51
-8	2	35	30
-8	3	88	91
-8	4	82	85
-8	5	112	125
-8	7	175	163
-8	8	125	100
-8	9	22	24
-8	10	95	79
-8	11	47	46
-8	12	10	15
-6	1	5	1
-6	2	70	75
-6	3	67	56
-6	4	36	40
-6	5	70	50
-6	6	178	144
-6	8	20	16
-6	9	55	59
-6	12	8	13
-6	13	69	64
-4	1	78	97
-4	3	61	71
-4	4	23	14
-4	5	146	148
-4	6	55	60
-4	7	51	51
-4	8	92	87
-4	9	34	32
-4	10	37	36
-4	11	55	54
-4	12	28	31
-2	1	37	28
-2	2	103	79
-2	3	91	92
-2	4	83	77
-2	5	147	140
-2	6	15	22
-2	7	158	150
-2	8	96	79
-2	10	20	15
-2	11	48	57
0	1	36	25
0	2	15	27
0	3	22	33
0	4	64	71
0	5	43	46
0	6	3	1
0	7	26	32
0	8	14	15
0	9	35	39
0	10	8	9
2	0	56	45
2	1	64	72
2	2	72	78
2	3	43	48
2	4	22	19
2	5	22	26
2	6	49	47
2	7	55	56
2	8	137	119
2	9	30	29
2	10	43	43
4	0	50	42
4	1	207	199
4	2	100	81
4	3	22	28
4	4	95	79
4	5	113	117
4	6	19	23
4	7	24	22
4	8	38	33
4	9	9	15
6	0	221	222
6	1	27	21
6	2	16	15
6	3	120	112
6	4	46	50
6	5	29	31
6	7	18	24
8	0	32	28
8	1	24	30
8	2	47	40
8	4	27	25
8	5	53	49
8	6	35	39
10	0	24	22
10	1	157	129
10	2	54	46
10	3	4	6
10	5	90	82
12	0	36	33
12	1	14	17
12	2	22	20
12	3	59	57
14	0	9	9
14	2	88	75
16	0	4	2

K = 1

H	L	FO	FC
-19	5	50	49
-19	6	27	29
-19	7	22	26
-19	9	31	36
-19	10	5	7
-19	12	16	21
-17	2	13	11
-17	3	5	5
-17	4	28	25
-17	7	99	95
-17	8	39	44
-17	9	15	25
-17	10	90	79
-17	13	37	39
-15	2	36	36
-15	3	44	41
-15	4	33	27
-15	5	73	70
-15	6	54	51
-15	9	73	64
-15	12	13	14
-13	2	167	132
-13	5	10	19
-13	6	32	35
-13	8	58	67
-13	9	84	89
-13	12	47	40
-11	1	77	75
-11	4	41	37
-11	6	13	21
-11	7	46	43
-11	8	45	49
-11	9	57	55
-11	10	166	141
-11	11	45	39
-11	12	7	9
-11	13	20	20
-9	1	46	48
-9	2	47	43
-9	3	198	185
-9	4	92	73
-9	5	69	73
-9	6	89	81
-9	7	41	46
-9	8	11	2
-9	10	29	14
-9	11	17	26
-7	2	113	105
-7	3	25	33
-7	4	18	14
-7	5	64	67
-7	6	32	25
-7	7	24	23
-7	8	42	46
-7	9	111	102
-7	10	27	30
-7	11	76	66
-7	12	66	61
-5	1	163	170
-5	2	34	43
-5	3	15	23
-5	4	206	188
-5	5	54	45
-5	7	46	43
-5	8	50	50
-5	9	72	62
-5	10	104	85
-5	11	10	9
-5	12	20	22
-3	1	107	110
-3	2	51	42
-3	3	260	235
-3	4	121	84
-3	5	38	41

				K = 2								K = 3			
-3	7	66	68	H	L	FO	FC	-4	6	37	44	H	L	FO	FC
-3	8	9	12	-18	6	81	72	-4	7	34	37	-13	5	12	15
-3	9	69	64	-18	9	43	40	-4	8	86	66	-13	6	8	13
-3	10	24	30	-16	5	41	36	-4	9	29	27	-13	8	45	45
-3	11	28	33	-16	6	5	9	-4	10	27	28	-13	9	57	58
-1	1	32	37	-16	8	24	22	-4	11	47	45	-11	1	47	47
-1	2	29	38	-16	11	72	66	-2	1	21	20	-11	4	19	21
-1	3	59	65	-14	1	12	14	-2	2	57	49	-11	6	10	16
-1	4	19	15	-14	2	8	10	-2	3	61	57	-11	7	25	24
-1	5	18	24	-14	3	45	43	-2	4	48	45	-11	8	31	32
-1	6	50	45	-14	4	77	71	-2	5	113	97	-11	9	37	35
-1	8	56	55	-14	5	53	55	-2	6	11	17	-9	1	24	26
-1	9	89	76	-14	7	33	33	-2	7	149	116	-9	2	23	22
-1	10	36	39	-14	8	48	42	-2	8	66	60	-9	3	125	112
-1	11	60	60	-14	9	28	31	-2	10	13	12	-9	4	46	41
1	0	14	24	-14	10	38	39	0	0	285	266	-9	5	39	40
1	1	39	48	-14	11	32	32	0	1	22	18	-9	6	57	49
1	2	66	68	-12	1	11	15	0	2	9	16	-9	7	24	28
1	3	36	41	-12	2	55	54	0	3	20	24	-9	10	22	12
1	4	273	250	-12	3	20	24	0	4	47	52	-7	2	64	57
1	5	60	48	-12	4	5	10	0	5	31	32	-7	5	33	35
1	6	36	31	-12	5	17	21	0	7	18	25	-7	6	13	11
1	7	13	11	-12	6	170	144	0	8	10	11	-7	7	9	14
1	8	54	55	-12	7	21	20	0	9	28	31	-7	8	33	31
1	9	48	45	-12	9	20	15	2	0	32	27	-7	9	71	64
3	0	86	78	-12	10	12	11	2	1	39	42	-5	1	102	86
3	1	138	142	-12	12	17	24	2	2	48	48	-5	2	18	23
3	2	25	19	-10	1	59	61	2	3	26	31	-5	4	112	99
3	3	57	44	-10	2	71	63	2	4	12	11	-5	5	33	28
3	4	59	48	-10	5	41	46	2	5	14	18	-5	7	34	30
3	6	40	46	-10	8	5	6	2	6	36	37	-5	8	33	34
3	7	47	46	-10	9	6	6	2	7	48	44	-5	9	45	40
3	8	12	14	-10	10	19	20	2	8	116	97	-3	1	48	53
3	9	5	8	-10	11	11	14	4	0	30	26	-3	2	20	20
5	0	19	25	-10	12	44	42	4	1	148	133	-3	3	143	122
5	1	31	36	-8	1	30	35	4	2	60	56	-3	4	61	42
5	3	48	53	-8	2	21	19	4	3	14	19	-3	5	17	19
5	5	80	68	-8	3	63	63	4	4	79	60	-3	7	42	42
5	6	45	44	-8	4	57	60	4	5	97	91	-1	1	11	16
5	7	8	9	-8	5	86	86	4	7	18	19	-1	2	13	19
5	8	78	71	-8	7	127	122	6	0	166	152	-1	3	30	31
7	0	10	9	-8	8	37	74	6	1	16	16	-1	5	7	11
7	1	49	45	-8	9	12	18	6	2	9	10	-1	6	27	26
7	2	62	70	-8	10	75	63	6	3	97	84	-1	8	37	35
7	3	36	39	-8	11	37	37	6	4	39	42	1	1	18	23
7	4	121	115	-8	12	10	13	6	5	20	25	1	2	37	36
7	5	21	21	-6	2	45	50	8	0	21	20	1	3	17	20
7	6	41	41	-6	3	31	31	8	1	14	21	1	4	173	144
9	0	43	47	-6	4	24	29	8	2	36	31	1	5	35	31
9	1	114	102	-6	5	39	32	8	4	19	18	1	6	16	19
9	3	29	31	-6	6	130	101	8	5	46	41	1	7	9	10
9	4	25	26	-6	8	10	11	10	0	17	16	3	0	39	34
11	1	8	14	-6	9	41	45	10	1	134	104	3	1	80	74
11	2	64	60	-6	11	4	1	10	2	45	35	3	2	8	9
11	3	40	43	-4	1	54	57	12	0	26	25	3	3	31	28
13	0	22	23	-4	3	38	44	12	1	12	14	3	4	30	25
13	2	57	58	-4	4	8	7	12	2	17	16	3	6	30	31
15	0	57	58	-4	5	107	99	14	0	7	7				

5	0	10	18
5	1	13	20
5	2	6	9
5	3	30	30
5	5	52	48
7	0	5	1
7	1	35	31
7	2	44	46
7	3	19	23
9	0	28	31
9	1	73	66

K = 4

H	L	FO	FC
-6	2	25	28
-6	3	17	19
-4	1	23	24
-4	2	6	10
-4	3	15	22
-2	1	9	12
-2	2	23	21
-2	3	24	28
0	0	159	126
0	1	9	10
2	0	8	10
2	1	13	17
2	2	22	26
4	0	11	10

APPENDIX F. OBSERVED AND CALCULATED STRUCTURE FACTORS FOR $CsScCl_3$

K = 0

H	L	FO	FC
0	2	122	133
0	4	102	95
0	6	39	37
1	1	55	58
1	2	45	46
1	3	37	37
1	4	3	3
1	5	18	18
1	6	5	8
1	7	6	6
2	0	58	56
2	1	126	133
2	2	82	83
2	3	86	87
2	4	29	28
2	5	50	47
2	6	20	22
3	0	68	72
3	1	8	7
3	2	25	25
3	3	4	5
3	4	35	32
3	6	5	6
4	0	34	33
4	1	86	83
4	2	57	56
4	3	64	61
4	4	19	20
4	5	34	35
4	6	15	17
5	0	9	9
5	1	23	22
5	2	32	30
5	3	17	15
5	4	5	6
5	5	5	7
6	0	73	68
6	2	44	42
6	4	38	39
7	0	4	5
7	1	17	17
7	2	4	8

K = 1

H	L	FO	FC
1	0	83	90
1	2	30	31
1	4	38	38
1	6	8	8
2	0	9	10
2	1	40	42
2	2	46	44
2	3	31	28
2	4	5	6
2	5	14	13
2	6	9	10
3	0	3	2
3	1	38	38
3	2	32	31
3	3	29	26
3	5	12	13
3	6	4	6
4	0	48	50
4	1	4	5
4	2	19	17
4	3	4	4
4	4	26	24
4	5	4	2
5	0	4	4
5	1	22	20
5	2	25	22
5	3	15	14
6	1	18	18
6	2	10	12
6	3	11	13
7	0	19	20

K = 2

H	L	FO	FC
2	0	129	134
2	2	82	81
2	4	68	68
2	6	27	28
3	0	3	3
3	1	36	34
3	2	22	22
3	3	25	24
3	5	12	12
4	0	23	23
4	1	62	59
4	2	42	40
4	3	46	45
4	4	13	15
4	5	25	26
5	0	33	31
5	1	5	6
5	2	10	10
5	3	4	5
5	4	14	15
6	0	8	12
6	1	31	33
6	2	22	23

K = 3

H	L	FO	FC
3	0	43	42
3	2	16	14
3	4	20	20
4	0	5	6
4	1	14	16
4	2	22	22
4	3	7	11
4	4	4	4
5	1	14	14
5	2	11	13

K = 4

H	L	FO	FC
4	0	53	51
4	2	28	31